Electronic Supplementary Material (ESI) for ChemComm.

Cryptand-imidazolium supported total synthesis of lasso peptide BI-32169 and its D-enantiomer

Ming Chen,*[a] Shuanglong Wang[b] and Xihan Yu[c]

[a] Laboratory of Natural Peptide Chemistry, College of Life Science, Yan'an University, Shendi Road 580, Yan'an 716000, China. E-mail: mingchen@mail.ecust.edu.cn

[b] CNRS-UPPA, Laboratoire de Chimie Analytique Bio-inorganique et Environnement, UMR5254, Hélioparc, 2, Av. Angot, 64053 Pau, France. E-mail: shuanglong.wang@univ-pau.fr

[c] College of Pharmacy, East China University of Science and Technology, Meilong Road 130, Shanghai 200237, China. E-mail: xh_yu@mail.ecust.edu.cn

Table of Contents

1. Materials

Solvent / Reagent	Supplier	Purity
DMF	TCI Chem. (Shanghai)	≥99.5%
2-MeTHF	TCI Chem. (Shanghai)	≥ 99.5%
THF	TCI Chem. (Shanghai)	≥99.5%
hexane	Scharlau (Spain)	≥ 99%
dimethyl ether	Daojing Chem. (Dongguan)	99.8%
acetonitrile	Alfa Aesar (China)	≥ 99.7%
NaCl	Jiawei Chem. (Nanjing)	≥ 99.5%
methanol	Lehua Chem. (Henan)	99.8%
phosphate buffer (pH=5.8)	Xingyi Pharma. (Shanghai)	AR
[2-HOM-MMIm][BAr^F_4]	Lanzhou Institute of Chemistry	97%
2-phenylpropan-2-yl 2-((4,5-bis(2-aminoethoxy)-2-nitrobenzyl)oxy)acetate	UHN R&D (Shanghai)	98.5%
((4,5-bis(2-iodoethoxy)-2-nitrobenzyl)oxy)(*tert*-butyl)diphenylsilane	UHN R&D (Shanghai)	98.2%
2,2'-oxydiacetyl chloride	TCI Chem. (Shanghai)	≥97.0%
BH_3-THF (1.0 M)	Shanghai Forxine Pharma.	97%
standard Fmoc-amino acids	GL Biochem. / Sigma-Aldrich (China)	95%-98%
N-Fmoc-2H,3H-2-carboxytryptophan	Hanhong Chem.	97%
EDCI	Alfa Aesar (China)	98%
OxymaPure®	Luxembourg Biotech.	99.5%
PyBOP	Sigma-Aldrich (China)	98%
DIPEA	Shanghai Ziye Chem. Eng.	99.9%
DIC	Alfa Aesar (China)	98%
DMAP	Hanhong Chem.	99%
N-methylmorpholine	Hanhong Chem.	99%
TAEA	Alfa Aesar (China)	97%
TFA	TCI Chem. (Shanghai)	≥99.0%
TBAF	Alfa Aesar (China)	98%
hydrazine	Sigma-Aldrich (China)	98%
phenol	Sheshan Chem. (Shanghai)	≥99.0%
TIPS	Alfa Aesar (China)	≥98.0%
sodium hydroxide	Tianli Chem. (Shanghai)	98%
citric acid	Dongting Chem. (Hunan)	≥99%
native peptide BI-32169	Hokkaido College of Pharmacy (Japan)	≥99%

2. Supplementary Methods

Fmoc-deprotection and coupling steps

Cryptand-imidazolium bounded peptide (2.0 mmol) was dissolved into 10.0 mL 2-MeTHF. TAEA (3.0 mL, 2924.6 mg, 20.0 mmol) was slowly added under stirring. More 2-MeTHF might be replenished if precipitation occurred. The solution was kept under stirring for 15 more minutes and washed with a phosphate buffer (pH= 5.8, ~20.0 mL×3), 20%(m/v) NaCl aqueous solution (~20.0 mL×4) and deionized water (~20.0 mL×2), respectively. Fmoc-protected amino acid (2.2 mmol), EDCI (742.1 mg, 3.0 mmol) and OxymaPure® (426.4 mg, 3.0 mmol) were mixed in 2-MeTHF (10.0 mL), allowed to stand for 15 minutes and added into the solution of cryptand-imidazolium bounded peptide. After 1 hour stirring, the solution was washed with 20%(m/v) NaCl aqueous solution (~20.0 mL×4) and deionized water (~20.0 mL×2) in a separation funnel.

HPLC and MS

Purity of the peptides was confirmed by analytical reversed-phase HPLC on an Agilent 1200 SL chromatograph with a Grace™ Vydac™ 208TP C8 (4.6 x 250mm, 5 µm particle size) and a mobile phase system consisting of A: 0.1% TFA in water and B: 0.1% TFA in acetonitrile with a flow rate of 1.0 mL/min. The UV-detection was at 220 nm. High resolution mass spectra analysis was performed on a Shimadzu LCMS-8030. 1 μL of sample (0.2 mM in 90% v/v acetonitrile/H_2O) was injected onto a Kinetex® C18 column (2.1 × 100 mm, 1.7 μm particle size). The MS analysis was carried out with a gradient of 5–95% B (solvent A = H_2O, 0.1% formic acid; B = acetonitrile, 0.1% formic acid) in 40 minutes and a flow rate of 0.2 ml/min at a column temperature of 40 °C.

NMR

Proton magnetic resonance (^{1}H NMR) and carbon magnetic resonance (^{13}C NMR) spectra were recorded on a Bruker ARX-400 equipped with a DCH cryoprobe. Chemical shifts (δ) are expressed in parts per million (ppm) relative to residual DMSO-d_6 as internal standards. ^{1}H NMR spectra were recorded at either 400 MHz. ^{13}C NMR spectra were recorded at 100 MHz. NMR acquisitions were performed at 295 K unless otherwise noted. Abbreviations are: s, singlet; d, doublet; t, triplet; q, quartet; br, broad, m, multiplet.

Circular dichroism

CD spectra were given on a Jasco J-810 spectropolarimeter (Japan) with a bandwidth at 1.0 nm and response time of 0.5 s. All experiments were carried out at room temperature and examined in far UV spectra region (190-250 nm). Peptide concentration was 100 μM in 20 μM sodium phosphate buffer at pH = 7.2. The blank buffer and peptide samples were each measured at 20°C using a 1 mm path length. Each spectrum was the average of four scans.

Glucagon receptor antagonism

Glucagon receptor antagonism assays were carried out using stably-transfected BHK cell lines expressing the cloned human glucagon receptor as earlier described method[1]. The cDNA coding for the human glucagon receptor, which was amplified from human liver mRNA by RT-PCR, was subsequently cloned into pcDNA3.1(+) vector. Baby hamster kidney cells (BHK-21[C-13]) were transfected with the expression construct for the human glucagon receptor and a stable transfected cell population was selected by growth in G418 (Geneticin) medium. The transfected BHK cells were preincubated in Krebs-Ringer bicarbonate HEPES (KRBH) buffer (10 mM Hepes, pH 7.4; 134 mM NaCl; 3.5 mM KCl; 1.2 mM KH_2PO_4; 0.5 mM $MgSO_4$; 1.5 mM $CaCl_2$; 5 mM $NaHCO_3$; 0.1% BSA; 11 mM glucose; 0.8 mM IBMX) in 96-well microtiter plates with various concentrations of peptide samples for 10 minutes at 37 °C, and glucagon (at concentration of 30 pM) was then added for 5 minutes. The reactions were quenched by adding 250 μL of 1.0 M HCl. cAMP concentrations were determined by using [125I] RIA Kit.

Serum stability assay

Peptide stabilities were assayed in diluted serum as previously described[2] with minor modifications. 2.0 mL of 25% human serum from adult male (Sigma-Aldrich) was centrifuged at 13,000 rpm for 10 minutes. The supernatant was then collected and incubated at 37°C for 15 minutes. The test peptides (final concentration of 100 μM) were incubated in serum at 37 °C. 80 μL aliquots of samples were collected for the following time points: 0, 2, 4, 8, 16, 24 and 36 hours. The aliquots were mixed with 80 μL of 15% TFA and incubated at 4°C for 15 minutes to precipitate serum proteins. The supernatant was collected for each sample after centrifugation at 13,000 rpm for 10 minutes and stored at -20°C. These assays were performed in triplicate. 40 μL of the collected samples were analyzed by HPLC using a Phenomenex™ Luna® C18 column (4.6 × 150 mm, 5 μm particle size) with a linear acetonitrile gradient (0-50% solvent B, 50 minutes).

3. Supplementary Procedure

Validation of complexation ability of synthesized cryptands with imidazolium salt

Cryptand assembly **2** and **16** were prepared using the method described earlier[3,4]. A solution of ((4,5-bis(2-iodoethoxy)-2-nitrobenzyl)oxy) (*tert*-butyl)diphenylsilane (365.76 mg, 0.50 mmol), Li_2CO_3 (209.11 mg, 2.83 mmol), LiI (44.17 mg, 0.33 mmol) in acetonitrile (30.0 mL) was refluxed with stirring for 1 hour at 40 °C. To the reaction mixture 2-phenylpropan-2-yl 2-((4,5-bis(2-aminoethoxy)-2-nitrobenzyl)oxy)acetate (212.26 mg, 0.49 mmol) was added with stirring, and the resulting mixture was refluxed for 2 days. The reaction mixture was cooled gradually to room temperature and then filtered. The filtrate was concentrated *in vacuo*, and the residue thereby obtained was purified *via* flash chromatography on neutral alumina (200-230 mesh) by eluting with 20% ethyl acetate/hexane. The dibenzo diazacrown analog (315.53 mg) was obtained and then mixed with 2,2'-oxydiacetyl chloride (59.84 mg, 0.35 mmol) in borane THF complex solution (1.0 M, 30.0 mL). The resulting mixture was refluxed for 24 hours. The mixture was cooled gradually to room

temperature and then filtered. The filtrate was concentrated *in vacuo*, and the residue thereby obtained was purified *via* flash chromatography on silica gel by eluting with 10% methanol/DCM. After aqueous extraction, the cryptand assembly (173.86 mg) was obtained and separated by chiral HPLC using CHIROBIOTIC V (250×4.6 mm inner diameter) with a mobile phase of THF/H_2O/TEA (2:8:0.01) at 10 °C (controlled by a Peltier heating/cooling HPLC column thermostat). The overall yields of (+)-/(-)-cryptands were 15.70% (75.4 mg, 0.077 mmol) and 19.54% (93.8 mg, 0.096 mmol). The chirality establishment is described in next chapter.

Imidazolium salt **1** (5.1 mg, 5.0 μmol) was methylated with the treatment of NH_3/MeOH (0.4 mL, 4.0 M) overnight. The solution was evaporated under reduced pressure and then mixed with (+)-/(-)-cryptand (4.9 mg, 5.0 μmol) to form a (+)-/(-)-cryptand-imidazolium complex in acetonitrile/water (5.0 mL, 80%). The resulting substance was washed with deionized water and hexane and evaporated to yield a light-yellow solid (9.9 mg). The methylated analogue of complex was used for study of the interactions between cryptand and imidazolium cation in next chapter.

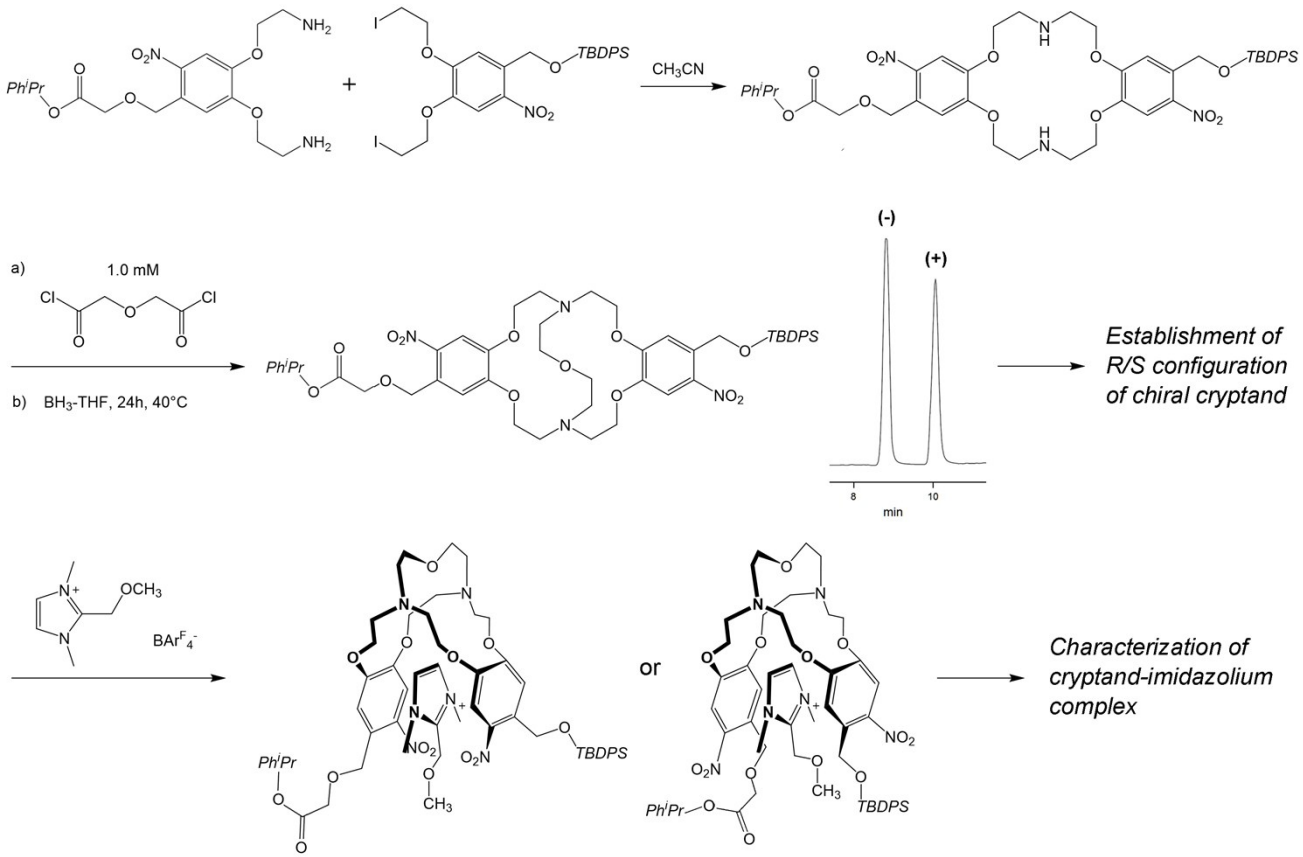

Figure **S1**. Synthesis of cryptand-imidazolium complex and chiral HPLC chromatogram of cryptand separation.

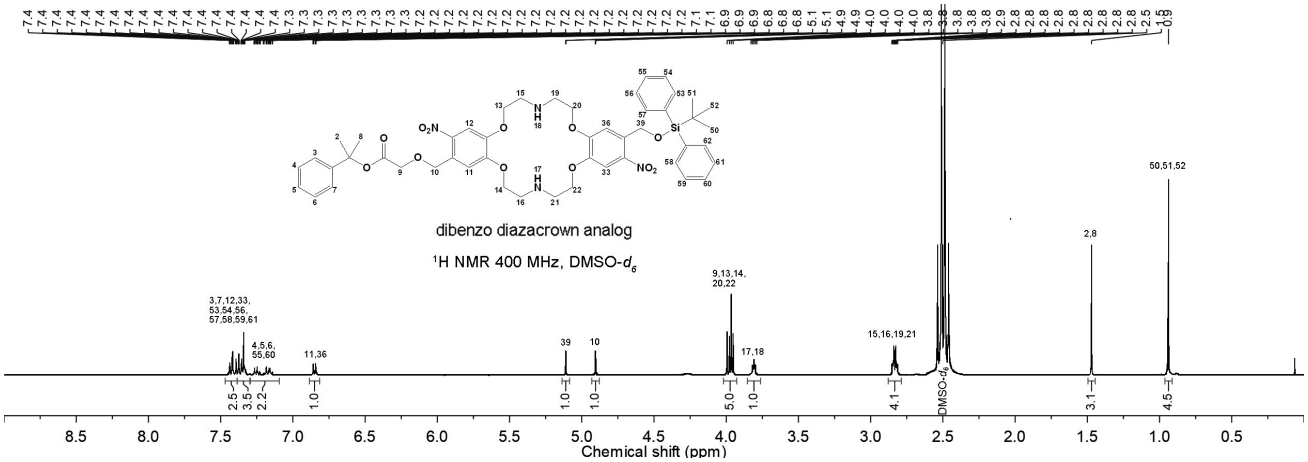

Figure **S2**. ^{1}H NMR spectrum of dibenzo diazacrown analog (400 MHz, DMSO-d_6, 0.3 mM, 22 °C), ESI-MS calculated for $C_{49}H_{58}N_4O_{12}Si$ $[M+Li]^+$: 929.3975; Found: 929.3272.

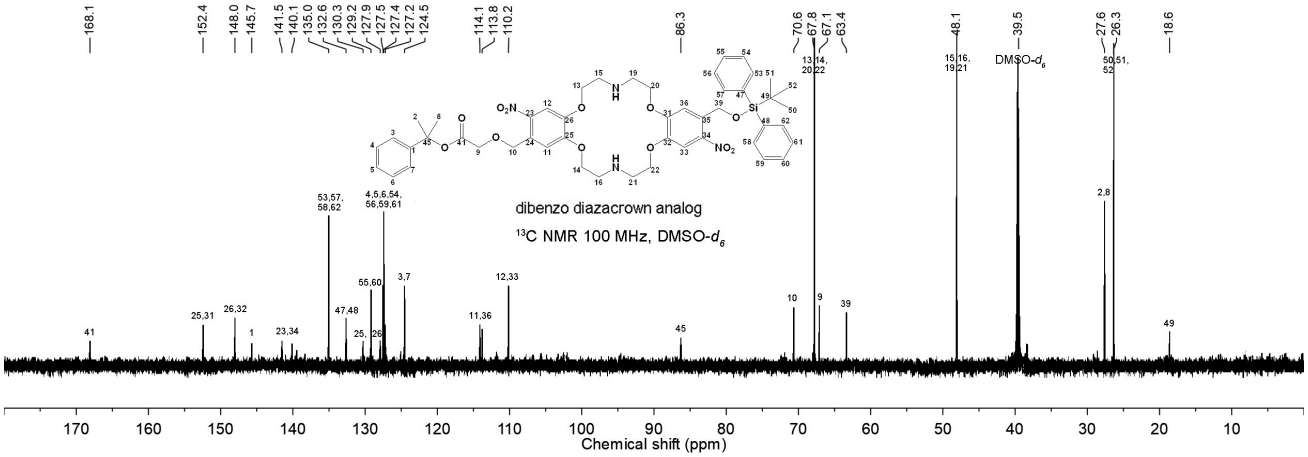

Figure **S3**. ^{13}C NMR spectrum of dibenzo diazacrown analog (100 MHz, DMSO-d_6, 0.3 mM, 22 °C).

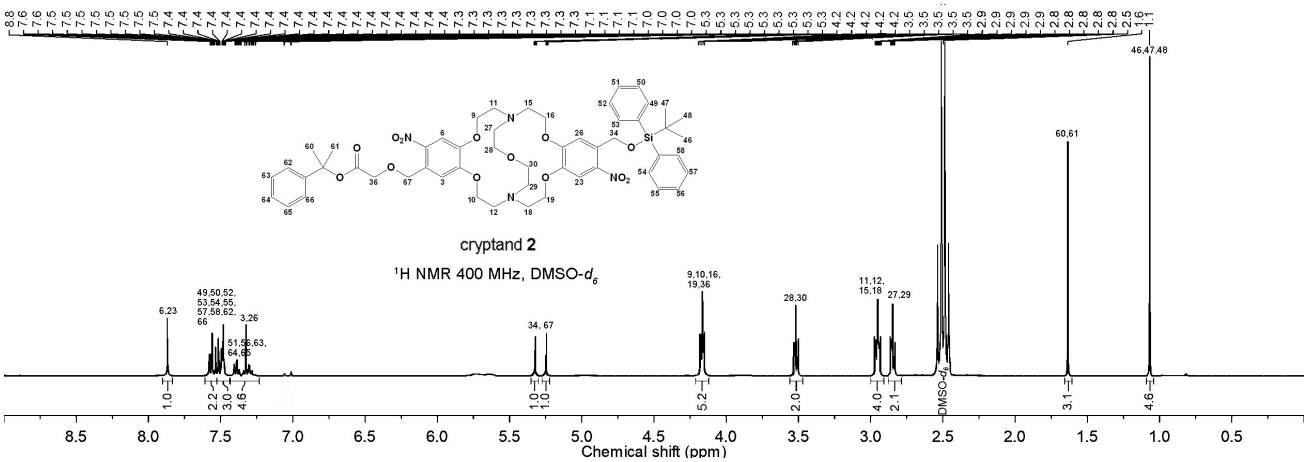

Figure **S4**. ^{1}H NMR spectrum of cryptand assembly **2** (400 MHz, DMSO-d_6, 0.3 mM, 22 °C), ESI-MS calculated for $C_{53}H_{64}N_4O_{13}Si$ $[M+H]^+$: 992.4239; Found: 992.4235.

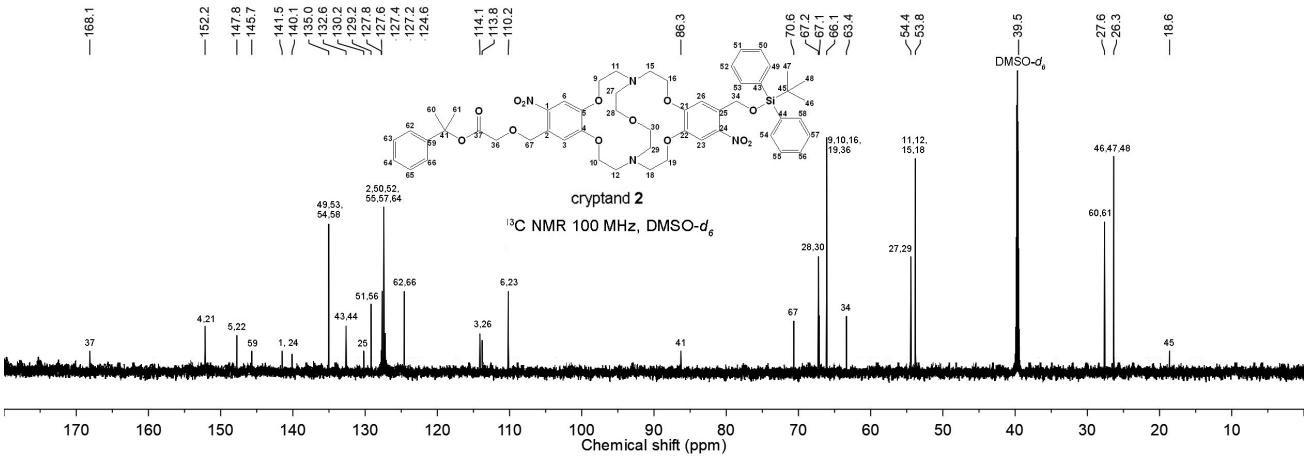

Figure **S5**. ^{13}C NMR spectrum of cryptand assembly **2** (100 MHz, DMSO-d_6, 0.3 mM, 22 °C).

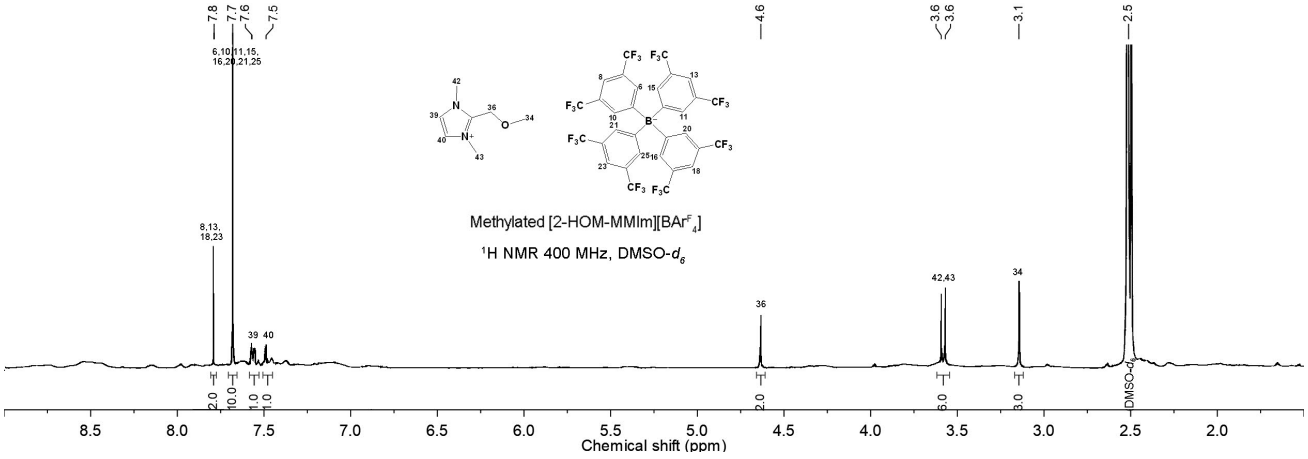

Figure **S6**. ^{1}H NMR spectrum of methylated [2-HOM-MMIm][BAr$^F_4$] (400 MHz, DMSO-d_6, 0.3 mM, 22 °C), ESI-MS calculated for $C_7H_{13}N_2O$ $[M]^+$: 141.1031; Found 141.1027.

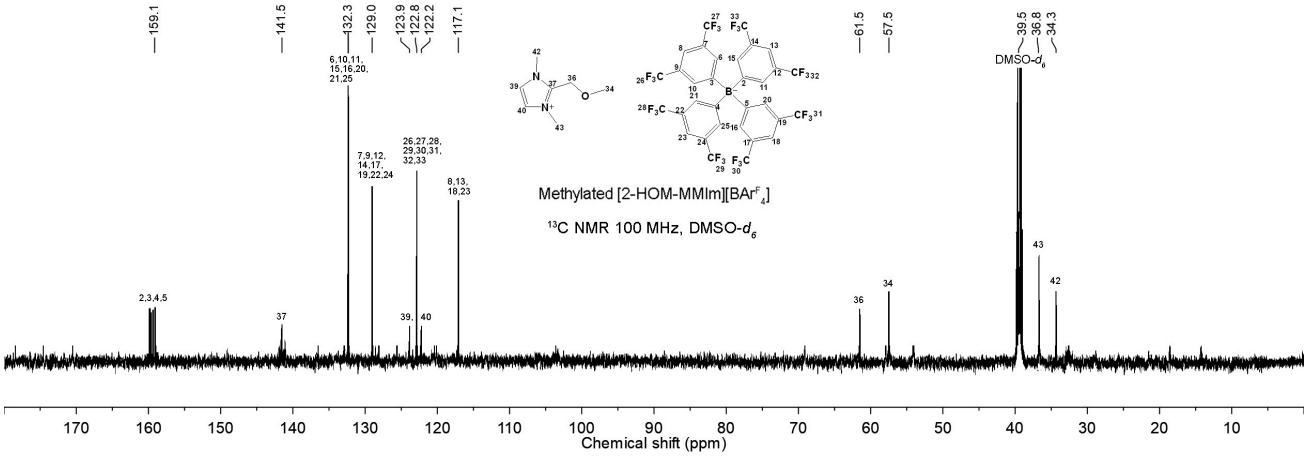

Figure **S7**. ^{13}C NMR spectrum of methylated [2-HOM-MMIm][BAr$^F_4$] (100 MHz, DMSO-d_6, 0.3 mM, 22 °C).

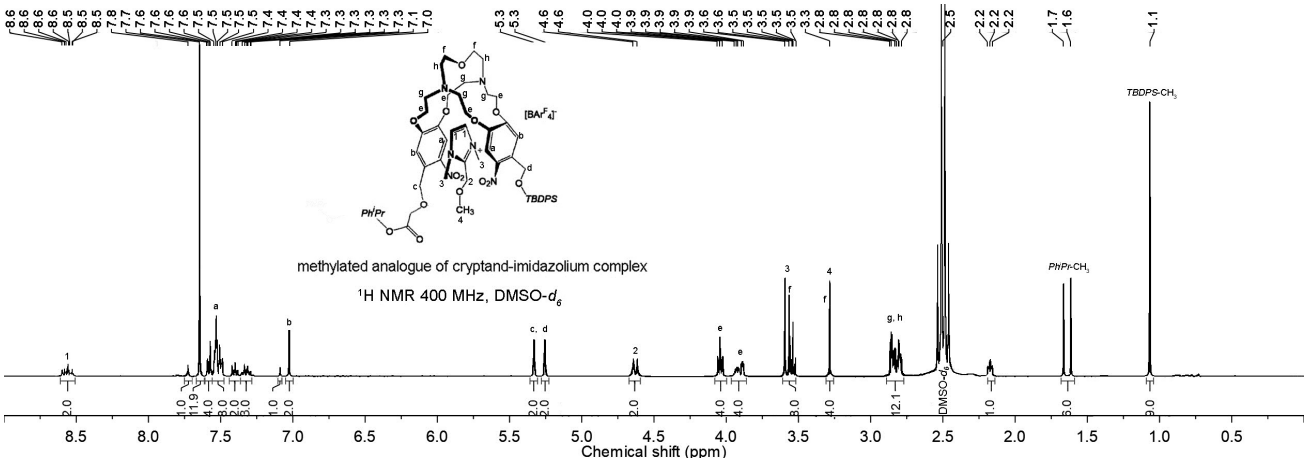

Figure **S8**. ^{1}H NMR spectrum of methylated analogue of cryptand-imidazolium complex (400 MHz, DMSO-d_6, 0.3 mM, 22 °C), ESI-MS calculated for $C_{60}H_{77}N_6O_{14}Si$ $[M]^+$: 1133.5262; Found 1133.5258.

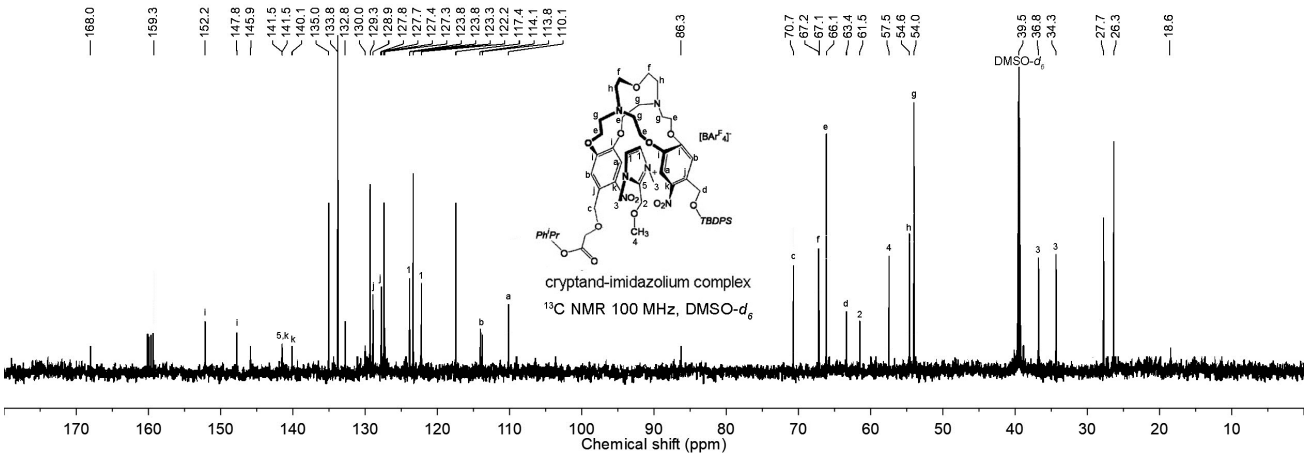

Figure **S9**. ^{13}C NMR spectrum of methylated analogue of cryptand-imidazolium complex (100 MHz, DMSO-d_6, 0.3 mM, 22 °C).

Characterization of cryptand-imidazolium complex

The resonance signal of protons H_1 in imidazolium assembly moved obviously to lower field (higher frequency) after complexation. This deshielding effect showed that the imidazolium cation should be transferred into the cavity of cryptand assembly and formed strong hydrogen bonds. The resonance signals of protons H_a and H_b in benzyl rings of cryptand assembly were changed towards higher filed (lower frequency) probably due to the shielding effect of π-π sandwich stacking between imidazolium cation and benzyl rings. Furthermore, variable temperature NMR measurement showed that the cryptand-imidazolium complex is still stable at 40°C.

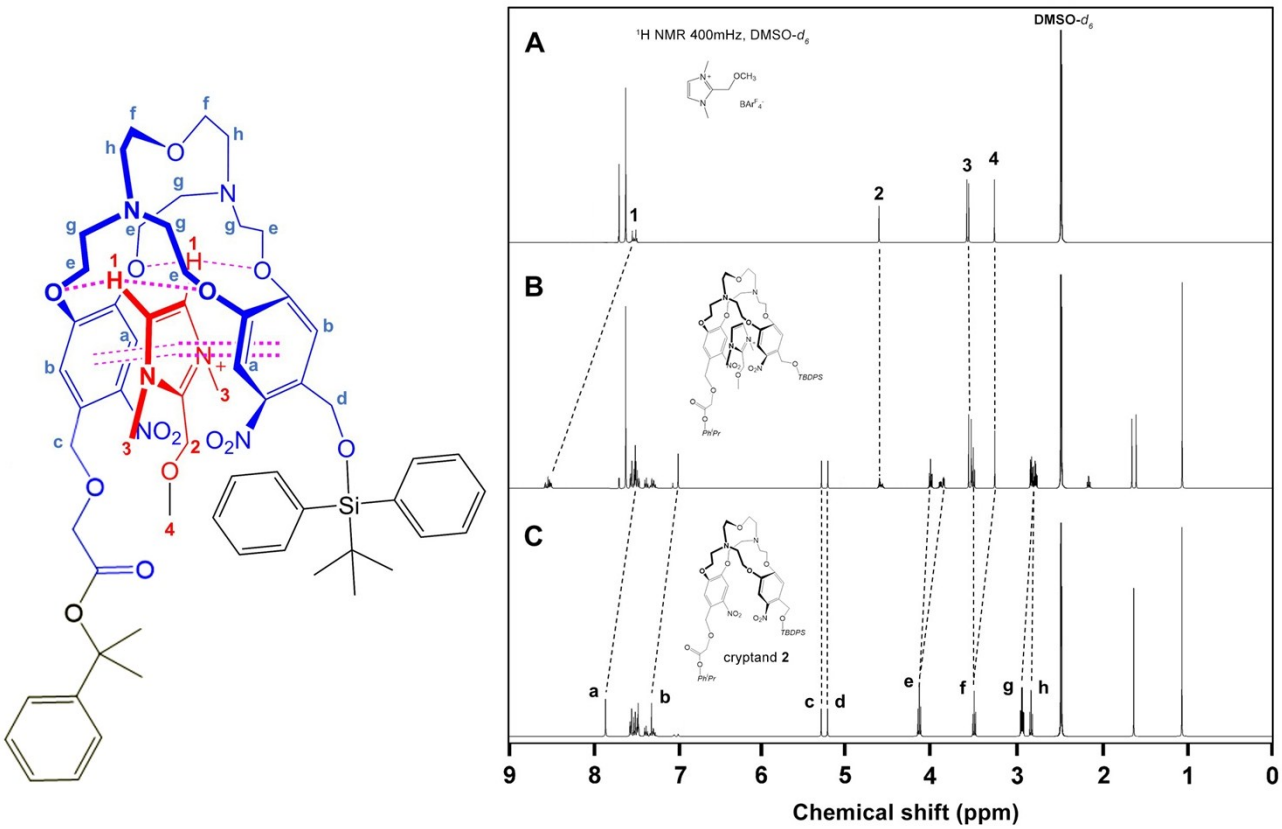

Figure **S10**. *Left*: The complexation between cryptand **2** (blue) and cation of imidazolium salt **1** (red). The interactions (hydrogen bonds and π-π stacking) were shown in purple. *Right*: ^{1}H NMR spectra of A) imidazolium salt **1**, B) equimolar mixture of **2** and **1** and C) cryptand **2** at 22 °C.

Establishment of R/S configuration of cryptands

To distinguish between the *R* and *S* configurations of separated cryptands, L-aspartic acid attached imidazolium was introduced as a chiral auxiliary. Fmoc-L-aspartic acid(Dmab) (4.0 mg, 6.0 μmol) was attached to imidazolium salt **1** (5.1 mg, 5.0 μmol) using EDCI (2.88 mg, 15.0 μmol)/OxymaPure® (2.1 mg, 15.0 μmol) in 2-MeTHF (5.0 mL, 1.0 mM). After washing with 20%(m/v) NaCl solution and deionized water, the Fmoc and Dmab groups of attached imidazolium were removed by 10.0 eq. TAEA (7.5 μL, 7.3 mg, 50.0 μmol) and hydrazine (0.1 mL, 102.1 mg, 3.2 mmol, 2% in solution), respectively. The resulting L-aspartic acid attached imidazolium salt was mixed (1:1) with (+)-/(-)-cryptand (4.9 mg, 5.0 μmol) in 2-MeTHF (5.0 mL). 2-3 drops of TFA (0.1-0.2 mL) were added to cleave the Ph^{i}Pr group of cryptand assembly. The deprotected carboxyl group generated an amide linkage with α-amino group of L-aspartic acid attached imidazolium. The TBDPS group of cryptand assembly was then removed by 3.0 eq. TBAF (3.9 mg, 15.0 μmol). The free hydroxyl group of **2** connected with the side chain of L-aspartic acid *via* an ester bond at 40°C using EDCI/OxymaPure®, while the esterification of hydroxyl group of **16** is spatially hindered.

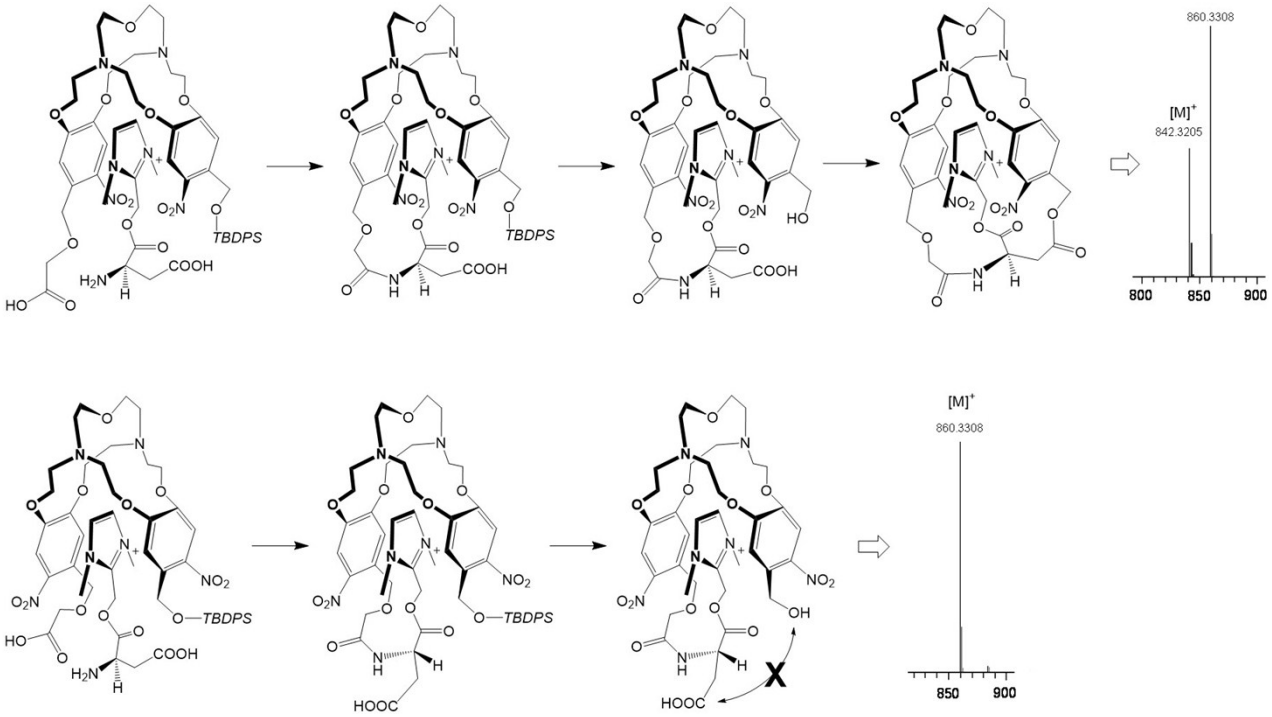

Figure **S11**. Establishment of *R*/*S* configuration of cryptands.

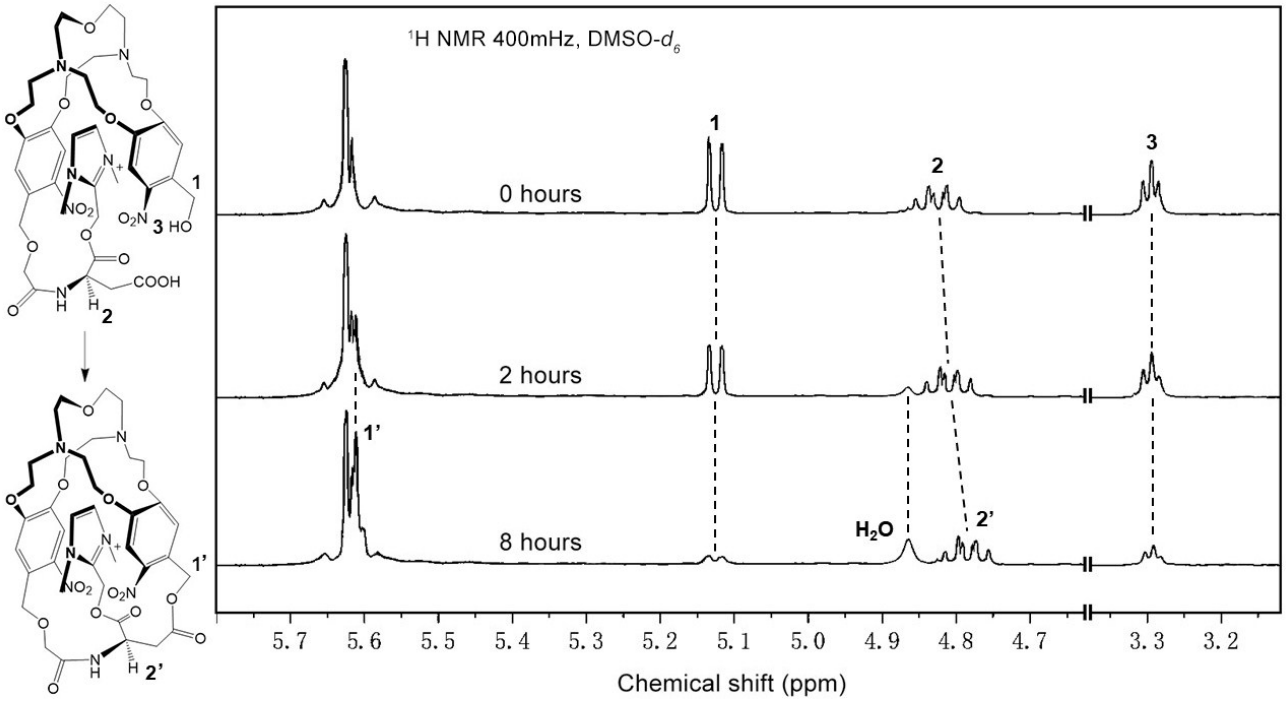

Figure **S12**. ^{1}H NMR spectra evolution as a function of time for esterification of cryptand **2** complex at 40°C.

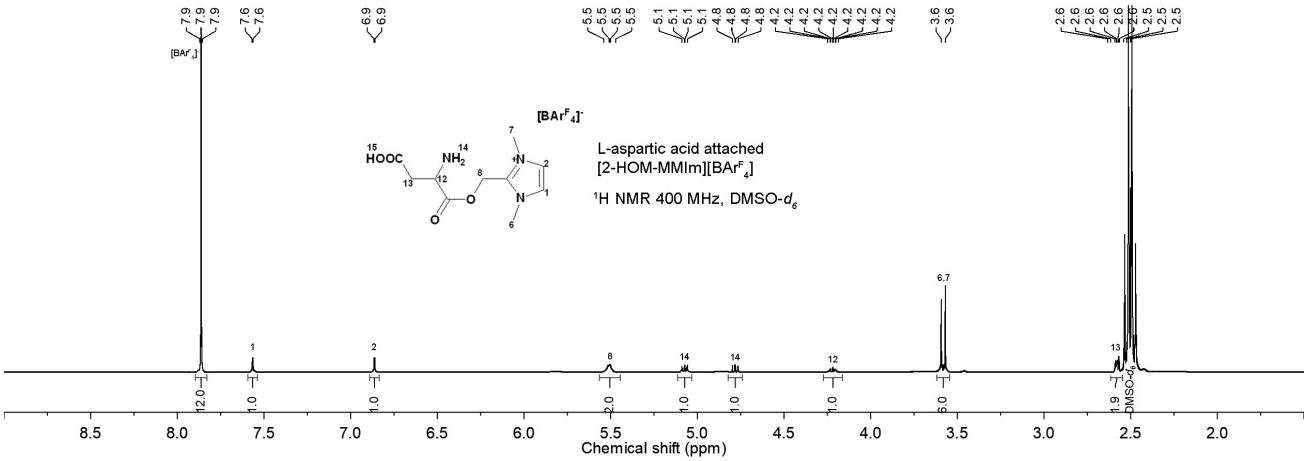

Figure **S13**. ^{1}H NMR spectrum of L-aspartic acid attached [2-HOM-MMIm][BAr^{F}_{4}] (400 MHz, DMSO-d_6, 0.3 mM, 22 °C), ESI-MS calculated for $C_{10}H_{16}N_3O_4$ $[M]^+$: 242.1135; Found: 242.1132.

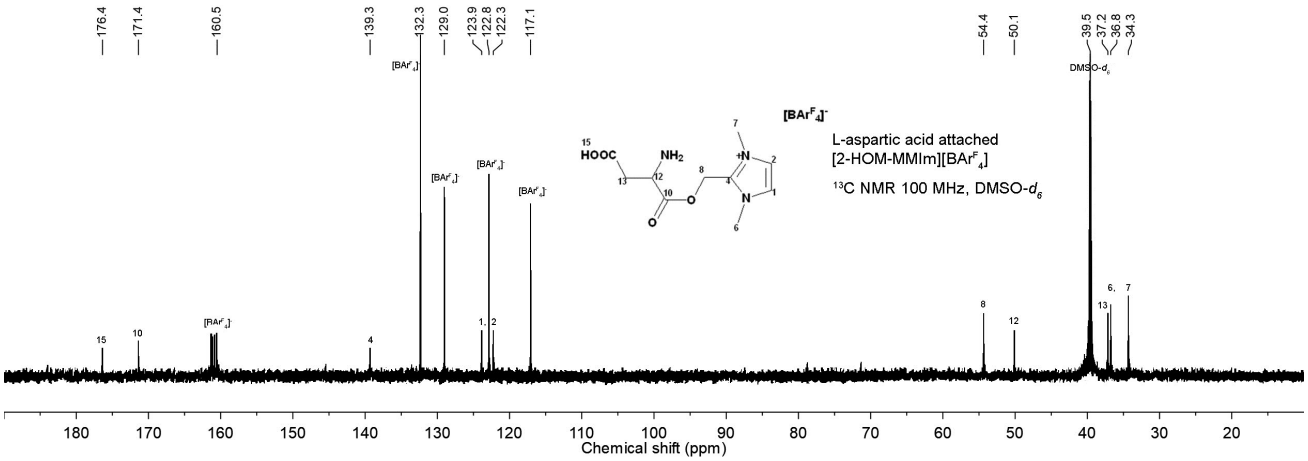

Figure **S14**. ^{13}C NMR spectrum of L-aspartic acid attached [2-HOM-MMIm][BAr^{F}_{4}] (100 MHz, DMSO-d_6, 0.3 mM, 22 °C).

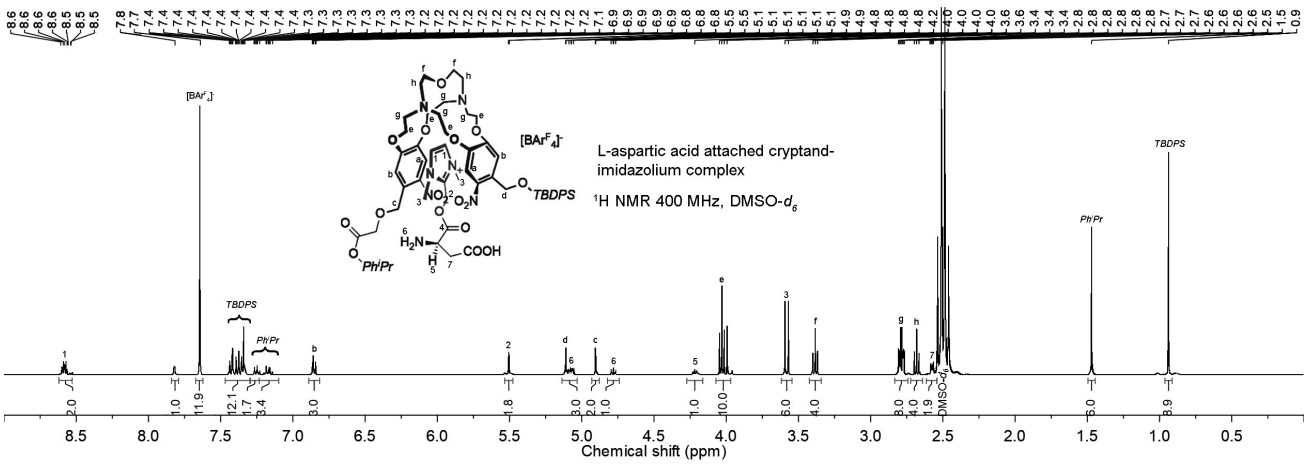

Figure **S15**. ^{1}H NMR spectrum of L-aspartic acid attached cryptand-imidazolium complex (400 MHz, DMSO-d_6, 0.3 mM, 22 °C), ESI-MS calculated for $C_{63}H_{80}N_7O_{17}Si$ $[M]^+$: 1234.5374; Found: 1234.5370.

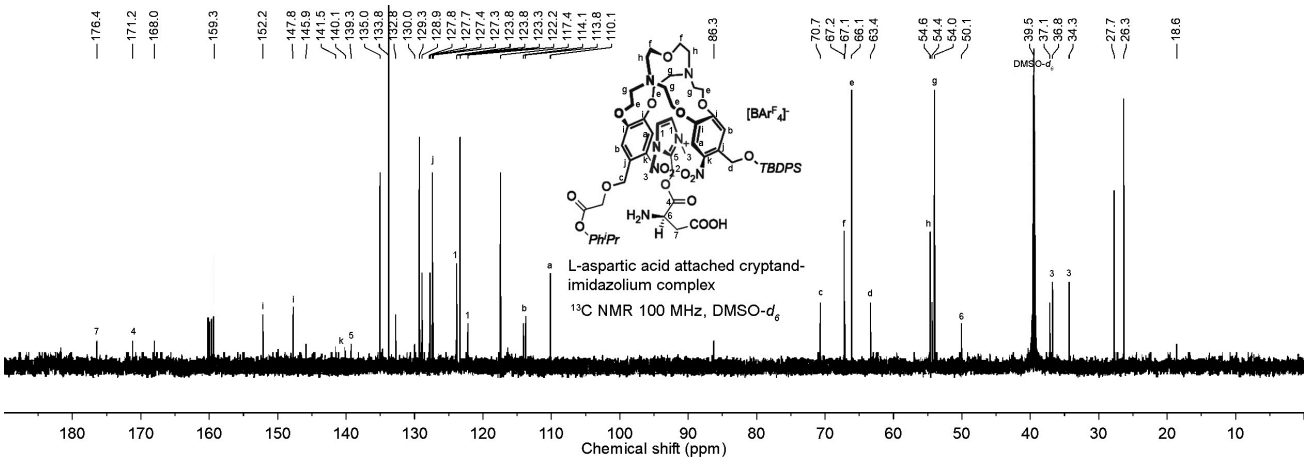

Figure **S16**. ^{13}C NMR spectrum of L-aspartic acid attached cryptand-imidazolium complex (100 MHz, DMSO-d_6, 0.3 mM, 22 °C).

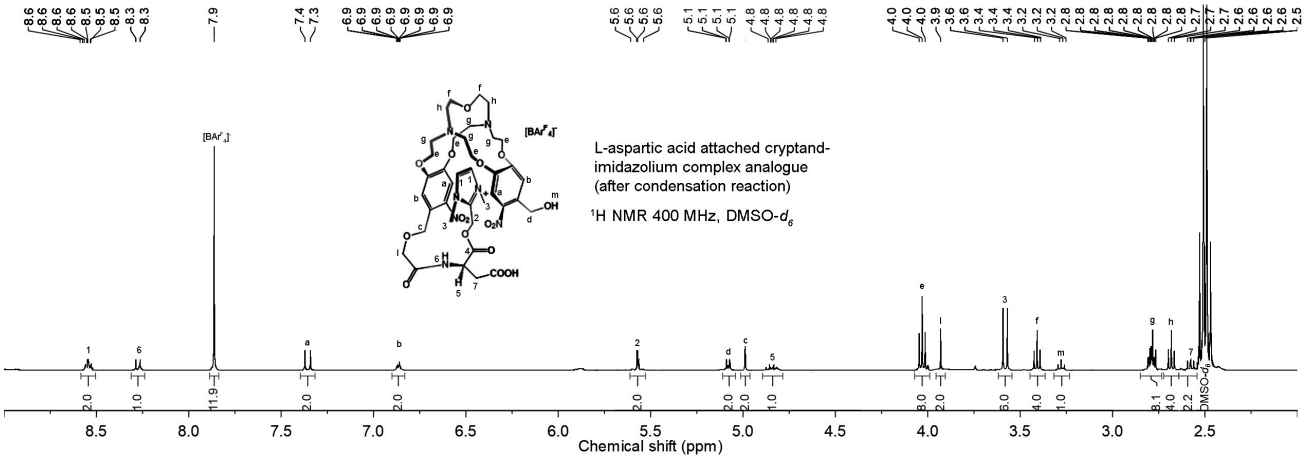

Figure **S17**. ^{1}H NMR spectrum of L-aspartic acid attached cryptand-imidazolium complex analogue (after condensation reaction) (400 MHz, DMSO-d_6, 0.3 mM, 22 °C), ESI-MS calculated for $C_{38}H_{50}N_7O_{16}$ $[M]^+$: 860.3309; Found: 860.3305.

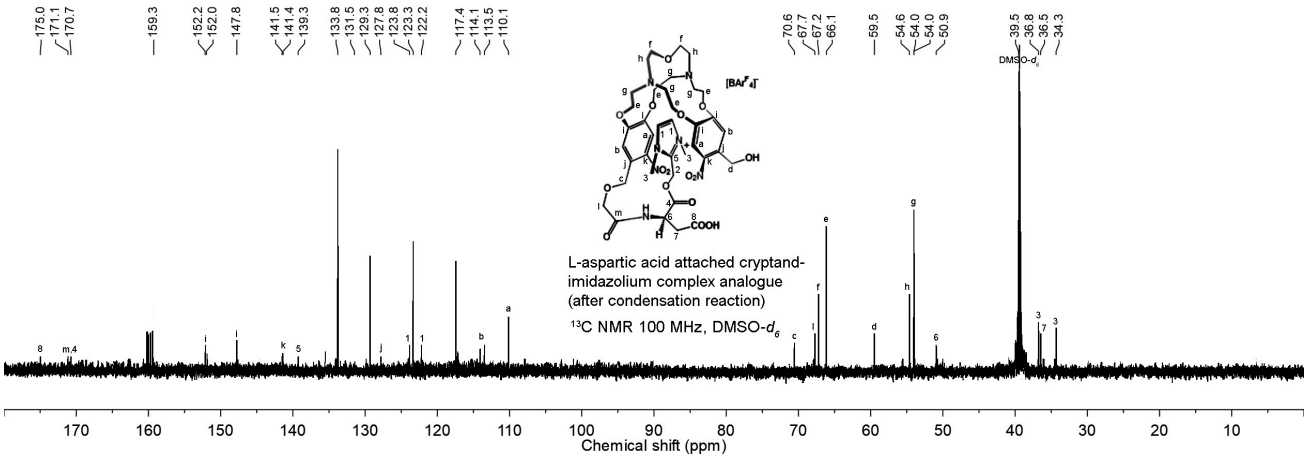

Figure **S18**. ^{13}C NMR spectrum of L-aspartic acid attached cryptand-imidazolium complex analogue (after condensation reaction) (100 MHz, DMSO-d_6, 0.3 mM, 22 °C).

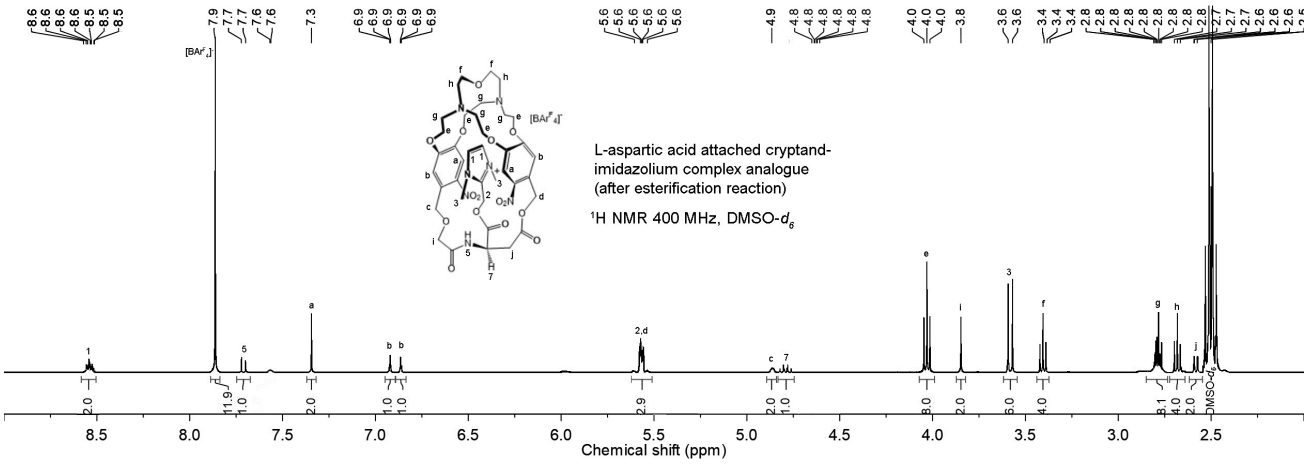

Figure **S19**. ^{1}H NMR spectrum of L-aspartic acid attached cryptand-imidazolium complex analogue (after esterification reaction) (400 MHz, DMSO-d_6, 0.3 mM, 22 °C), ESI-MS calculated for $C_{38}H_{48}N_7O_{15}$ $[M]^+$: 842.3203; Found: 842.3199.

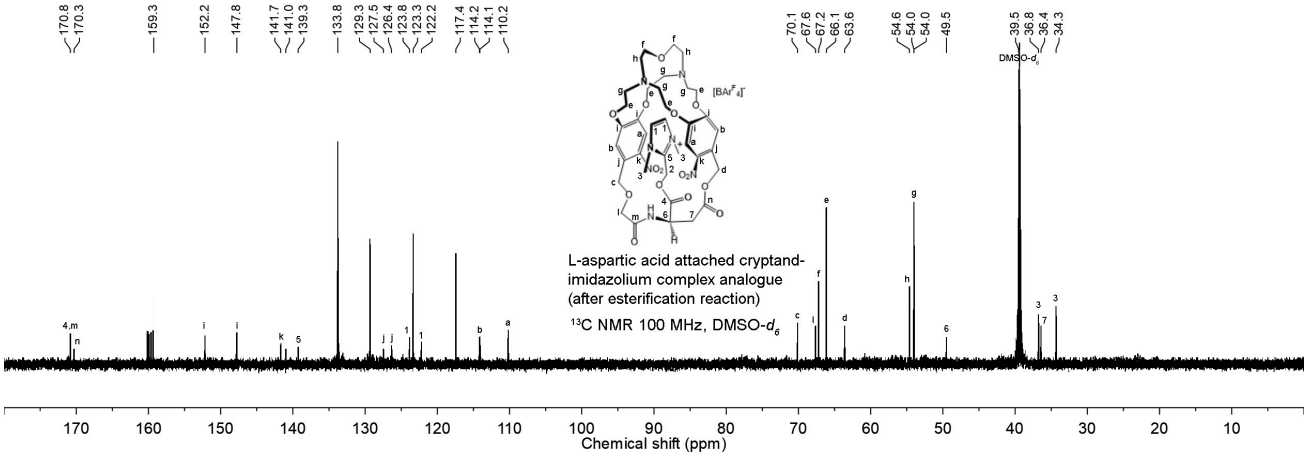

Figure **S20**. ^{13}C NMR spectrum of L-aspartic acid attached cryptand-imidazolium complex analogue (after esterification reaction) (100 MHz, DMSO-d_6, 0.3 mM, 22 °C).

Photolytic conversion of 1-nitroveratryloxycarbonyl(NVOC) protected-2H,3H-tryptophan into tryptophan

The *N*-Fmoc-1-NVOC protected 2*H*,3*H*-tryptophan (65.4 mg, 0.1 mmol) was first dissolved in 2-MeTHF (5.0 ml) to give a clear solution, which was placed in a 3.5 mL glass cuvette and exposed under ultraviolet irradiation for 45 minutes using a 150W Xe lamp (SCHOTT AG, Germany) with a 330-nm filter. The solution was evaporated under reduced pressure, washed with ether and dissolved in DCM (5.0 mL). Polymer-based piperazine (1.0 g, 1.0 mmol, 200-400 mesh, 1.0-2.0 mmol/g loading, 2% cross-linked with divinylbenzene) was added. The reaction mixture was stirred for 30 minutes and filtered. The filtrate was lyophilized to yield a white powder (43.8 mg, 99%). After lyophilization, the crude 1-NVOC protected 2*H*,3*H*-tryptophan was dissolved in water/acetonitrile (50:50) and purified by reversed-phase HPLC (gradient: 0-40% acetonitrile in water + 0.1% TFA, in 120 minutes). Fractions of 500 μL were examined by MS (ESI-MS calculated for $C_7H_{13}N_2O$

[M+H]$^+$: 205.0976; Found 205.0973) and NMR (Fig. S21). The results showed that the 1-NVOC protected 2*H*,3*H*-tryptophan has been converted into tryptophan instead of 2*H*,3*H*-tryptophan during the photolytic release of protecting group NVOC. Considering the photolytic mechanisms of NVOC and 1-acyl-7-nitroindolines[5,6], a provisional mechanism is given below, in which UV light leads to the radical decarboxylation of NVOC group and the cleavage of resulting 1,3-dihydrobenzo[c]isoxazole group promoted the dehydrogenation of indoline.

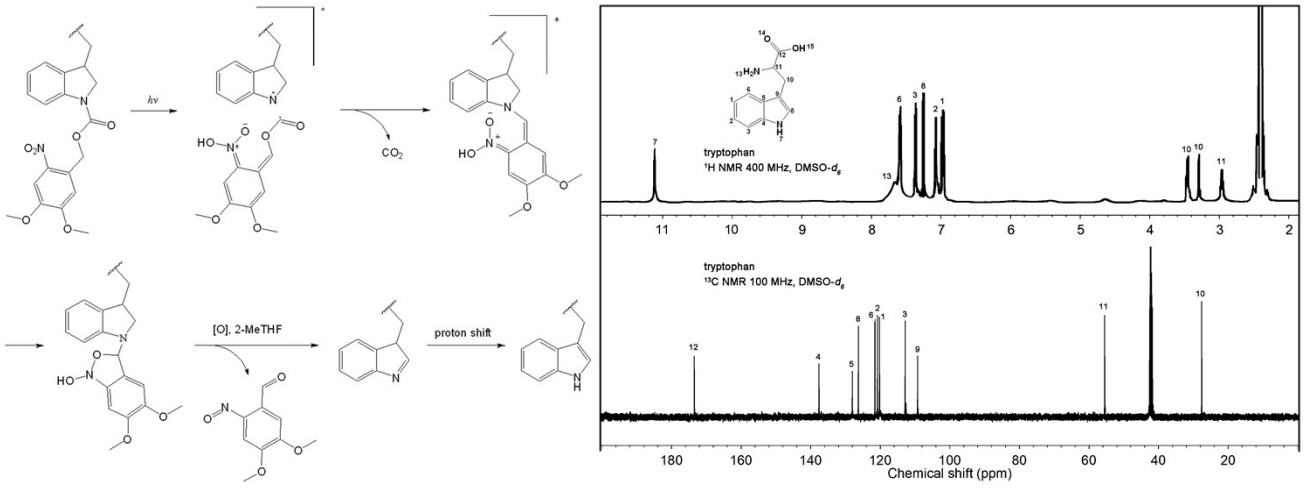

Figure **S21**. Postulated mechanism of photolytic conversion of 1-NVOC protected 2*H*,3*H*-tryptophan assembly and NMR spectra of the product tryptophan (DMSO-d_6, 0.6 mM, 22 °C).

Synthesis of unthreaded peptide topoisomer

Linear peptide **G**^{1}**LPWGCPSDIPGWNTPWAC**^{19} was prepared by stepwise Fmoc-SPPS on an Advanced ChemTech (ACT-396) automated peptide synthesizer on 2-chlorotrityl chloride resin (300.0 mg, 100-200 mesh, 1.06 mmol/g) with *in situ* activation protocols to couple Fmoc-protected amino acid (1.3 mmol, 4.0 eq. to resin loading) to the resin using PyBOP (676.5 mg, 1.3 mmol) as coupling reagent in the presence of *N*-methylmorpholine (0.29 mL, 263.0 mg, 2.6 mmol). The Fmoc group was deprotected with 20% piperidine/DMF. The side chain ODmab of residue **D**^{9} was selectively removed using 2% hydrazine in DMF. The cyclization *via* isopeptide bond between **G**^{1} and **D**^{9} was carried out using PyBOP (676.5 mg, 1.3 mmol) and *N*-methylmorpholine (0.29 mL, 263.0 mg, 2.6 mmol). Cyclized peptide was cleaved from the resin at room temperature in TFA/phenol/water/TIPS (88:5:5:2) for 3 hours. Cold diethyl ether was then added to the filtered cleavage mixture and the peptide precipitated out. Pure peptide (0.2 mM) was oxidized by stirring at room temperature in 0.1 M NH_4OAc/ DMF for 12 hours after washing with further cold diethyl ether. The oxidized peptide was purified by semipreparative reversed-phase HPLC equipped with a Waters XBridgeTM BEH3000 C18 column (4.6 × 150 mm) at a flow rate of 10.0 ml/min in 0-50% acetonitrile/0.1% TFA gradient and then lyophilized overnight.

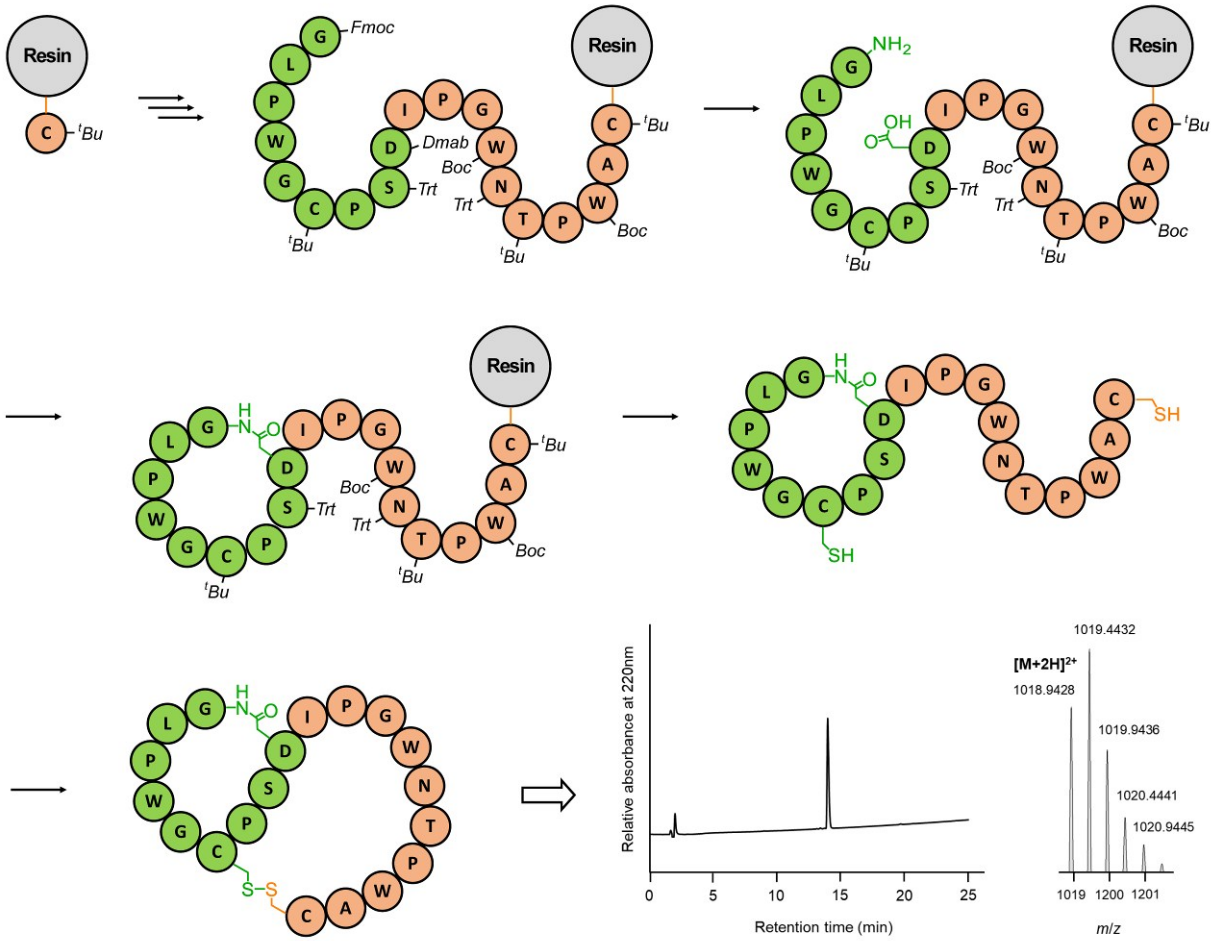

Figure **S22**. Synthesis of unthreaded topoisomer of BI-32169 (ESI-MS calculated for $C_{95}H_{125}N_{23}O_{24}S_2$ $[M+2H]^{2+}$: 1018.9433; Found 1018.9429).

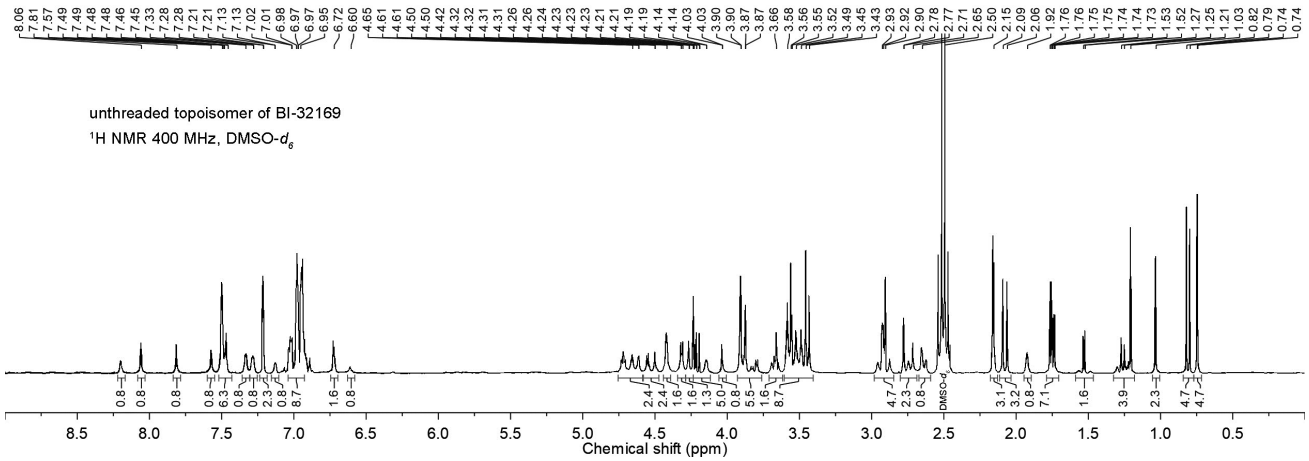

Figure **S23**. ^{1}H NMR spectrum of unthreaded topoisomer of BI-32169 (400 MHz, DMSO-d_6, 0.2 mM, 40 °C).

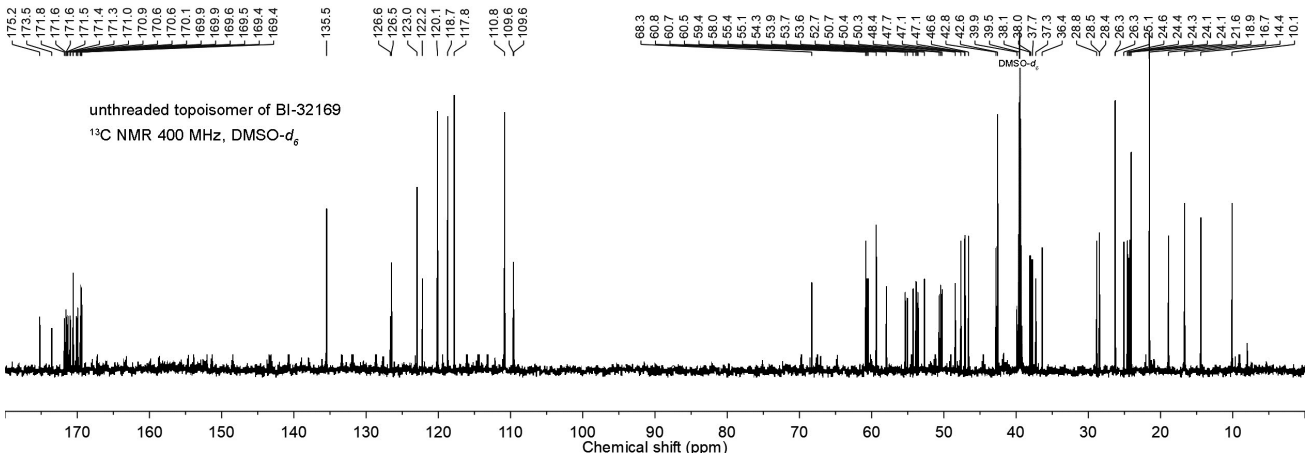

Figure **S24**. ^{13}C NMR spectrum of unthreaded topoisomer of BI-32169 (100 MHz, DMSO-d_6, 0.2 mM, 40 °C).

*Synthesis of **5** (first anchoring)*

Fmoc-L-cysteine(^{t}Bu)-OH (87.89 mg, 0.22 mmol), EDCI (46.58 mg, 0.30 mmol) and OxymaPure® (42.64 mg, 0.30 mmol) were first mixed in 2-MeTHF (10.0 mL) and allowed to stand for 15 minutes. Imidazolium salt **1** (198.08 mg, 0.20 mmol) and further 10.0 mL 2-MeTHF were added to give a clear solution. More 2-MeTHF might be replenished if precipitation occurred. The solution was stirred for 4 hours and washed with 20%(m/v) NaCl aqueous solution (~20.0 mL×4) and deionized water (~20.0 mL×2) in a separation funnel. The solution was concentrated under reduced pressure to give crude **5** (brown oil, 246.19 mg) (ESI-MS calculated for $C_{28}H_{34}N_3O_4S$ $[M]^+$: 508.2270; Found 508.2263).

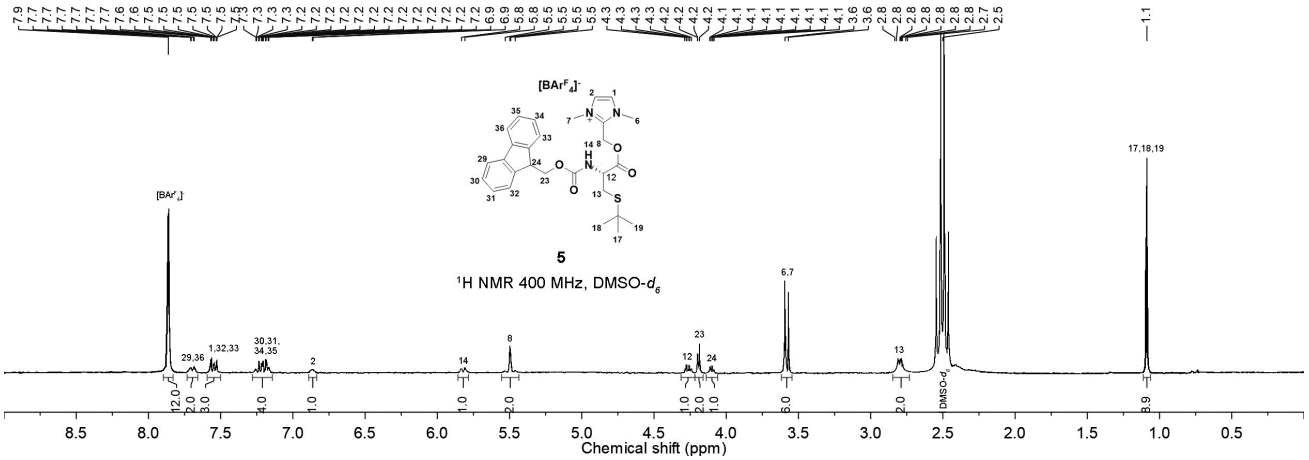

Figure **S25**. ^{1}H NMR spectrum of **5** (400 MHz, DMSO-d_6, 0.4 mM, 40 °C).

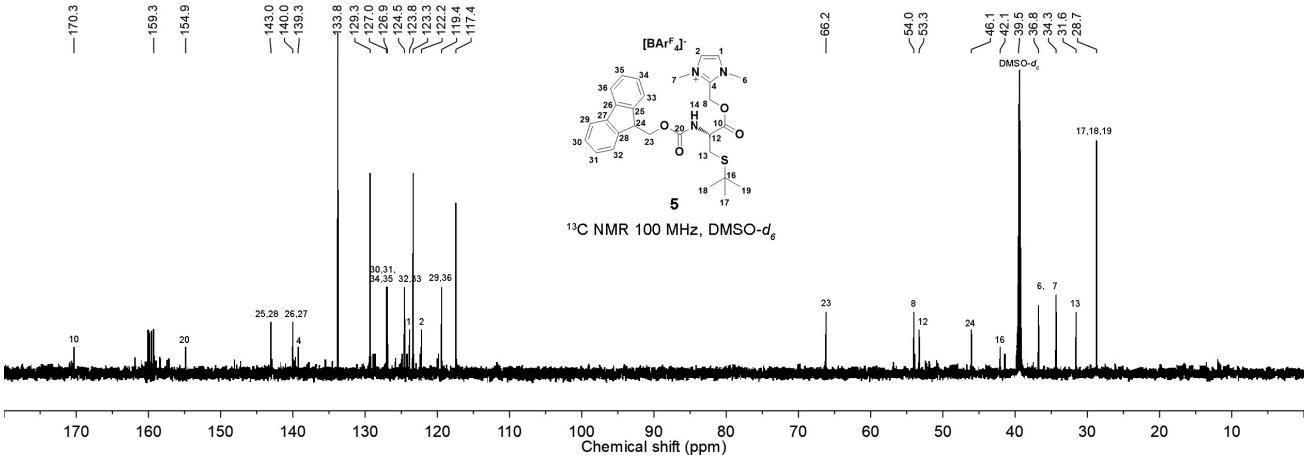

Figure **S26**. ^{13}C NMR spectrum of **5** (100 MHz, DMSO-d_6, 0.4 mM, 40 °C).

Synthesis of 7

Compound **5** was dissolved into 12.0 mL 2-MeTHF. TAEA (3.0 mL, 2924.6 mg, 20.0 mmol) was slowly added under stirring. The solution was kept under stirring for 15 more minutes and washed with a phosphate buffer (pH= 5.8, ~20.0 mL×2), 20%(m/v) NaCl aqueous solution (~20.0 mL×4) and deionized water (~20.0 mL×2). Fmoc-L-alanine-OH (68.50 mg, 0.22 mmol), EDCI (46.58 mg, 0.30 mmol) and OxymaPure® (42.64 mg, 0.30 mmol) were mixed in 2-MeTHF (10.0 mL) and allowed to stand for 15 minutes. The mixed reagents were then added into the solution. After 4 hours stirring, the solution was washed with 20%(m/v) NaCl aqueous solution (~20.0 mL×4) and deionized water (~20.0 mL×2) in a separation funnel. The solution was concentrated under reduced pressure to give crude **7** (brown oil, 245.96 mg) (ESI-MS calculated for $C_{31}H_{39}N_4O_5S$ $[M]^+$: 579.2641; Found 579.2635).

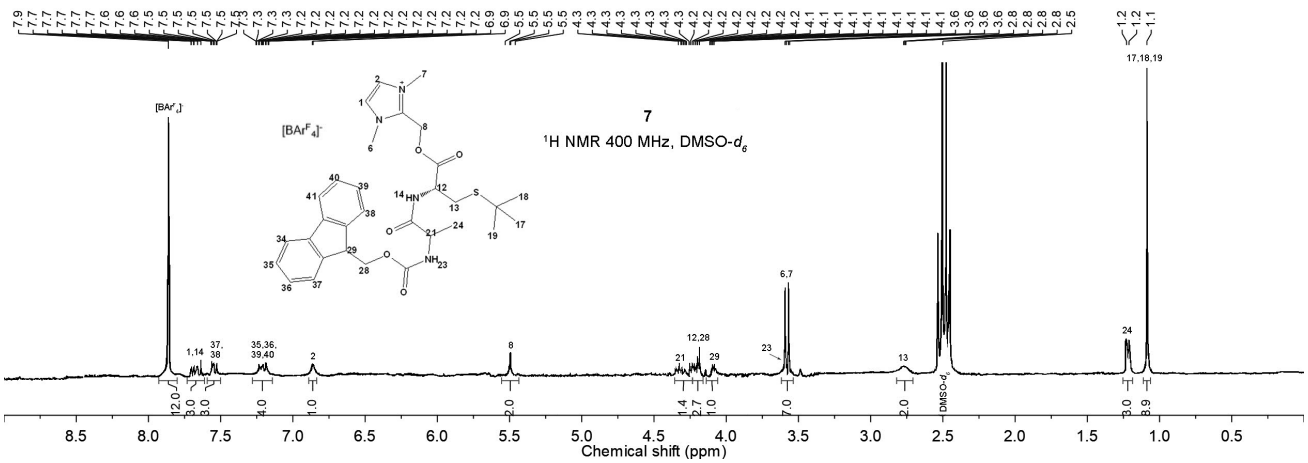

Figure **S27**. ^{1}H NMR spectrum of **7** (400 MHz, DMSO-d_6, 0.4 mM, 40 °C).

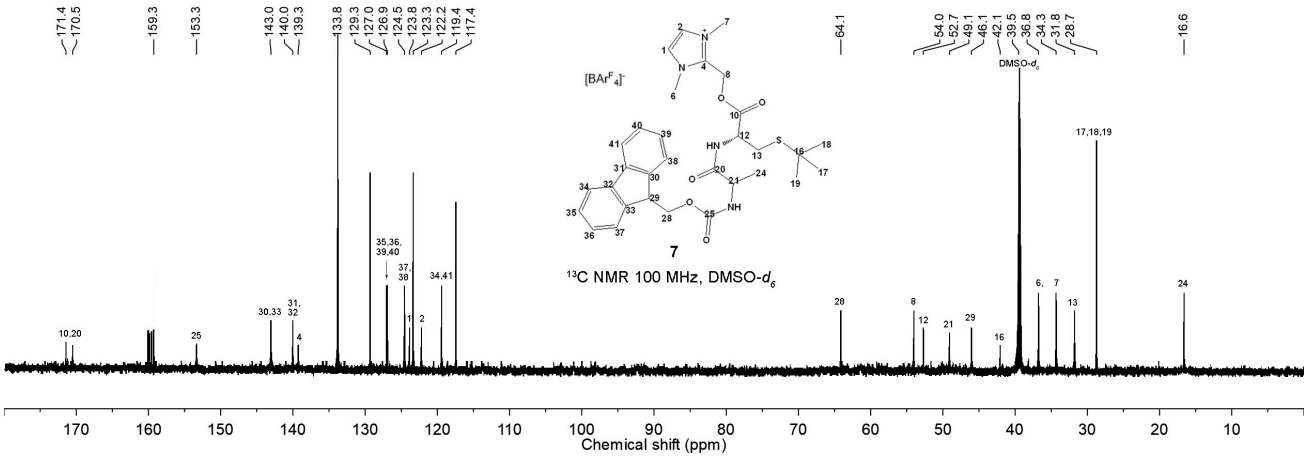

Figure **S28**. ^{13}C NMR spectrum of **7** (100 MHz, DMSO-d_6, 0.4 mM, 40 °C).

*Preparation of **8** (complexation of **7** with **2**)*

7 and cryptand **2** (203.60 mg, 0.21 mmol) were mixed in 20.0 mL 2-MeTHF under stirring. The solution was concentrated to 6.0-7.0 mL under reduced pressure and dropped slowly into 50.0 mL cold hexane. The resulting precipitate was filtered off, washed with cold hexane (~50.0 mL×4) and deionized water (~50.0 mL) and concentrated under reduced pressure to yield **8** (brown solid, 414.62 mg) (ESI-MS calculated for $C_{84}H_{103}N_8O_{18}SSi$ $[M]^+$: 1571.6880; Found 1571.6861).

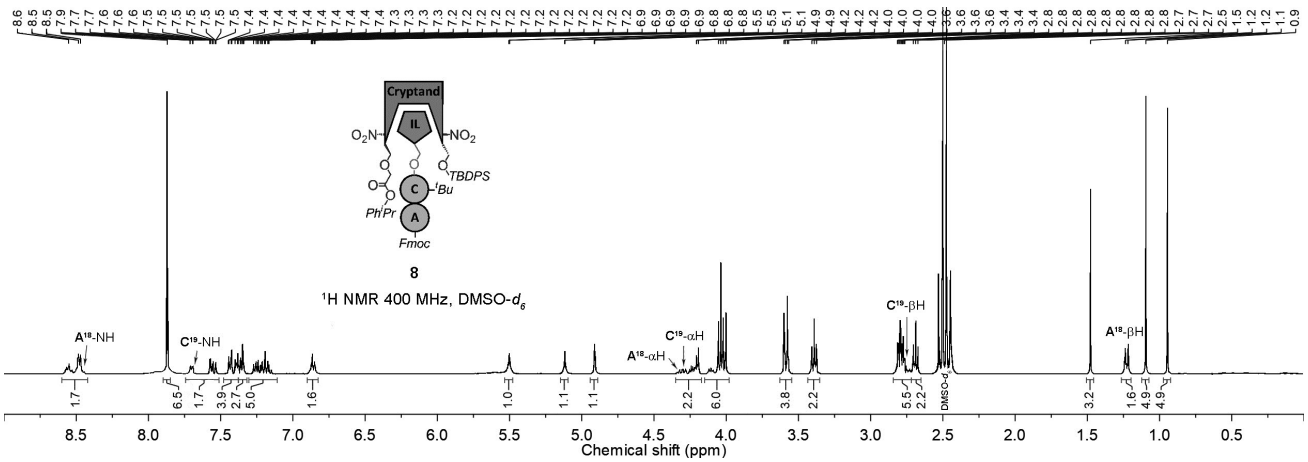

Figure **S29**. ^{1}H NMR spectrum of **8** (400 MHz, DMSO-d_6, 0.2 mM, 40 °C).

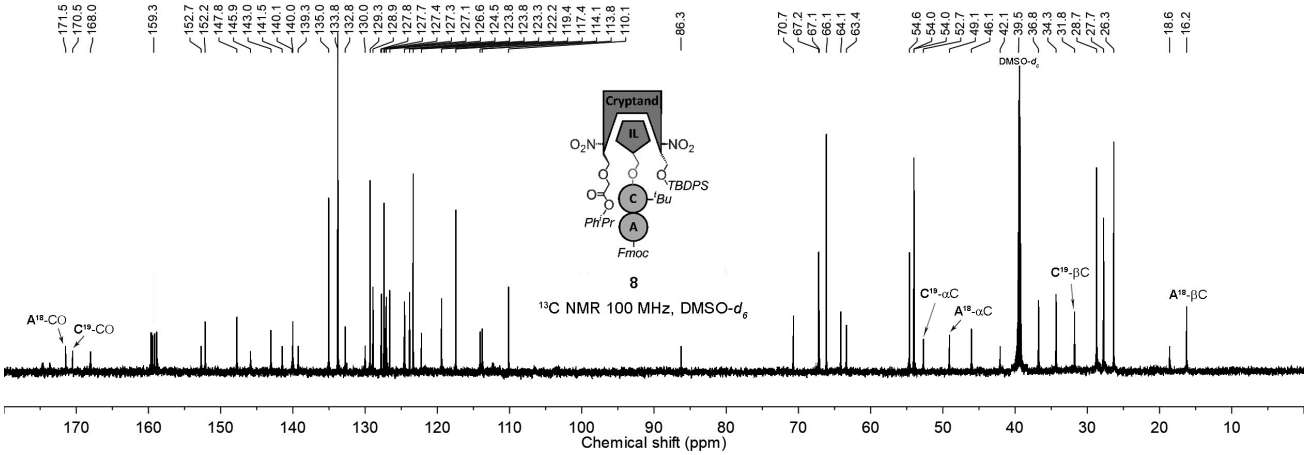

Figure **S30**. ^{13}C NMR spectrum of **8** (100 MHz, DMSO-d_6, 0.2 mM, 40 °C).

*Synthesis of **10** (second anchoring)*

Compound **9** was accomplished by sequential coupling of following protected amino acids: Fmoc-L-tryptophan(Boc)-OH (115.85 mg, 0.22 mmol), Fmoc-L-proline-OH (74.22 mg, 0.22 mmol), Fmoc-L-threonine(^{t}Bu)-OH (87.44 mg, 0.22 mmol), Fmoc-L-asparagine(Trt)-OH (131.27 mg, 0.22 mmol), Fmoc-L-tryptophan-OH (93.82 mg, 0.22 mmol), Fmoc-*L*-glycine-OH (65.41 mg, 0.22 mmol), Fmoc-L-proline-OH (74.22 mg, 0.22 mmol), Fmoc-*L*-isoleucine-OH (77.75 mg, 0.22 mmol), Fmoc-L-aspartic acid(Dmab)-OH (146.69 mg, 0.22 mmol) and Fmoc-L-serine(Trt)-OH (125.34 mg, 0.22 mmol). 2% TFA/2-MeTHF solution (30.0 mL) was added into the resulting solution at 0 °C. The reaction mixture was kept under stirring for 5 minutes at 0 °C and washed with 20%(m/v) NaCl aqueous solution (20.0 mL), 1.0 mM sodium hydroxide solution (~20.0 mL×2), 20%(m/v) NaCl aqueous solution (~20.0 mL×4) and deionized water (~20.0 mL×2). EDCI (93.16 mg, 6.0 mmol) and OxymaPure® (85.28 mg, 6.0 mmol) were added after washing. The solution was stirred for 12 hours, then washed with 1.0 mM calcium hydroxide solution (~20.0 mL×2) and centrifuged. The precipitate was filtered off, washed with 20%(m/v) NaCl aqueous solution (~20.0 mL×6) and deionized water (~20.0 mL×2) and concentrated under reduced pressure to yield **10** (brown solid, 307.81 mg) (ESI-MS calculated for $C_{183}H_{225}N_{22}O_{38}SSi$ $[M+H]^{2+}$: 1700.2934; Found 1700.2932).

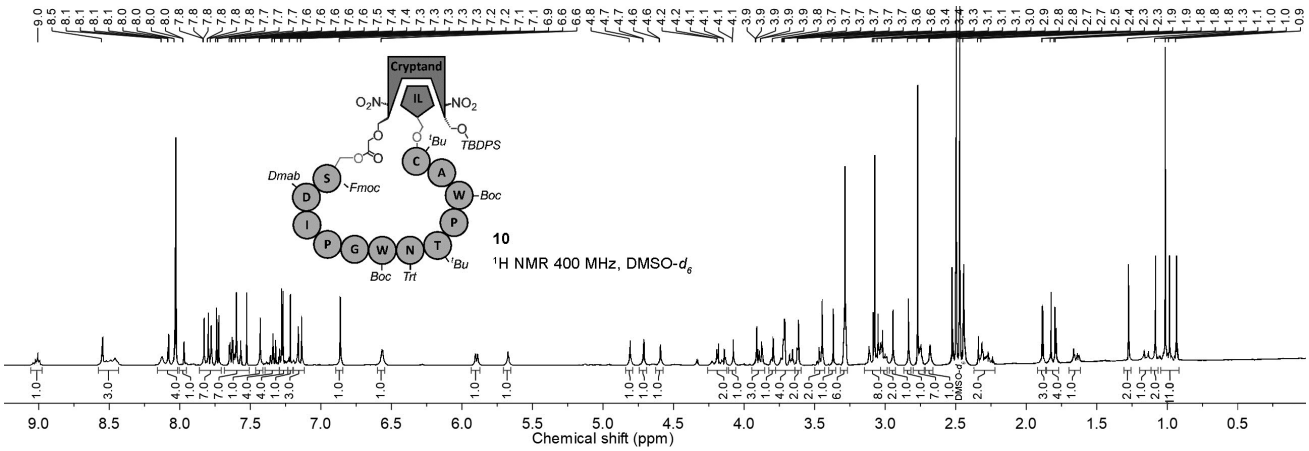

Figure **S31**. ^{1}H NMR spectrum of **10** (400 MHz, DMSO-d_6, 0.2 mM, 40 °C).

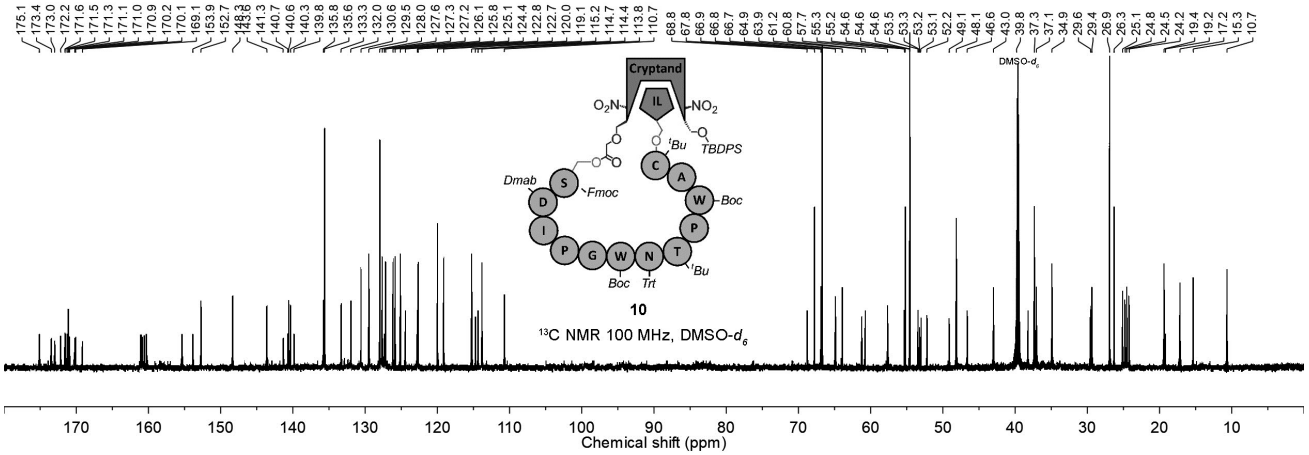

Figure **S32**. ^{13}C NMR spectrum of **10** (400 MHz, DMSO-d_6, 0.2 mM, 40 °C).

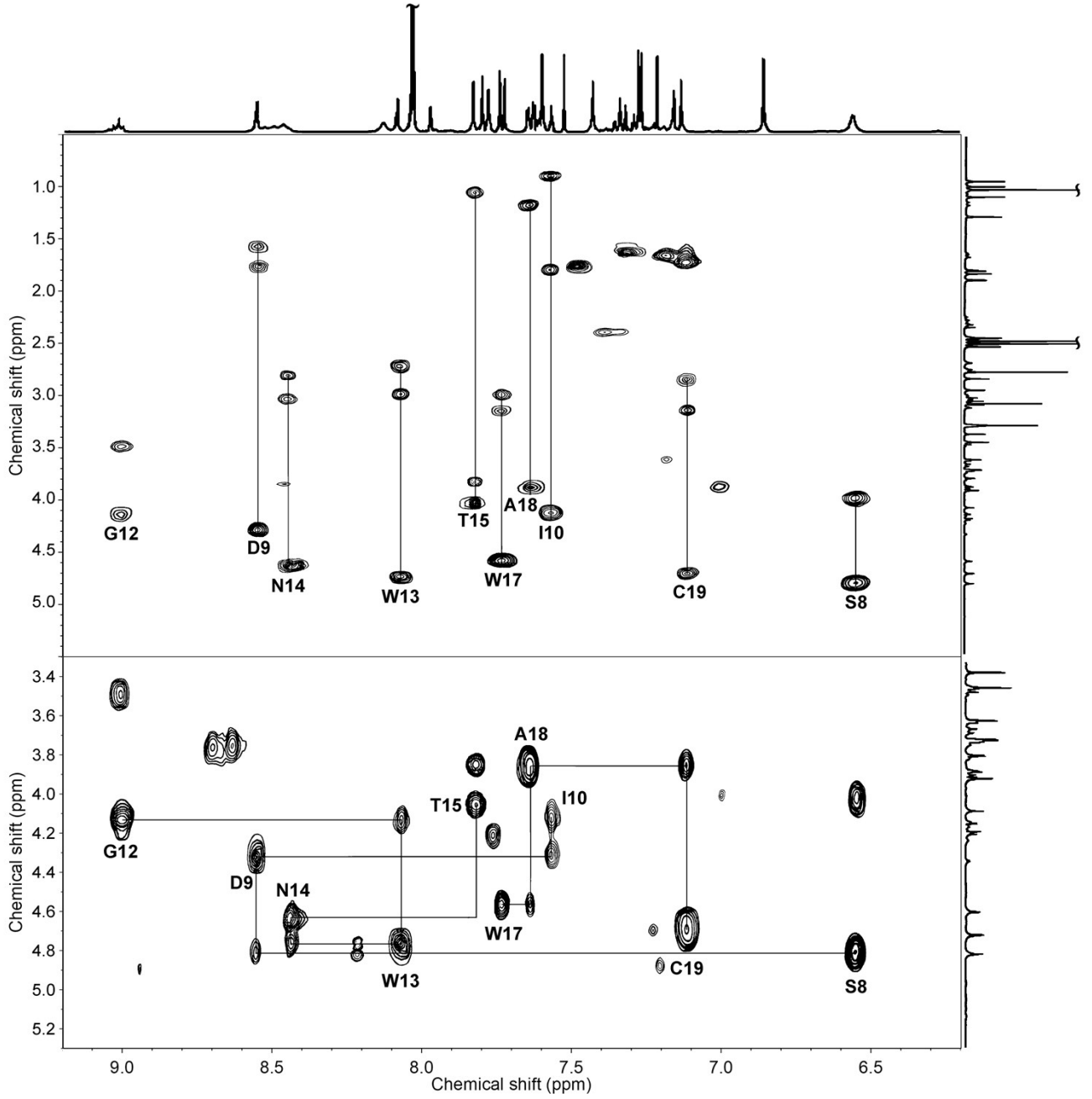

Figure **S33**. NMR spectra of compound **10** (400 MHz, DMSO-d_6, 0.2 mM, 40 °C). *Top*: TOCSY spectrum (100 ms). Amino acid spin systems are labeled. *Bottom*: Fingerprint region of the NOESY spectrum (150 ms) showing sequential connectivity between the residues.

*Synthesis of **12** (third anchoring)*

Compound **11** was accomplished by sequential coupling of following protected amino acids: Fmoc-L-proline-OH (74.22 mg, 0.22 mmol), Fmoc-L-cysteine(*t*Bu)-OH (87.89 mg, 0.22 mmol), Fmoc-L-glycine-OH (65.41 mg, 0.22 mmol) and Fmoc-L-2*H*,3*H*-1-carboxytryptophan(*p*NB)-OH (130.15 mg, 0.22 mmol). TBAF trihydrate (1893.0 mg, 6.0 mmol) in 2.0 mL 2-MeTHF was added dropwise into the resulting solution. The reaction mixture was kept under stirring for 8 hours. 5.0 g Dowex® 50WX8 (hydrogen form, 200-400 mesh), 1.6 g calcium carbonate and further 10.0 mL 2-MeTHF were added into the reaction mixture. The resulting suspension was stirred for 1 hour and then filtered. The organic phase was washed with a phosphate buffer (pH= 5.8, ~20.0 mL×3), 20%(m/v) NaCl aqueous solution (~20.0 mL×4) and deionized water (~20.0 mL×2). The attempt to join the free side chain of **W′**4 with the free linker of support using EDCI/OxymaPure® offered only a low crude yield of esterification (27% of **12**). Switching to other common combination of coupling reagents, such as *N,N′*-diisopropylcarbodiimide (DIC)/4-dimethylaminopyridine (DMAP) or benzotriazol-1-yl-oxytripyrrolidinophosphonium hexafluorophosphate (PyBOP)/*N,N*-diisopropylethylamine (DIPEA), did not alleviate this problem as well. The anchoring was then achieved by increasing the temperature to 37°C and conducting esterification twice as following described. EDCI (93.16 mg, 0.60 mmol) and OxymaPure® (85.28 mg, 0.60 mmol) were added. The reaction mixture was stirred for 12 hours at 37 °C, then washed with 1.0 mM calcium hydroxide solution (~20.0 mL×2) and centrifuged. The precipitate was filtered off and washed with 20%(m/v) NaCl aqueous solution (~20.0 mL×6) and deionized water (~20.0 mL×2). These anchoring and washing operations were repeated one more time. The solution was concentrated under reduced pressure to yield **12** (brown solid, 166.98 mg) (ESI-MS calculated for $C_{195}H_{246}N_{27}O_{41}S_2$ $[M+H]^{2+}$: 1844.3750; Found 1844.3748).

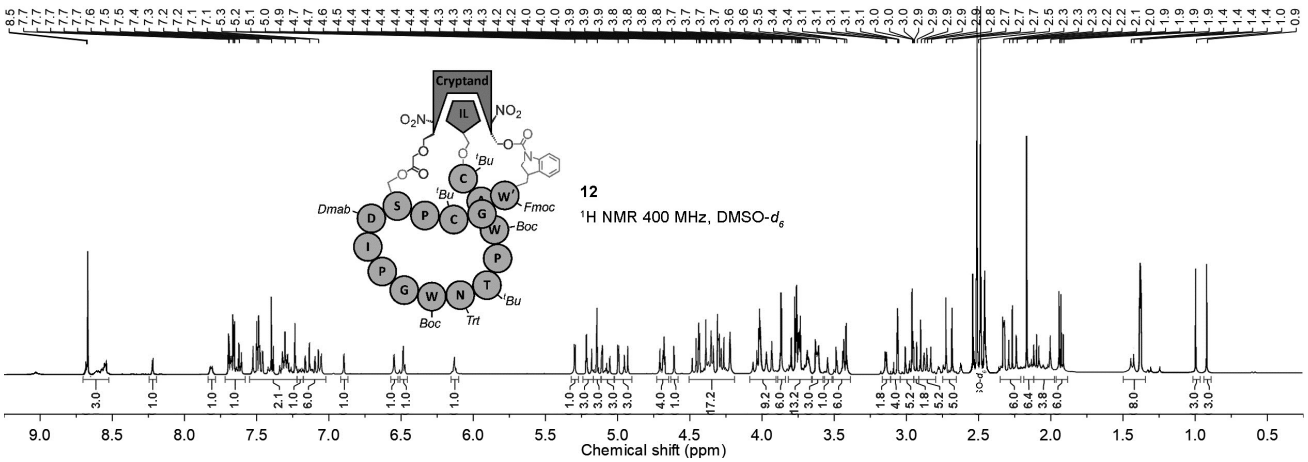

Figure **S34**. ^{1}H NMR spectrum of **12** (400 MHz, DMSO-d_6, 0.2 mM, 40 °C).

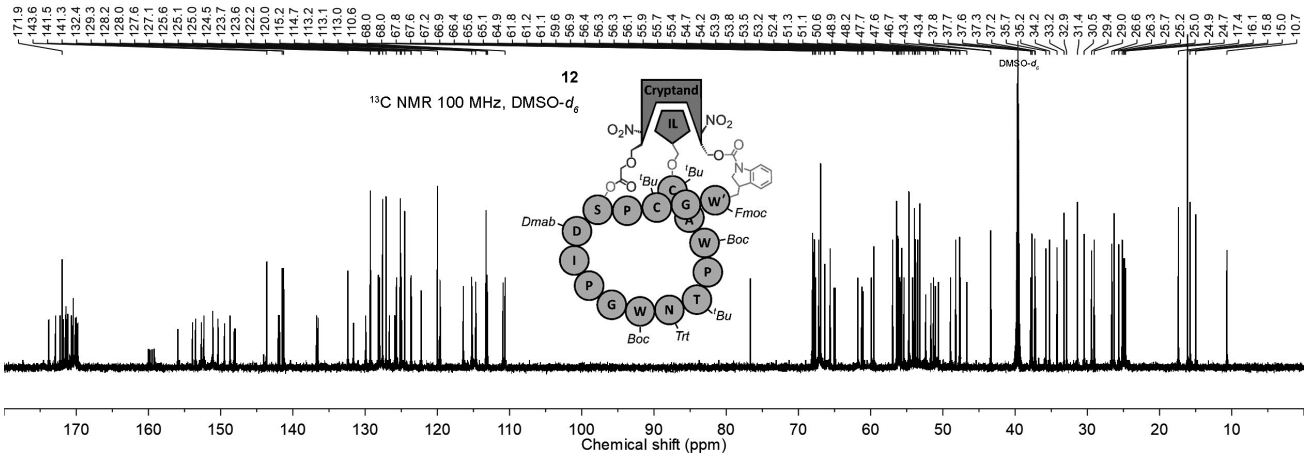

Figure **S35**. ^{13}C NMR spectrum of **12** (400 MHz, DMSO-d_6, 0.2 mM, 40 °C).

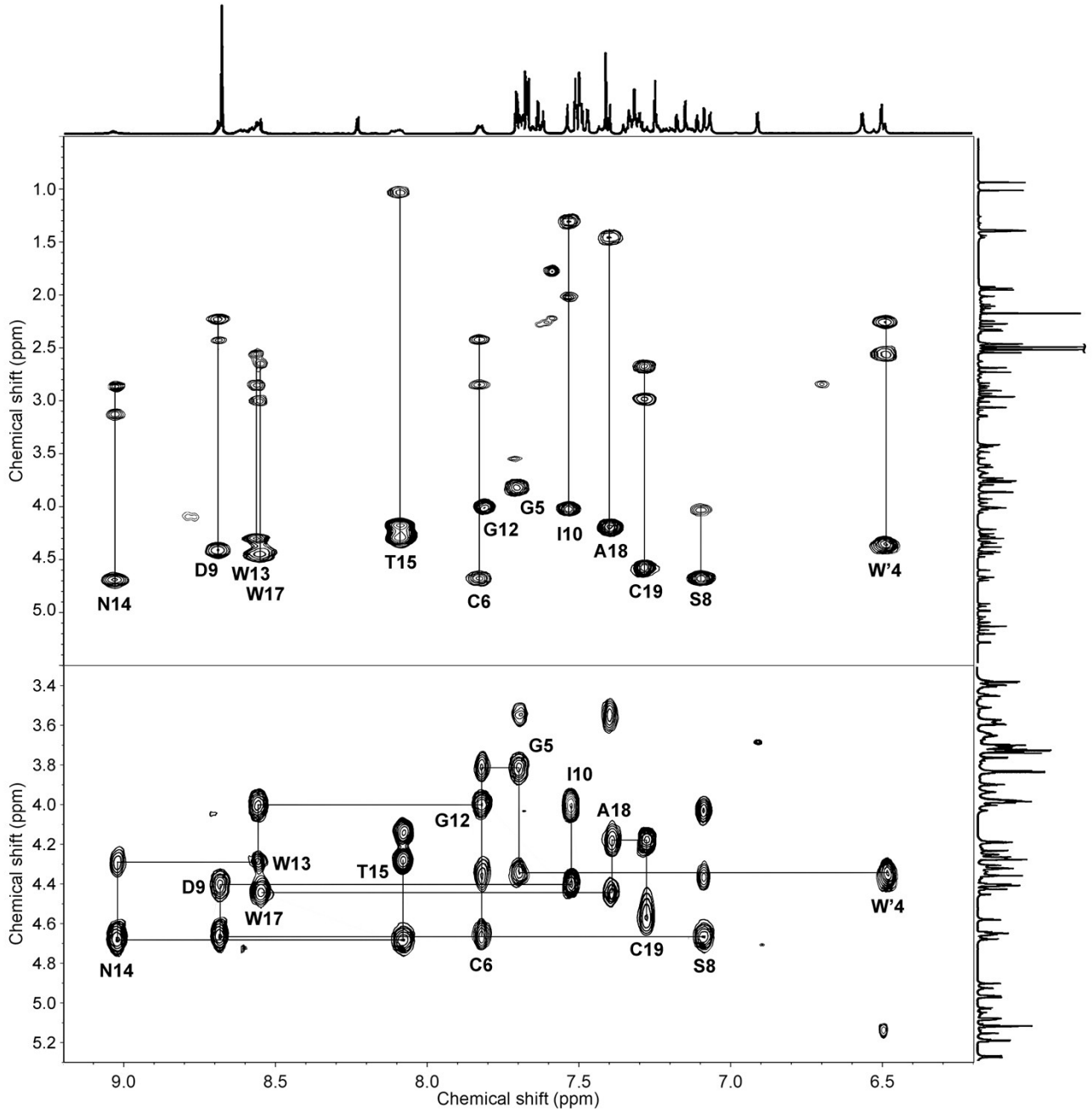

Figure **S36**. NMR spectra of compound **12** (400 MHz, DMSO-d_6, 0.2 mM, 40 °C). *Top*: TOCSY spectrum (100 ms). Amino acid spin systems are labeled. *Bottom*: Fingerprint region of the NOESY spectrum (150 ms) showing sequential connectivity between the residues.

*Synthesis of **14***

Compound **13** was accomplished by sequential coupling of following protected amino acids: Fmoc-L-proline-OH (74.22 mg, 0.22 mmol), Fmoc-L-leucine-OH (77.75 mg, 0.22 mmol) and Fmoc-L-glycine-OH (65.41, 0.22 mmol). 0.6 mL hydrazine (61.26 mg, 1.91 mmol) in 2.0 mL 2-MeTHF was added into the resulting solution. The reaction mixture was kept under stirring for 15 minutes and washed with a phosphate buffer (pH= 5.8, ~20.0 mL×3), 20%(m/v) NaCl aqueous solution (~20.0 mL×4), deionized water (~20.0 mL×2) and cold hexane (~50.0 mL×3). EDCI (93.16 mg, 0.60 mmol) and OxymaPure® (85.28 mg, 0.60 mmol) were then added. The reaction mixture was stirred for 12 hours and washed with 20%(m/v) NaCl aqueous solution (~20.0 mL×6) and deionized water (~20.0 mL×2). The solution was concentrated under reduced pressure to yield **14** (brown solid, 109.11 mg) (ESI-MS calculated for $C_{171}H_{224}N_{29}O_{41}S_2$ $[M+H]^{2+}$: 1702.7903; Found 1702.7901).

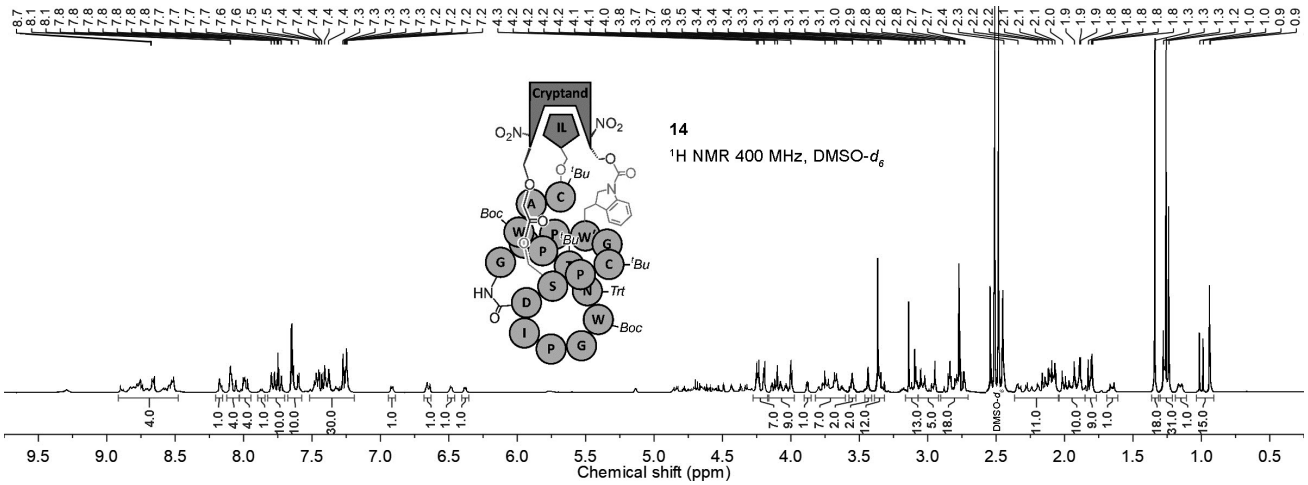

Figure **S37**. ^{1}H NMR spectrum of **14** (400 MHz, DMSO-d_6, 0.2 mM, 40 °C).

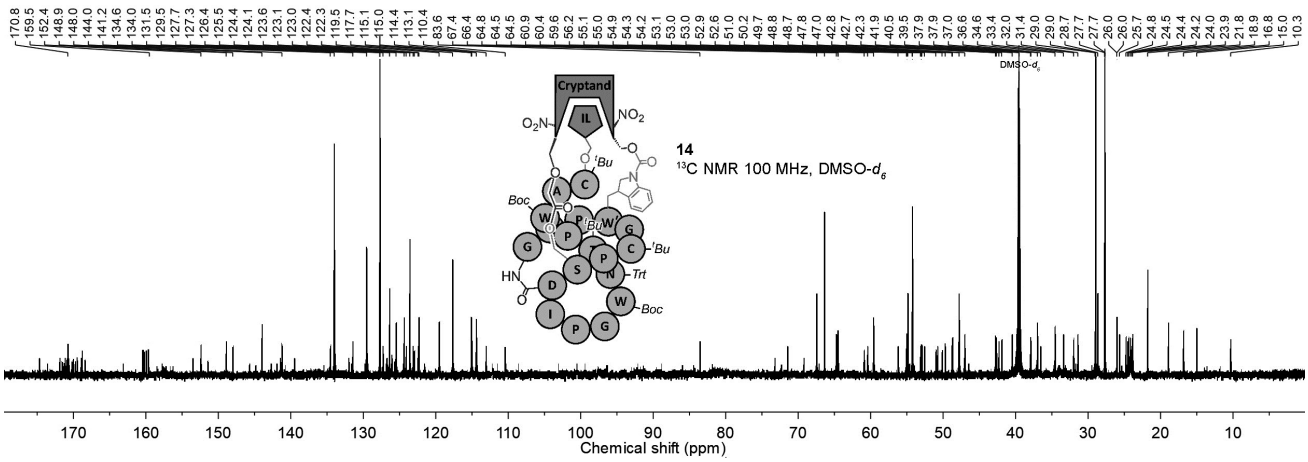

Figure **S38**. ^{13}C NMR spectrum of **14** (400 MHz, DMSO-d_6, 0.2 mM, 40 °C).

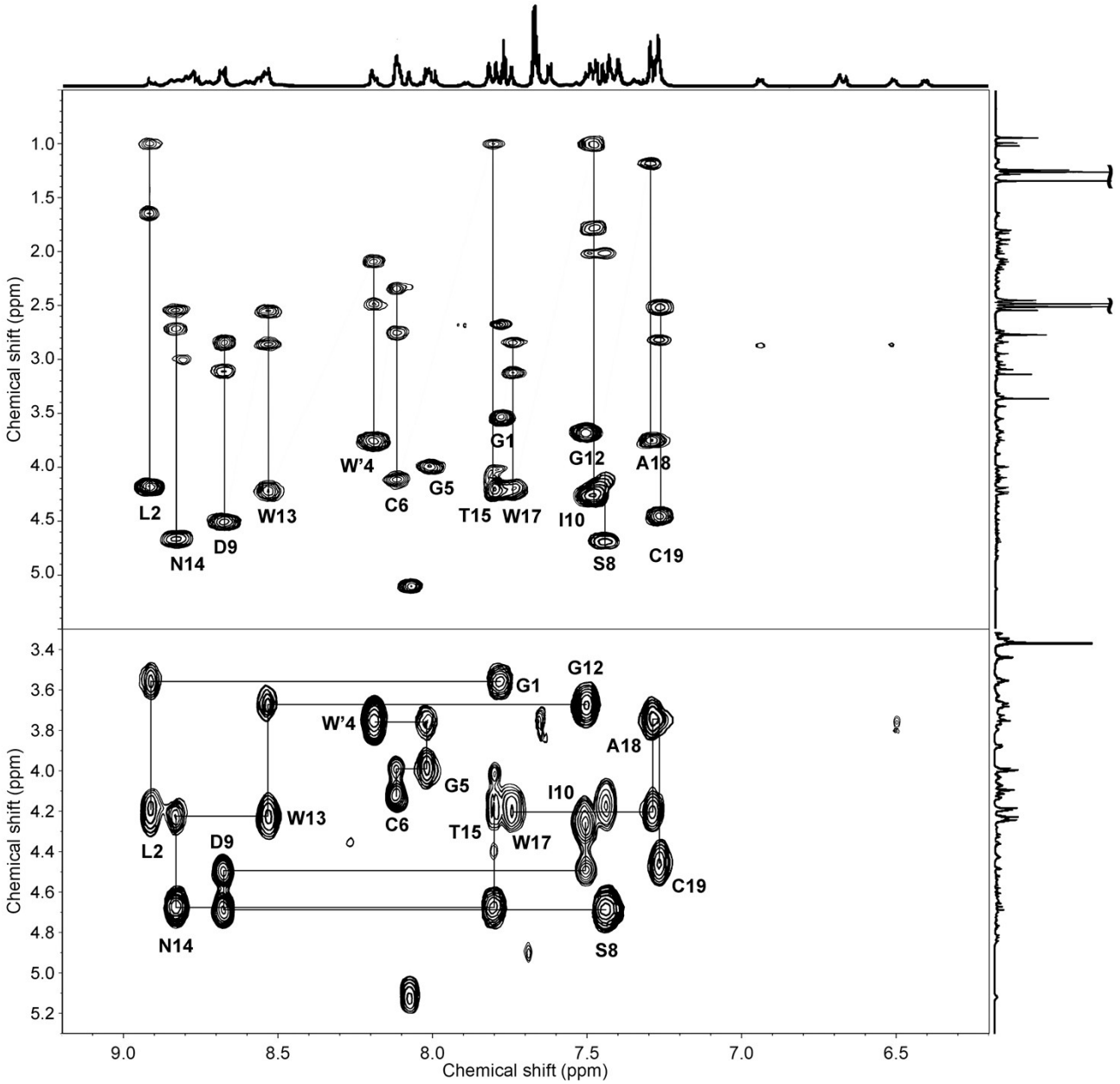

Figure **S39**. NMR spectra of compound **14** (400 MHz, DMSO-d_6, 0.2 mM, 40 °C). *Top*: TOCSY spectrum (100 ms). Amino acid spin systems are labeled. *Bottom*: Fingerprint region of the NOESY spectrum (150 ms) showing sequential connectivity between the residues.

Peptide-liberation

Compound **14** was dissolved in 2-MeTHF (10.0 ml) and prewarmed to ~30°C to give a clear solution, which was placed in a 14.0 ml ES quartz glass cuvette (45mm × 42.5mm × 12.5mm) and exposed under ultraviolet irradiation in a 30°C water bath for 45 minutes using a 150W Xe lamp (SCHOTT AG, Germany) with a 330-nm filter. The solution was evaporated under reduced pressure and washed with cold hexane (~50.0 mL×4). The washed residue was then dissolved in 10.0 mL

TFA/phenol/water/TIPS (88:5:5:2) under argon atmosphere. A certain amount of dichloromethane might be added if the peptide was not fully dissolved. The reaction mixture was stirred for 15 minutes and dropped slowly into 100.0 mL cold hexane (50.0 mL×2). It should be noted that cold ether is not applicable for separation due to its high dissolving capability for the compounds with [BAr^F_4] anion. The resulting precipitate was separated by centrifugation, washed with deionized water (~50.0 mL) and cold hexane (~50.0 mL×6), and concentrated under reduced pressure to yield **15** (brown solid, 69.62 mg, ESI-MS calculated for $C_{127}H_{166}N_{29}O_{34}S_2$ $[M]^+$: 2705.1594; Found 2705.1548). Compound **15** and sodium hydroxide (20.00 mg, 0.50 mmol) were dissolved in THF/H_2O (3:1, 5.0 mL). In this step, utilizing a higher concentration (1.0 M) solution of sodium hydroxide could obviously shorten the liberation time, yet led to an undesirable opening of the *N*-terminal ring and thus destroyed the lasso conformation. The mixture was then stirred under argon atmosphere for 6 hours and then exposed to air for 12 hours. The solution was acidified to pH= ~6.0 with 0.1 M aqueous citric acid and evaporated under reduced pressure. The resulting substance was washed with deionized water (50.0 mL×2) and ether (50.0 mL×6) to yield crude BI-32169 (42.81 mg). The characterization of purified synthetic BI-32169 (10.064 mg, 50 μmol, 2.47%, white solid) is described in next chapters.

Synthesis of D-enantiomer of BI-32169

The peptide D-enantiomer of BI-32169 was synthesized using cryptand **16** and corresponding D-amino acids in the same manner as BI-32169 (Figure S40-S54). The characterization of D-BI-32169 is described in next chapters.

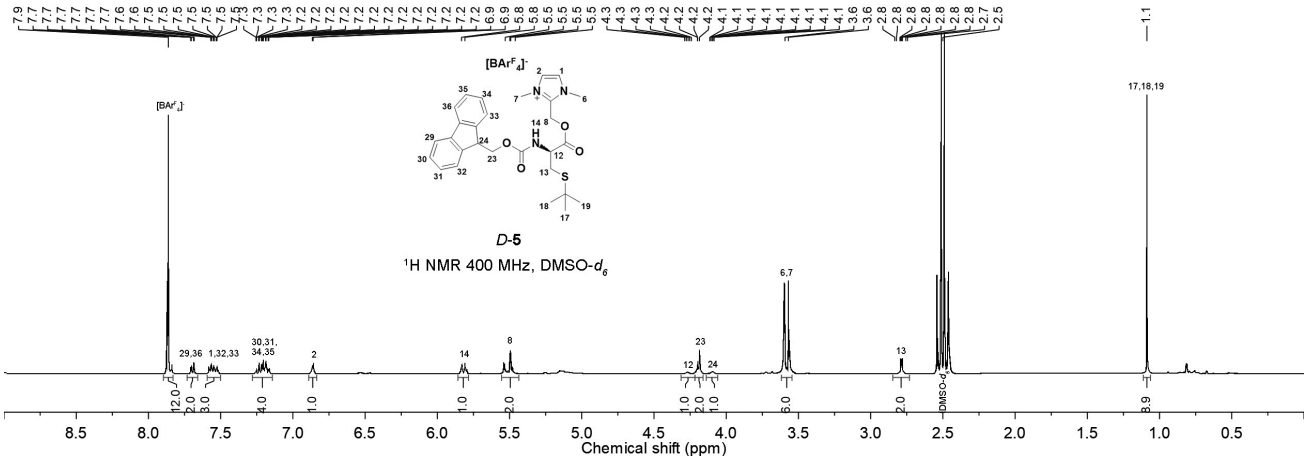

Figure **S40**. ^{1}H NMR spectrum of D-enantiomer of **5** (400 MHz, DMSO-d_6, 0.4 mM, 40 °C); ESI-MS calculated for $C_{28}H_{34}N_3O_4S$ $[M]^+$: 508.2270; Found 508.2264.

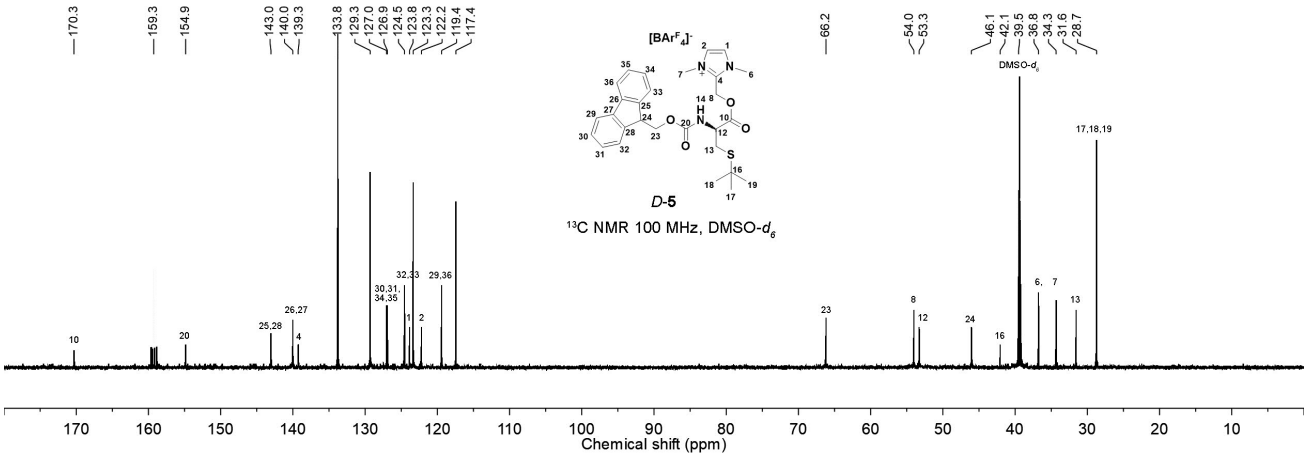

Figure **S41**. ^{13}C NMR spectrum of D-enantiomer of **5** (400 MHz, DMSO-d_6, 0.4 mM, 40 °C).

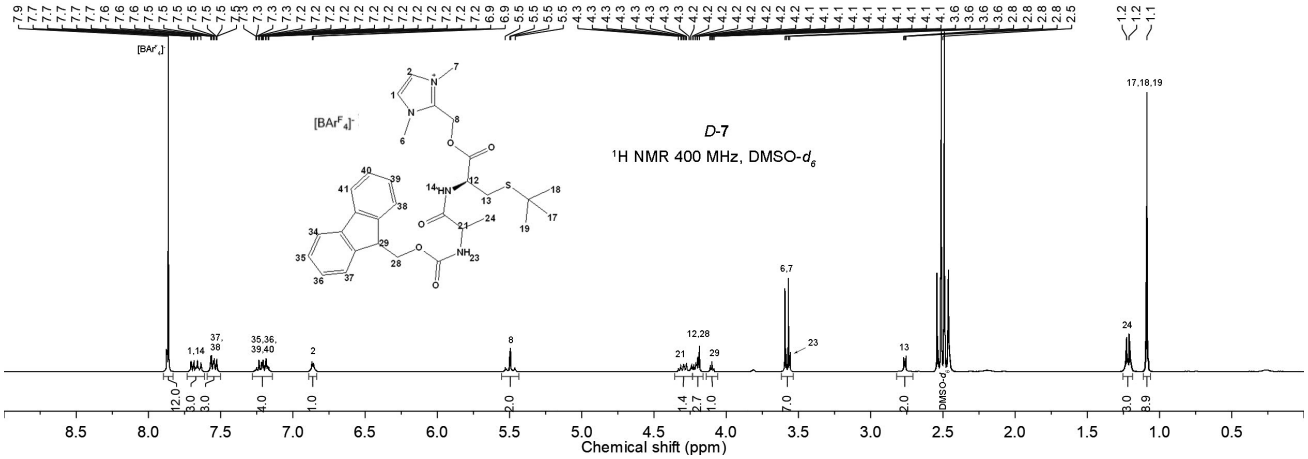

Figure **S42**. ^{1}H NMR spectrum of D-enantiomer of **7** (400 MHz, DMSO-d_6, 0.4 mM, 40 °C), ESI-MS calculated for $C_{31}H_{39}N_4O_5S$ $[M]^+$: 579.2641; Found 579.2639.

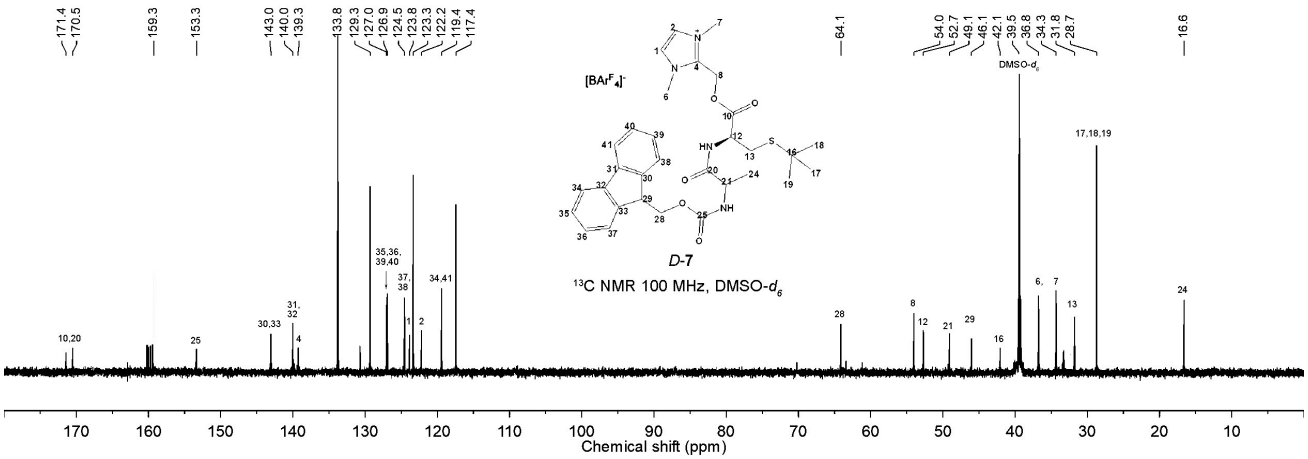

Figure **S43**. ^{13}C NMR spectrum of D-enantiomer of **7** (400 MHz, DMSO-d_6, 0.4 mM, 40 °C).

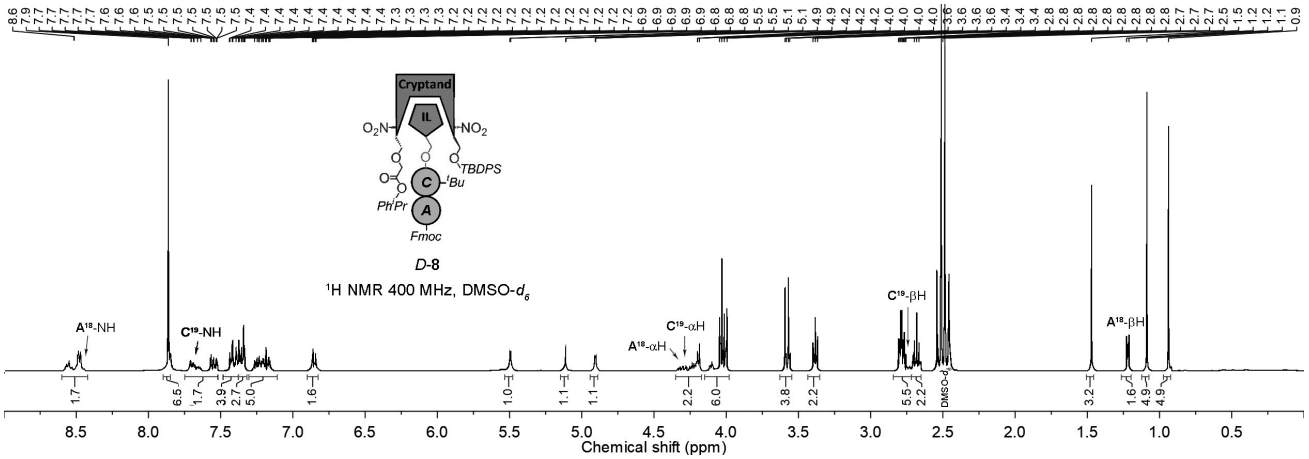

Figure **S44**. ^{1}H NMR spectrum of D-enantiomer of **8** (400 MHz, DMSO-d_6, 0.2 mM, 40 °C), ESI-MS calculated for $C_{84}H_{103}N_8O_{18}SSi$ $[M]^+$: 1571.6880; Found 1571.6867.

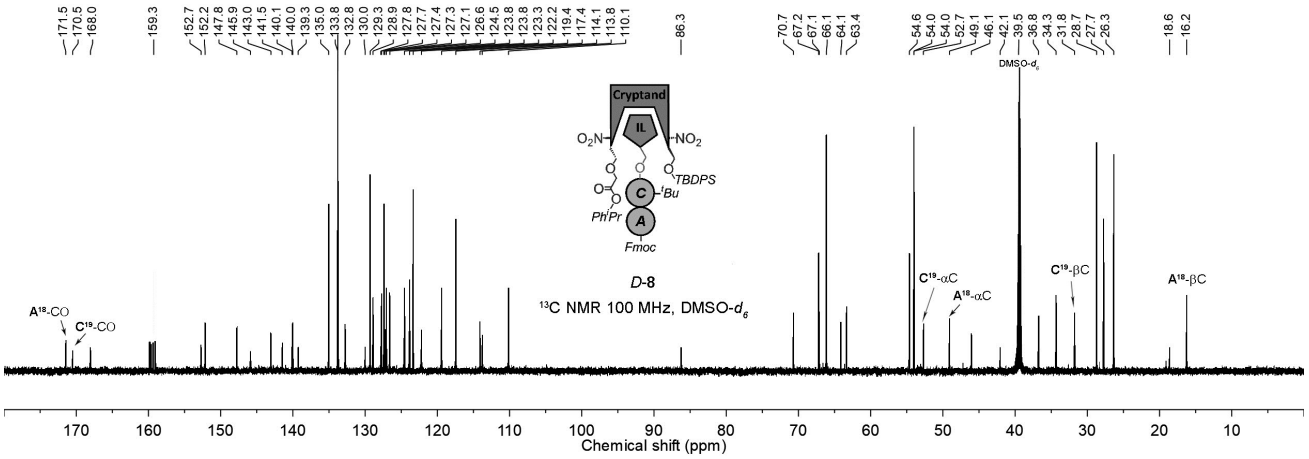

Figure **S45**. ^{13}C NMR spectrum of D-enantiomer of **8** (400 MHz, DMSO-d_6, 0.2 mM, 40 °C).

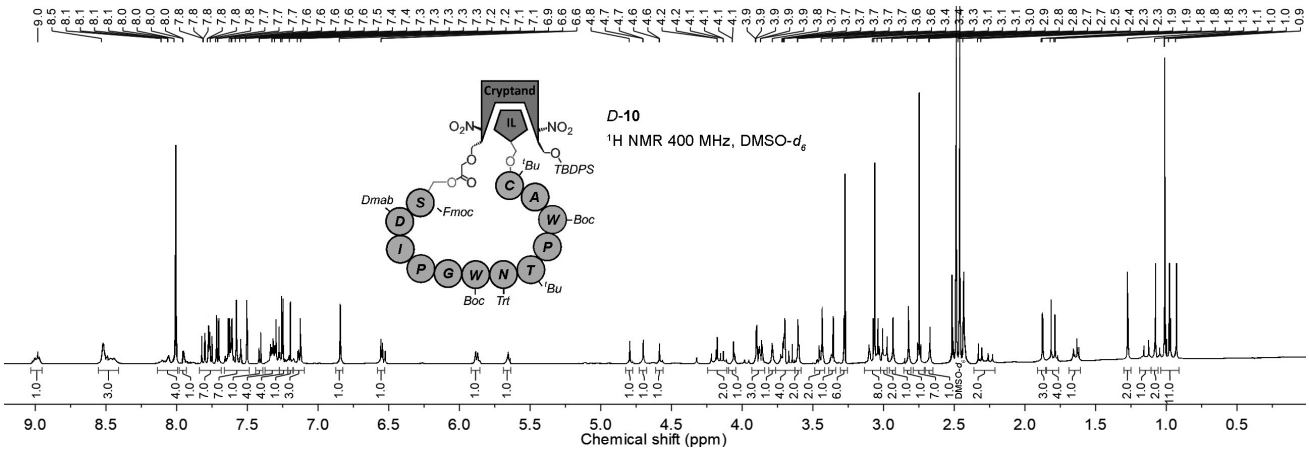

Figure **S46**. ^{1}H NMR spectrum of D-enantiomer of **10** (400 MHz, DMSO-d_6, 0.2 mM, 40 °C), ESI-MS calculated for $C_{183}H_{225}N_{22}O_{38}SSi$ $[M+H]^{2+}$: 1700.2934; Found 1700.2930.

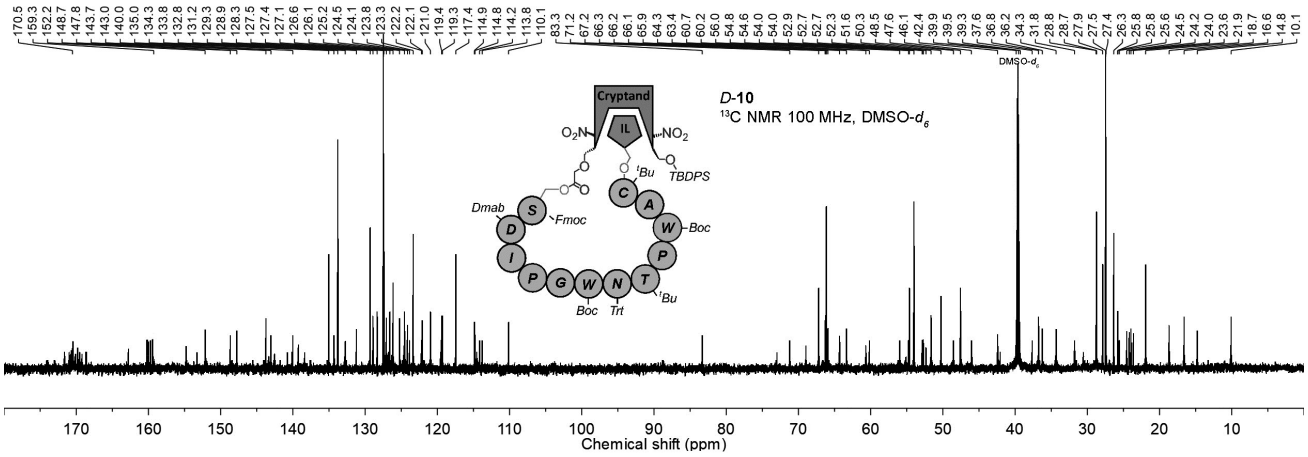

Figure **S47**. ^{13}C NMR spectrum of D-enantiomer of **10** (400 MHz, DMSO-d_6, 0.2 mM, 40 °C).

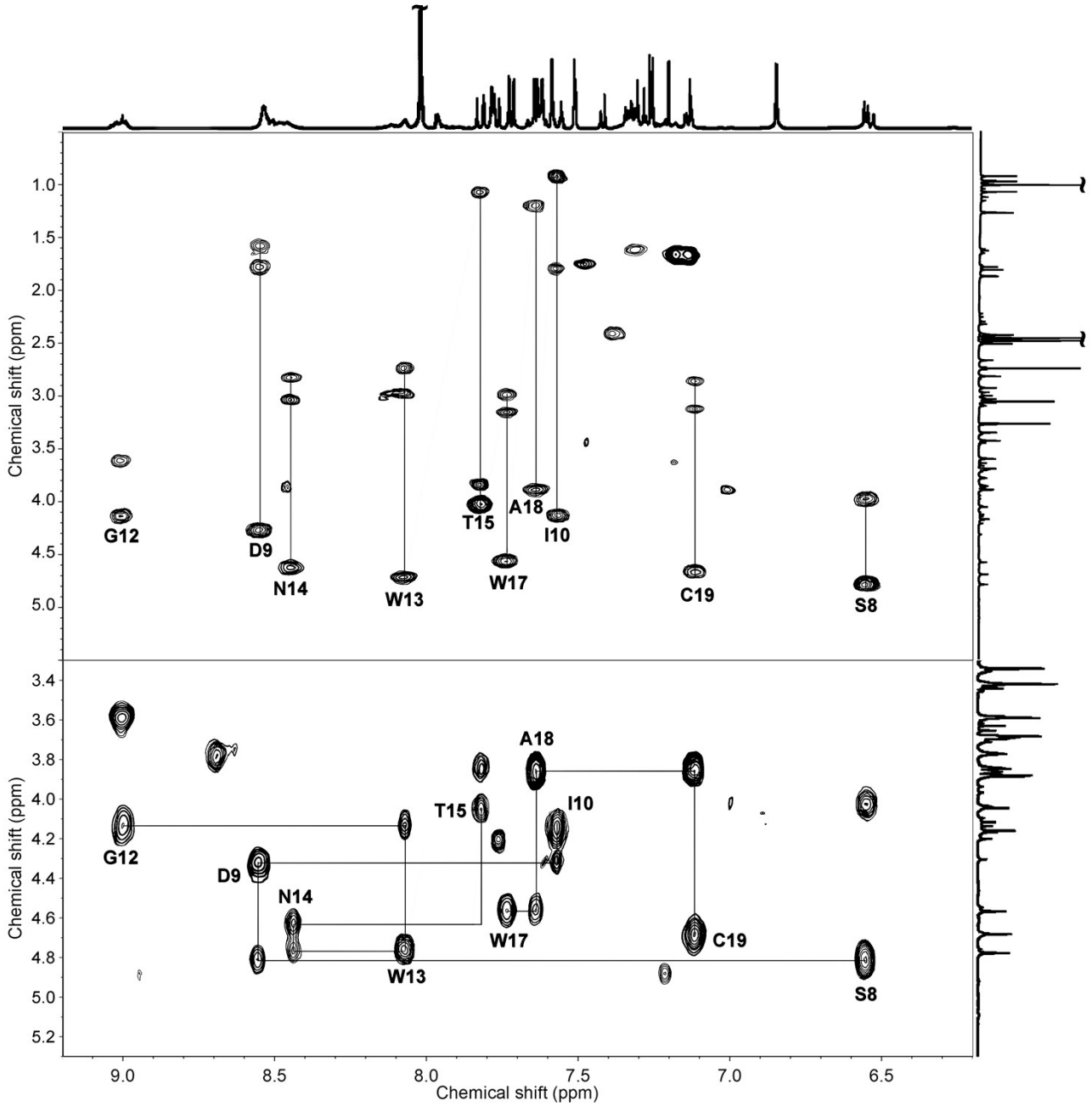

Figure **S48**. NMR spectra of D-enantiomer of compound **10** (400 MHz, DMSO-d_6, 0.2 mM, 40 °C). *Top*: TOCSY spectrum (100 ms). Amino acid spin systems are labeled. *Bottom*: Fingerprint region of the NOESY spectrum (150 ms) showing sequential connectivity between the residues.

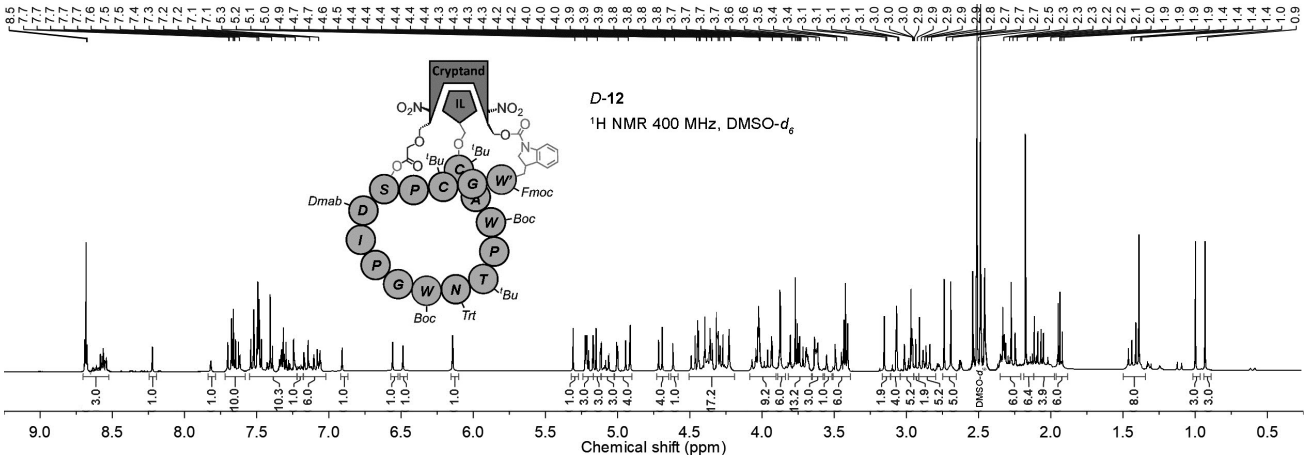

Figure **S49**. ^{1}H NMR spectrum of D-enantiomer of **12** (400 MHz, DMSO-d_6, 0.2 mM, 40 °C), ESI-MS calculated for $C_{195}H_{246}N_{27}O_{41}S_2$ $[M+H]^{2+}$: 1844.3750; Found 1844.3747.

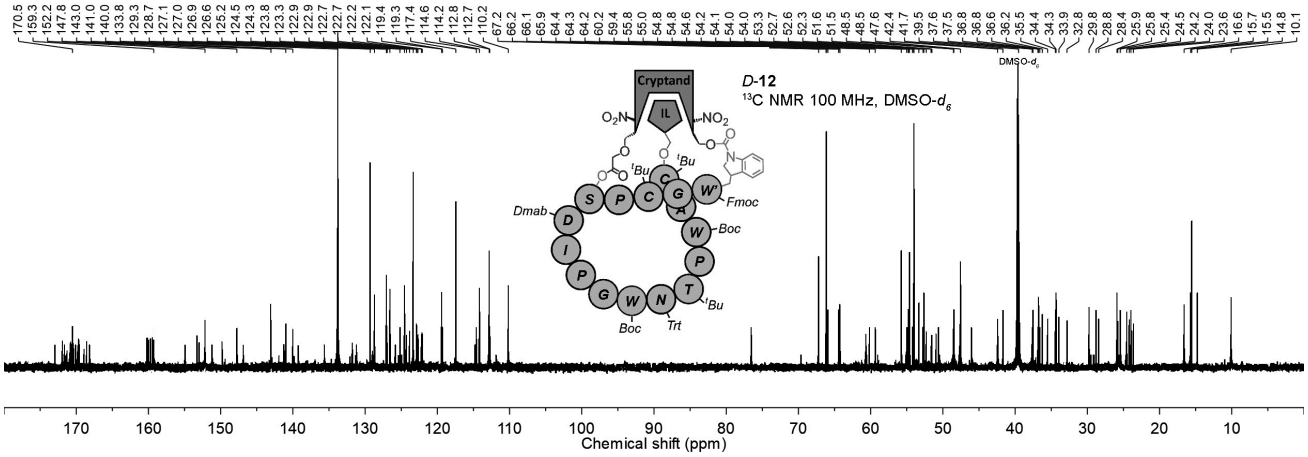

Figure **S50**. ^{13}C NMR spectrum of D-enantiomer of **12** (400 MHz, DMSO-d_6, 0.2 mM, 40 °C).

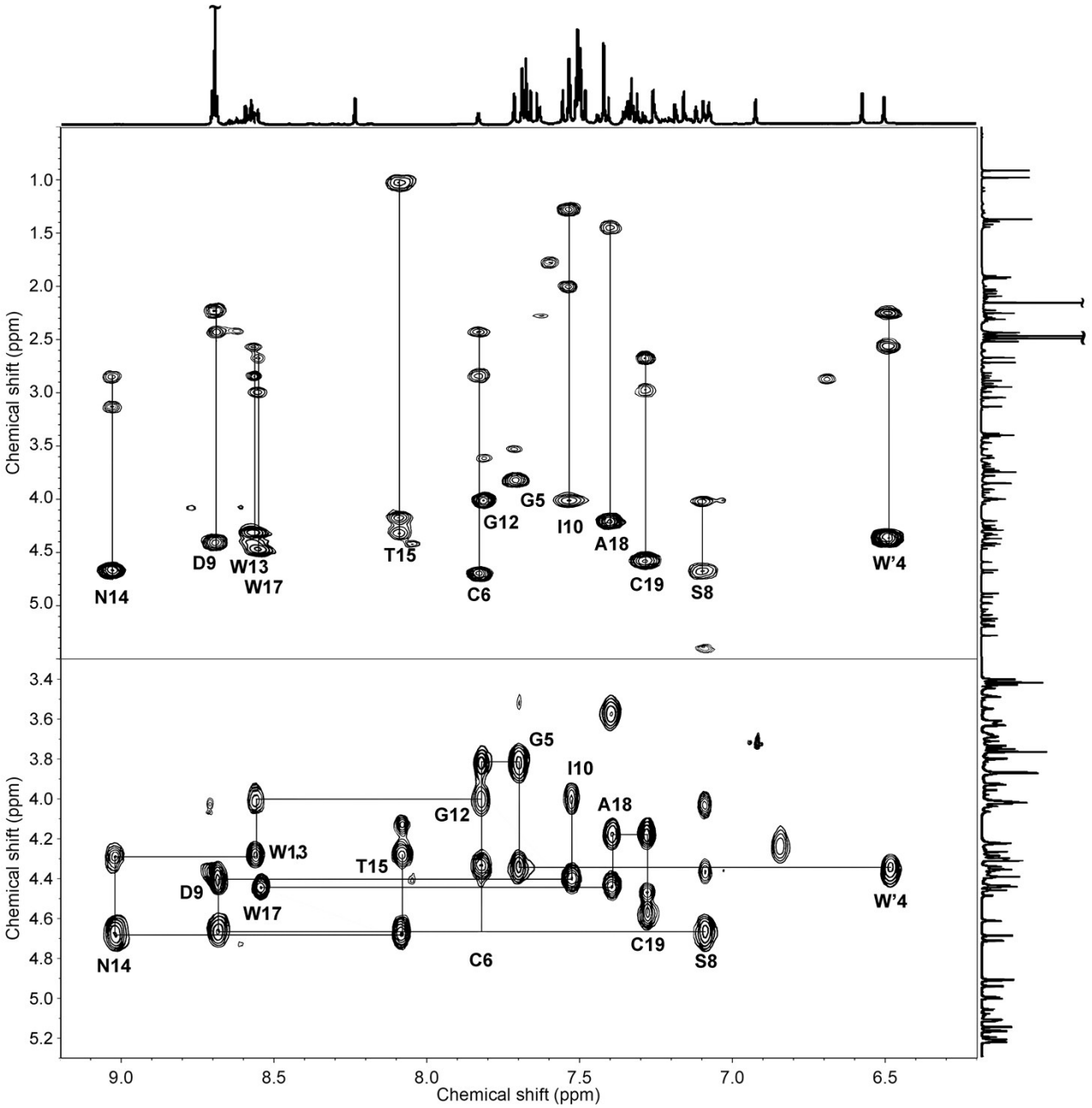

Figure **S51**. NMR spectra of D-enantiomer of compound **12** (400 MHz, DMSO-d_6, 0.2 mM, 40 °C). *Top*: TOCSY spectrum (100 ms). Amino acid spin systems are labeled. *Bottom*: Fingerprint region of the NOESY spectrum (150 ms) showing sequential connectivity between the residues.

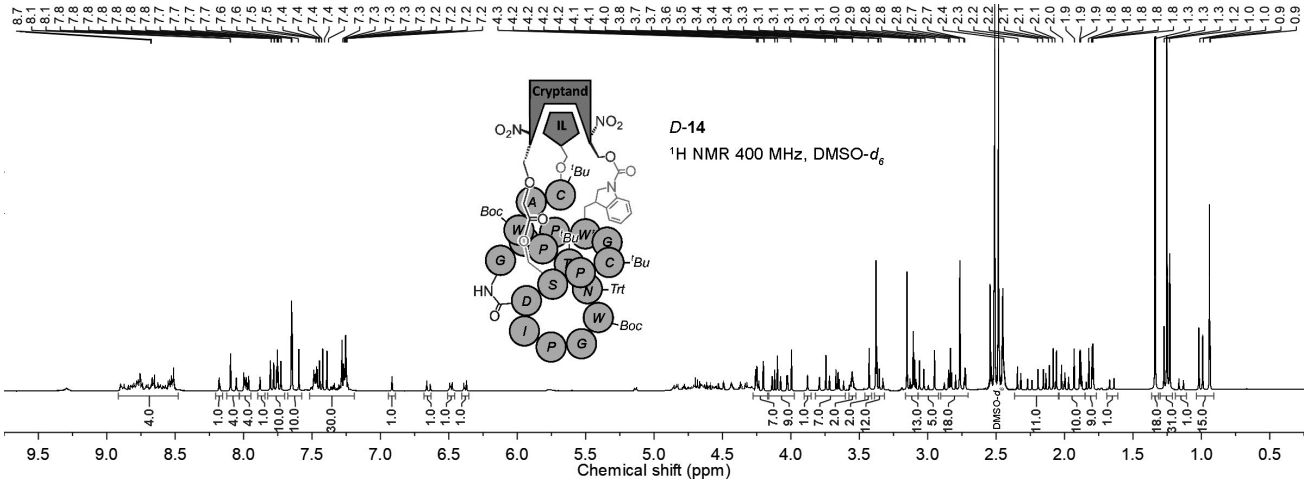

Figure **S52**. ^{1}H NMR spectrum of D-enantiomer of **14** (400 MHz, DMSO-d_6, 0.2 mM, 40 °C), ESI-MS calculated for $C_{171}H_{224}N_{29}O_{41}S_2$ $[M+H]^{2+}$: 1702.7903; Found 1702.7900.

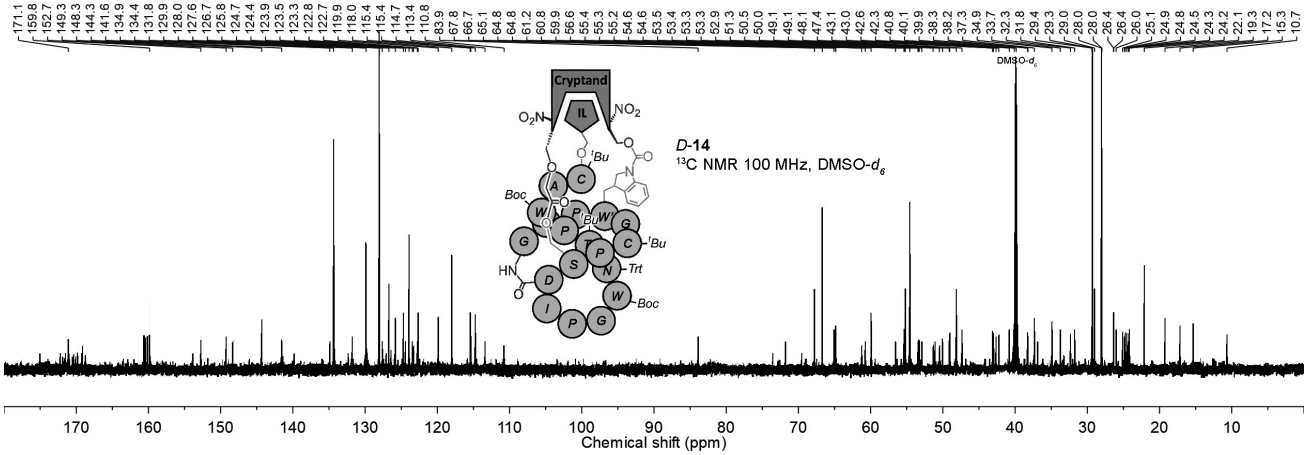

Figure **S53**. ^{13}C NMR spectrum of D-enantiomer of **14** (400 MHz, DMSO-d_6, 0.2 mM, 40 °C).

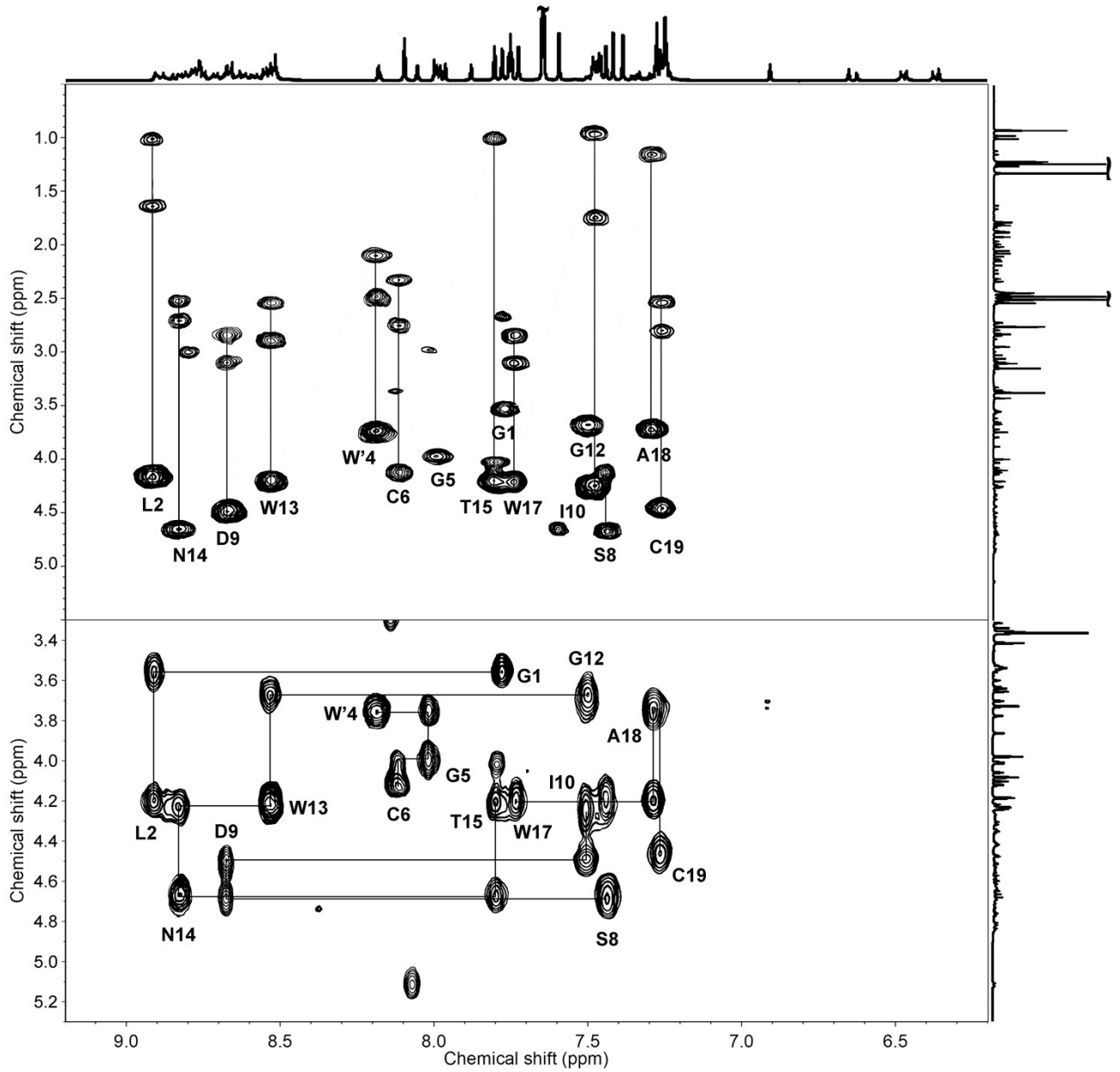

Figure **S54**. NMR spectra of D-enantiomer of compound **14** (400 MHz, DMSO-d_6, 0.2 mM, 40 °C). *Top*: TOCSY spectrum (100 ms). Amino acid spin systems are labeled. *Bottom*: Fingerprint region of the NOESY spectrum (150 ms) showing sequential connectivity between the residues.

4. Supplementary Characterization of synthetic BI-32169 and its D-

enantiomer

HPLC and MS spectrum of synthetic BI-32169

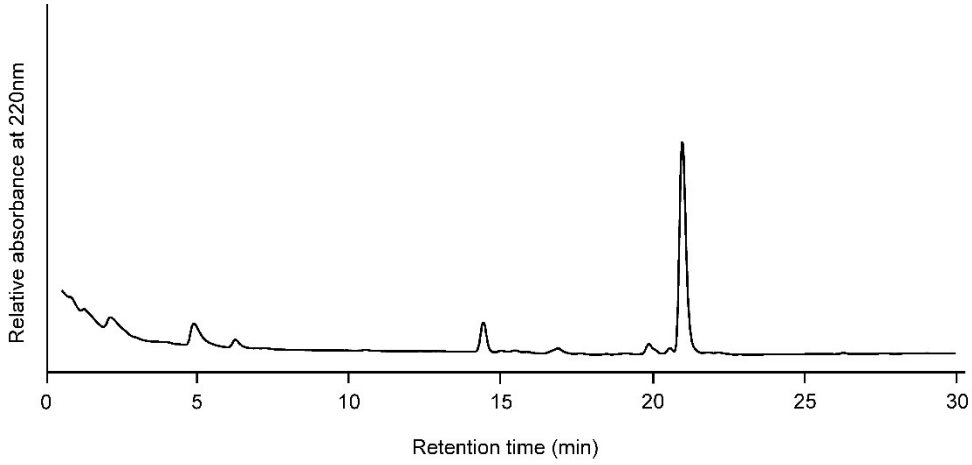

Figure **S55**. HPLC Chromatogram of crude synthesized BI-32169 (gradient: 0-40% acetonitrile in water + 0.1% TFA, at 1.0 mL/min, in 40 minutes).

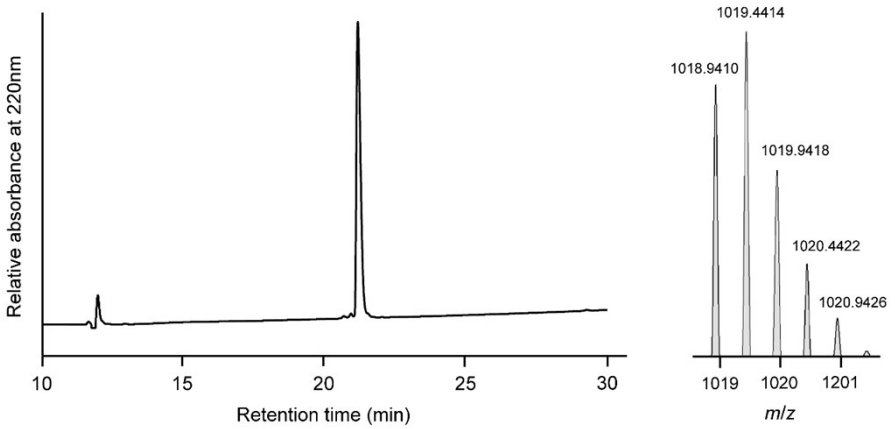

Figure **S56**. HPLC Chromatogram and ESI-FT mass spectrum of purified synthesized BI-32169 (T_R= 21.7 minutes, gradient: 0-40% acetonitrile in water + 0.1% TFA, at 1.0 mL/min, in 40 minutes; ESI-MS calculated for $C_{95}H_{125}N_{23}O_{24}S_2$ $[M+2H]^{2+}$: 1018.9433; Found 1018.9410).

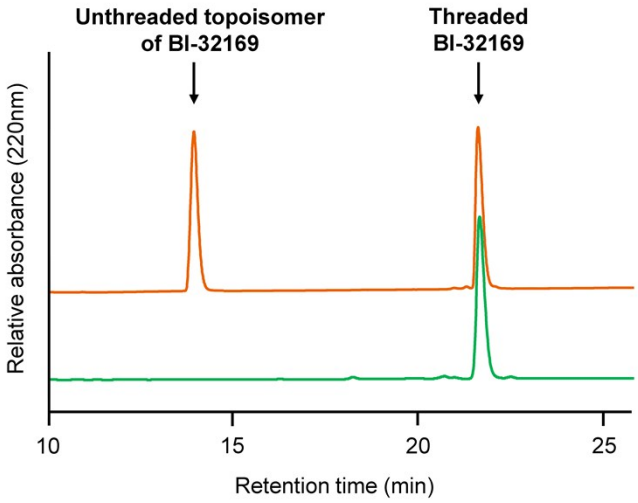

Figure **S57.** HPLC profiles of purified synthesized BI-32169 (gradient: 0-40% acetonitrile in water + 0.1% TFA, at 1.0 mL/min, in 40 minutes). The green line shows the co-injection of synthesized BI-32169 and its native standard. The orange line shows the co-injection of synthesized BI-32169 and its unthreaded topoisomer synthesized by SPPS method.

NMR spectrum of synthetic BI-32169

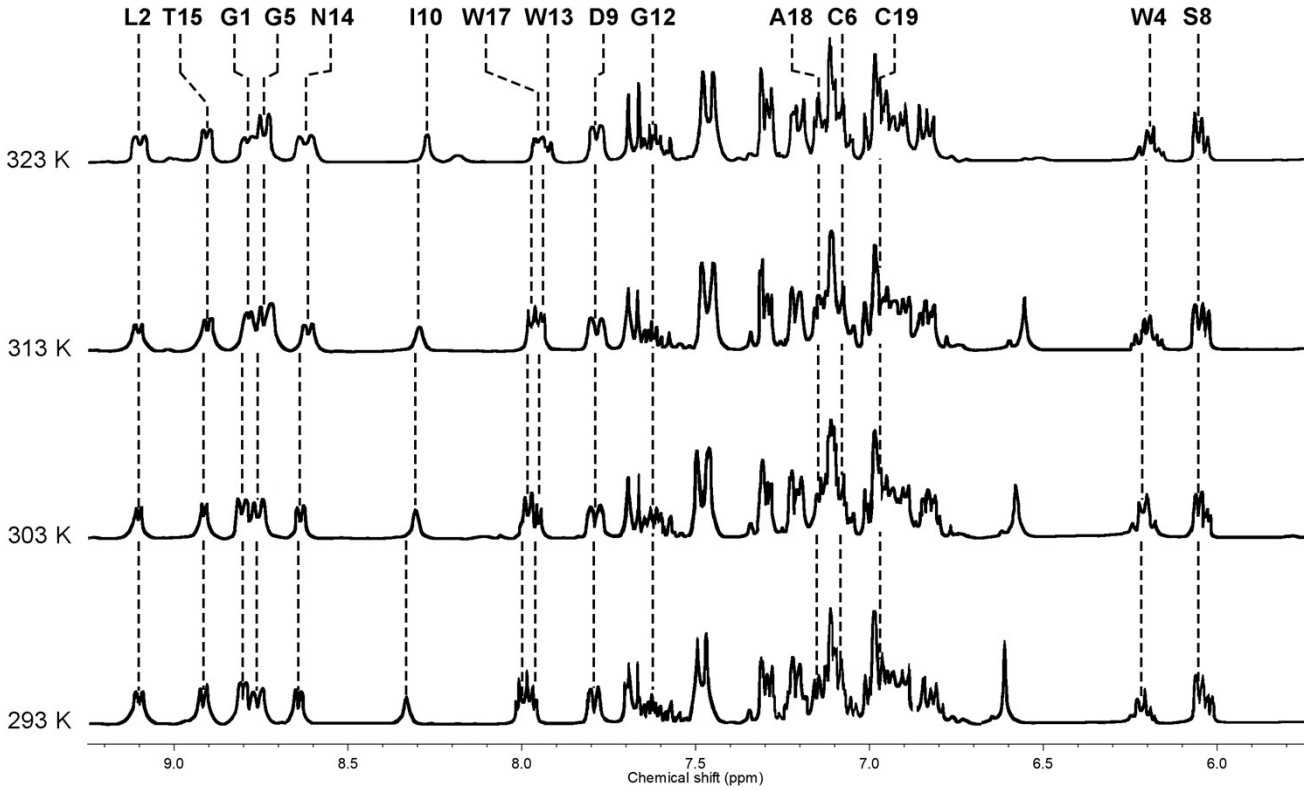

Figure **S58**. Amide proton region of ^{1}H spectra of synthetic BI-32169 in DMSO-d_6 at variable temperatures. The temperature dependence of chemical shifts is shown by dashed lines.

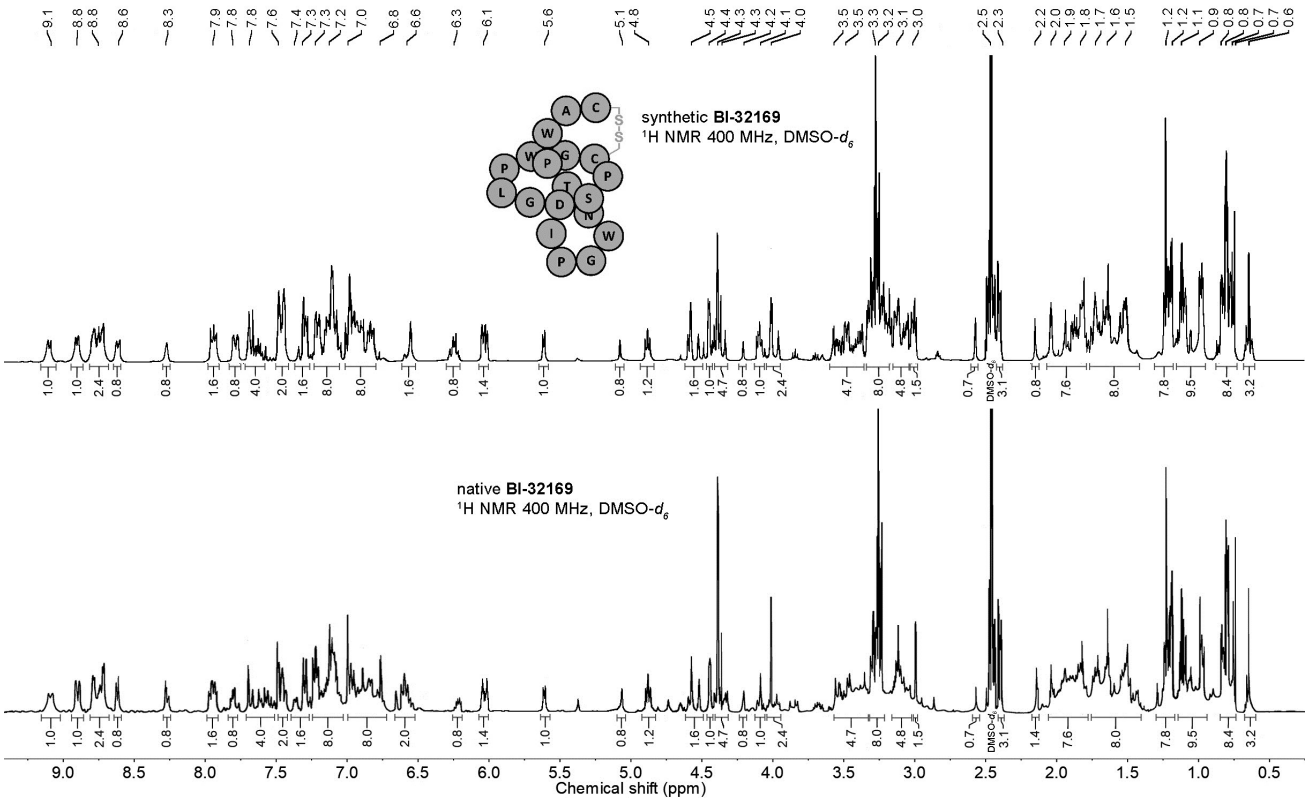

Figure **S59**. ^{1}H NMR spectra of synthetic BI-32169 and its native standard (400 MHz, DMSO-d_6, 0.2 mM, 40 °C).

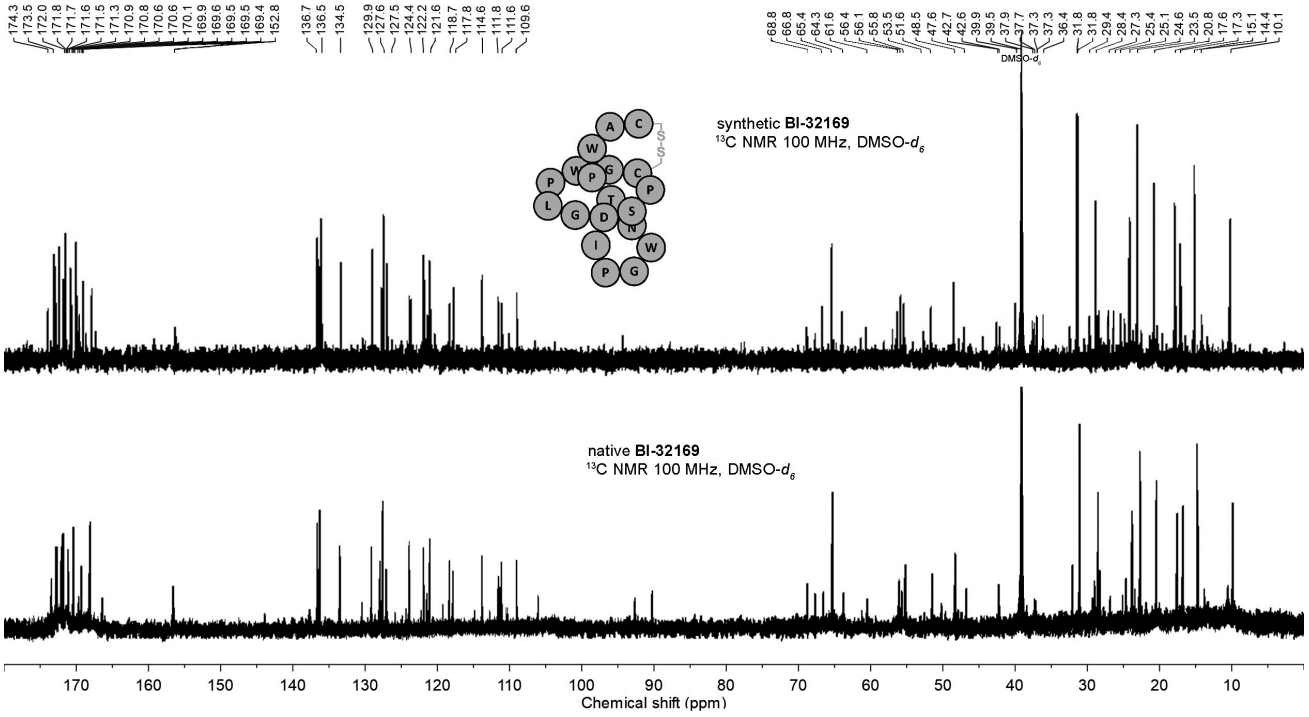

Figure **S60**. ^{13}C NMR spectra of synthetic BI-32169 and its native standard (100 MHz, DMSO-d_6, 0.2 mM, 40 °C).

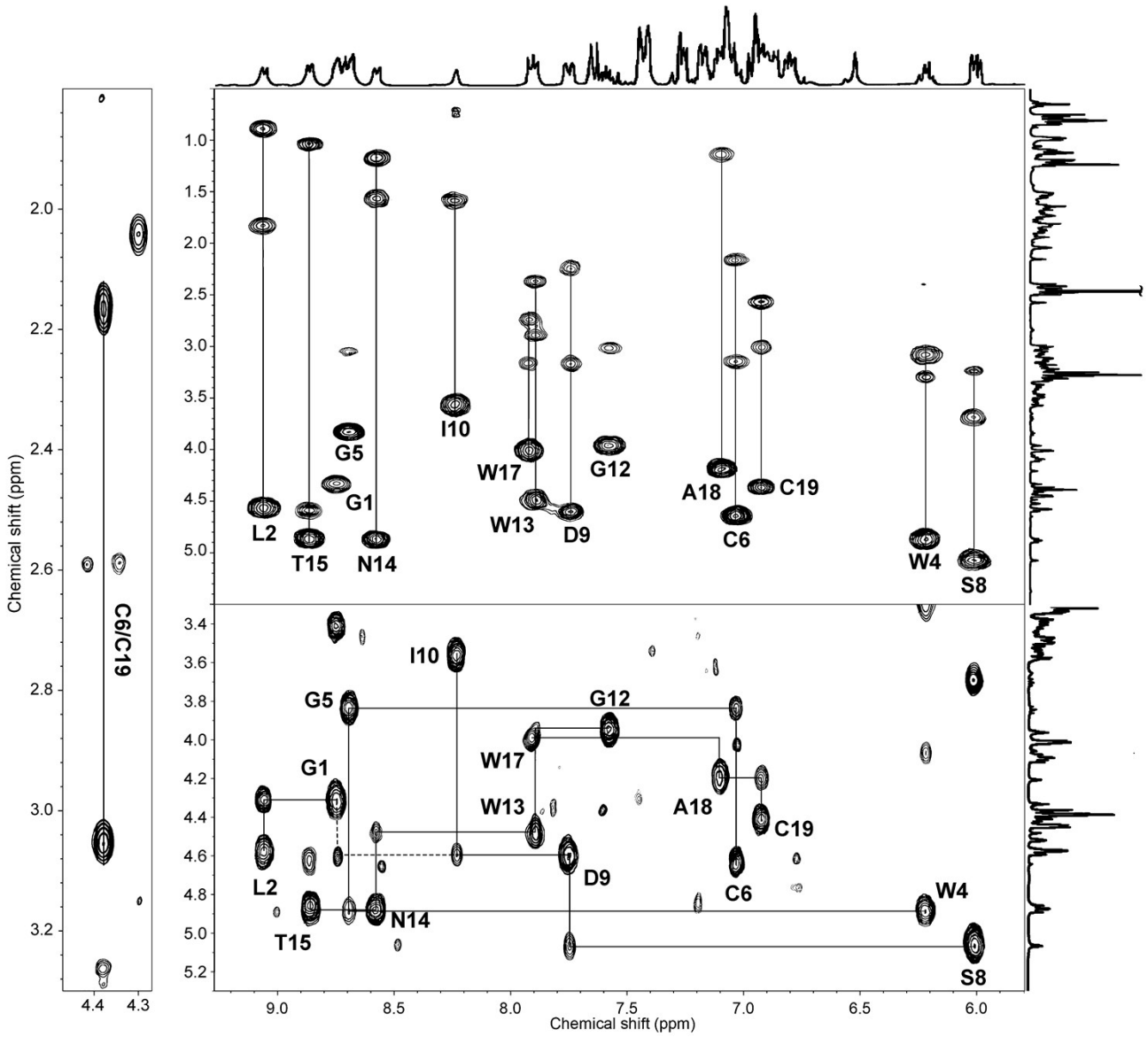

Figure **S61**. NMR spectra of synthetic BI-32169 (400 MHz, DMSO-d_6, 0.2 mM, 40 °C). *Top-right*: TOCSY spectrum (100 ms). Amino acid spin systems are labeled. *Bottom-right*: Fingerprint region of the NOESY spectrum (150 ms) showing sequential connectivity between the residues (solid line) and the isopeptide bond between **G**^{1} and **D**^{9} (dashed line). *Left*: Hα-Hβ region of NOESY spectrum (150 ms) showing the disulfide bond between **C**^{6} and **C**^{19}.

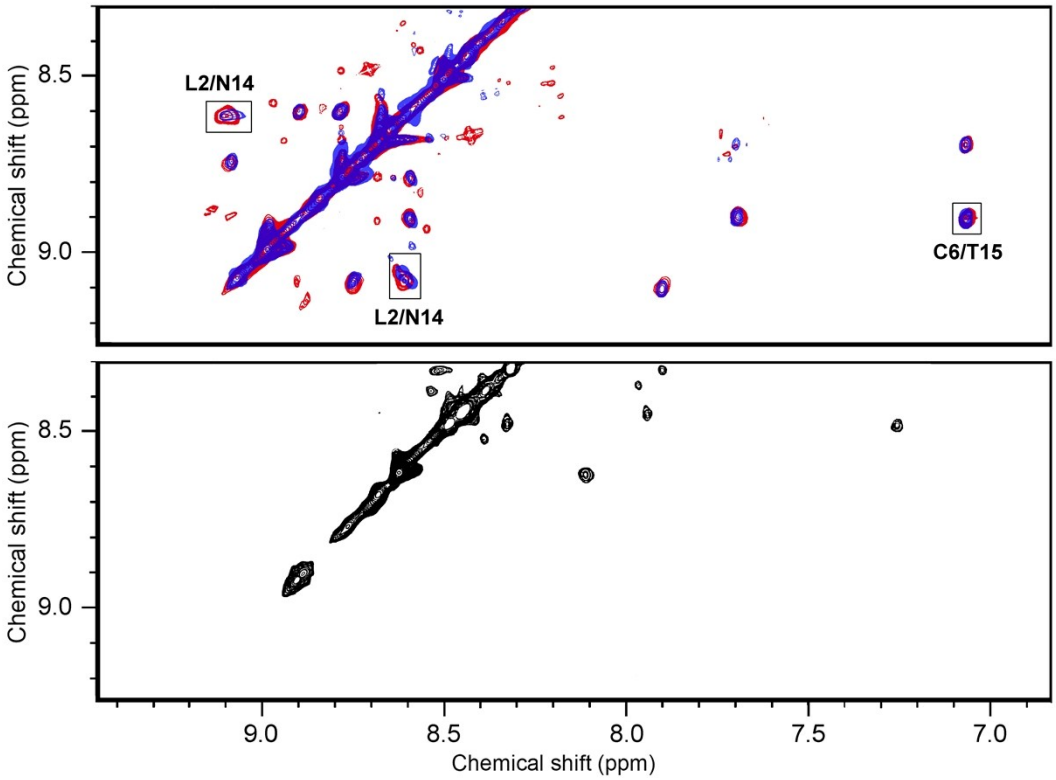

Figure **S62**. *Top*: the NH/NH regions of NOESY spectra overlay of synthetic BI-32169 (blue) and native BI-32169 (red). The apparent long-range NOEs between the amide protons of $\mathbf{L}^{2}$ with $\mathbf{N}^{14}$ and $\mathbf{C}^{6}$ with $\mathbf{T}^{15}$ of synthetic BI-32169 are indicated, showing the lasso configuration of BI-32169. *Bottom*: the NH/NH region of NOESY spectrum of the unthreaded topoisomer of BI-32169.

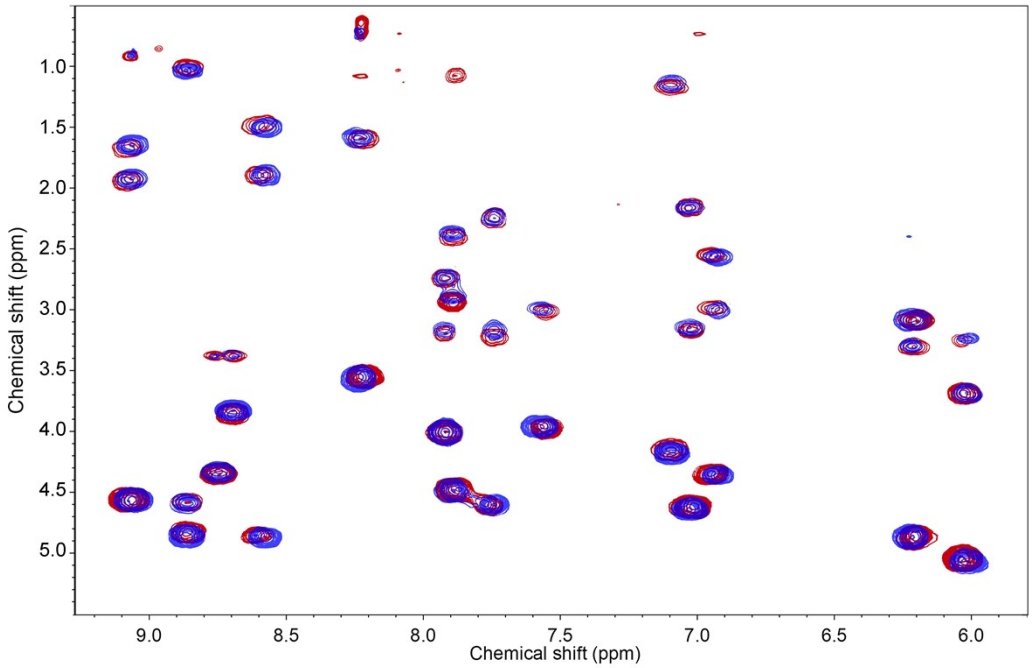

Figure **S63**. Superimposed TOCSY spectra (100 ms) of synthetic BI-32169 (blue) and native BI-32169 (red).

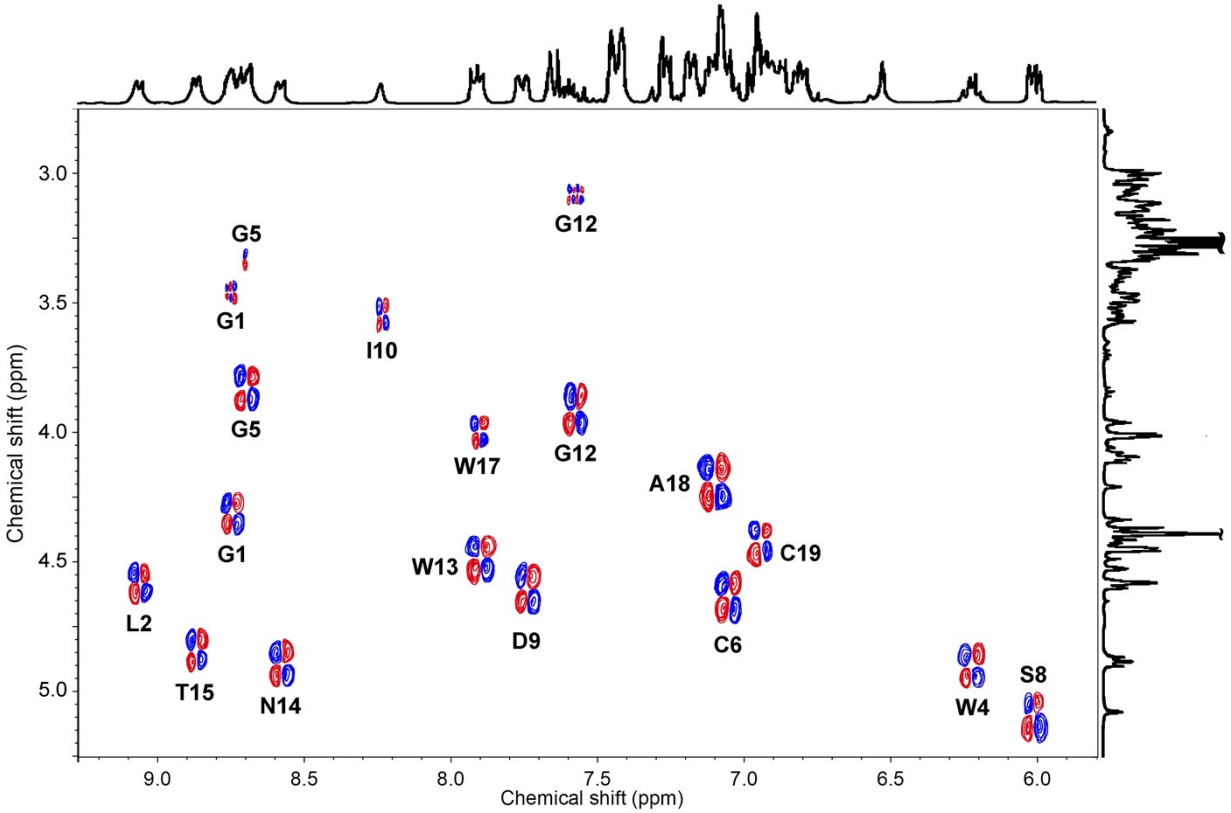

Figure **S64**. Fingerprint region of the 2D DQF-COSY spectrum of synthetic BI-32169 (400 MHz, DMSO-d_6, 0.2 mM, 40 °C).

Table **S1**. Comparison of assigned ^{1}H NMR chemical shifts of synthetic and native BI-32169

AA	Proton chemical shifts (synthetic/native, deviation), in DMSO-d_6 at 40°C (ppm)				
	NH	αH	βH	γH	others
G[1]	8.75/8.75, ±0.00	3.39/3.39, ±0.00 4.32/4.32, ±0.00	-	-	-
L[2]	9.07/9.08, -0.01	4.59/4.59, ±0.00	1.65/1.67, -0.02 1.91/1.92, -0.01	1.83/1.82, +0.01	δH: 0.90/0.90, ±0.00 δH: 0.99/0.99, ±0.00
P[3]	-	4.16/4.17, -0.01	1.61/1.61; ±0.00 1.99/2.00; -0.01	1.76/1.71, ±0.00 1.87/1.86, +0.01	δH: 3.39/3.38, +0.01 δH: 3.58/3.58, ±0.00
W[4]	6.22/6.20, +0.02	4.83/4.83, ±0.00	3.09/3.09, ±0.00 3.30/3.30, ±0.00	-	2H$_{indole}$: 7.25/7.25, ±0.00 NH$_{indole}$: 10.85/10.86, -0.01 4H$_{indole}$: 7.55/7.55, ±0.00 5H$_{indole}$: 7.05/7.05, ±0.00 6H$_{indole}$: 7.21/7.21, ±0.00 7H$_{indole}$: 7.42/7.41, +0.01
G[5]	8.73/8.73, ±0.00	3.34/3.35, -0.01 3.82/3.82, ±0.00	-	-	-
C[6]	7.07/7.07, ±0.00	4.65/4.66, -0.01	2.19/2.19, ±0.00 3.14/3.13, +0.01	-	-
P[7]	-	4.88/4.88, ±0.00	1.91/1.91, ±0.00 2.32/2.32, ±0.00	1.89/1.89, ±0.00 2.04/2.03, +0.01	δH: 3.58/3.58, ±0.00
S[8]	6.01/6.03, -0.02	5.17/5.18, -0.01	3.23/3.24, -0.01 3.70/3.70, ±0.00	-	-
D[9]	7.75/7.76, -0.01	4.62/4.62, ±0.00	2.24/2.24, ±0.00 3.19/3.21, -0.02	-	-
I[10]	8.27/8.26, +0.01	3.58/3.57, +0.01	1.60/1.61, -0.01	CH_2: 1.22/1.22, ±0.00 1.74/1.74, ±0.00 CH_3: 0.91/0.92, -0.01	δH: 0.91/0.90, +0.01
P[11]	-	4.32/4.32, ±0.00	1.66/1.66, ±0.00 2.10/2.09, +0.01	1.79/1.79, ±0.00 2.14/2.15, -0.01	δH: 3.26/3.26, ±0.00 δH: 3.87/3.88, -0.01
G[12]	7.59/7.57, +0.02	3.03/3.05, -0.02; 3.95/3.95, ±0.00	-	-	-
W[13]	7.91/7.91, ±0.00	4.49/4.49, ±0.00	2.38/2.40, -0.02 2.90/2.92, -0.02	-	2H$_{indole}$: 6.96/6.95, +0.01 NH$_{indole}$: 10.80/10.80, ±0.00 4H$_{indole}$: 7.12/7.12, ±0.00 5H$_{indole}$: 6.85/6.86, -0.01 6H$_{indole}$: 7.14/7.15, +0.01 7H$_{indole}$: 7.38/7.38, ±0.00
N[14]	8.60/8.62, -0.02	4.89/4.88, +0.01	1.50/1.49, +0.01 1.89/1.89, ±0.00	-	-
T$_{15}$	8.89/8.89, ±0.00	4.87/4.86, +0.01	4.60/4.60, ±0.00	1.20/1.19, +0.01	-
P[16]	-	4.48/4.48, ±0.00	1.48/1.48, ±0.00 2.25/2.25, ±0.00	1.57/1.57, ±0.00 1.71/1.71, ±0.00	δH: 3.70/3.70, ±0.00 δH: 3.96/3.95, +0.01
W[17]	7.95/7.95, ±0.00	4.01/4.01, ±0.00	2.17/2.17, ±0.00 3.19/3.20, -0.01	-	2H$_{indole}$: 7.41/7.41, ±0.00 NH$_{indole}$: 11.14/11.12, +0.02 4H$_{indole}$: 7.66/7.66, ±0.00 5H$_{indole}$: 7.12/7.12, ±0.00 6H$_{indole}$: 7.19/7.18, +0.01 7H$_{indole}$: 7.40/7.41, -0.01
A[18]	7.18/7.18; ±0.00	4.20/4.19, +0.01	1.13/1.15, -0.02	-	-
C[19]	6.93/6.95; -0.02	4.36/4.36, ±0.00	2.59/2.58, +0.01 3.01/3.00, +0.01	-	-

Table **S2**. *J* values and torsion angles of synthetic BI-32169 measured from DQF-COSY spectrum

AA	peak position (ppm-ppm)	assignment	*J* value (Hz)	backbone angle φ	sidechain angles χ1
G[1]	8.75-4.32	$^3J_{HHA3}$	11.2	-	
L[2]	9.07-4.59	$^3J_{HHA}$	9.8	-120°±30°	60°±30°
	4.59-1.91	$^3J_{HAHB3}$	9.8		
W[4]	6.22-4.83	$^3J_{HHA}$	9.8	-120°±30°	60°±30°
	4.83-3.30	$^3J_{HAHB3}$	6.6		
G[5]	8.73-3.82	$^3J_{HHA3}$	10.5	-	
C[6]	7.07-4.65	$^3J_{HHA}$	10.5	-120°±30°	-30°±30°
	4.65-3.14	$^3J_{HAHB3}$	6.0		
S[8]	6.01-5.17	$^3J_{HHA}$	9.8	-120°±30°	60°±30°
	5.17-3.70	$^3J_{HHB3}$	5.6		
D[9]	7.75-4.62	$^3J_{HHA}$	10.8	-120°±30°	60°±30°
	4.62-3.19	$^3J_{HAHB3}$	7.2		
I[10]	8.27-3.58	$^3J_{HHA}$	5.5	-60°±30°	-
	3.58-1.60	$^3J_{HAHB}$	10.8		
G[12]	7.59-3.95	$^3J_{HHA3}$	13.0	-	
W[13]	7.91-4.49	$^3J_{HHA}$	10.5	-120°±30°	-30°±30°
	4.49-2.90	$^3J_{HAHB3}$	5.5		
N[14]	8.60-4.89	$^3J_{HHA}$	10.0	-120°±30°	150°±30°
	4.89-1.89	$^3J_{HAHB3}$	10.5		
T$_{15}$	8.89-4.87	$^3J_{HHA}$	8.0	-120°±30°	-
	4.87-4.60	$^3J_{HAHB}$	13.5		
W[17]	7.95-4.01	$^3J_{HHA}$	7.5	-60°±30°	-30°±30°
	4.01-3.19	$^3J_{HAHB3}$	5.7		
A[18]	7.18-4.20	$^3J_{HHA}$	9.5	-120°±30°	-
	4.20-1.13	$^3J_{AB}$	7.7		
C[19]	6.93-4.36	$^3J_{HHA}$	8.0	-120°±30°	-30°±30°
	4.36-3.01	$^3J_{HAHB3}$	5.5		

* Conversion of *J* values into the torsion angle constraints was solved by a Karplus equation[9]. The information of χ1 rotameric state was obtained from ^{3}J-coupling constants and the NOE strengths between NH and βHs[10].

MS^2 analysis of synthetic BI-32169

To characterize the synthesized lasso-structured peptide, tandem mass spectrometry was applied to identify the structure of synthetic BI-32169. According to the previous reports[7,8], the rigid cyclic part of lasso peptides usually gave a weak overall fragmentation, while the exocyclic part produced high intensities of some characteristic fragment ions.

The main fragmentation patterns are showed in the following figures upper marked by numbers. Although the MS^2 fragmentation behaviors of the synthetic BI-32169 (Figure S49; e.g. weak fragmentation, the most intense ion ***10*** (in red) resulted from the loss of $\mathbf{I}^{10}$) matched the work of Knappe *et al.* well, similar fragmentation behaviors could be also caused by the fact that two bond breakages are required in unthreaded bicyclic peptide[7]. Thus, the tandem mass spectrometry studies of reduced BI-32169 and its unthreaded topoisomer were performed. We found that the intensities of the fragment ions resulting from peptide bond cleavages in internal sequence $\mathbf{P}^{11}\mathbf{GWNTPW}^{17}$ of reduced BI-32169 (Figure S50; ions ***12***, ***13***, ***14***, ***15*** in various colors) were significantly weaker than those in unthreaded one (Figure S51; ions ***11***, ***12***, ***13***, ***14***, ***15*** in various colors).

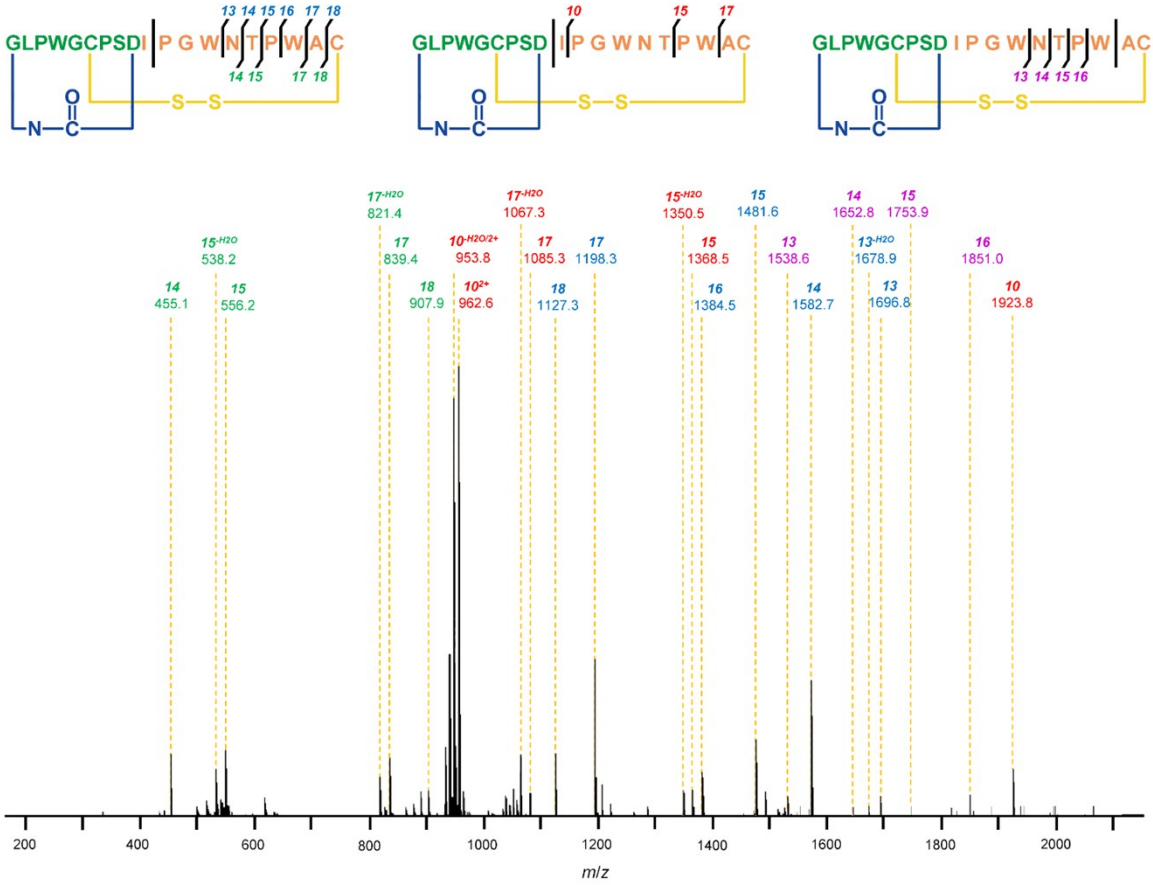

Figure **S65**. MS^2 spectrum of oxidized BI-32169. Four series of fragment ions (singly and doubly protonated fragments) and their corresponding peaks (marked with italic serial numbers) were showed in green, red, blue and purple, respectively.

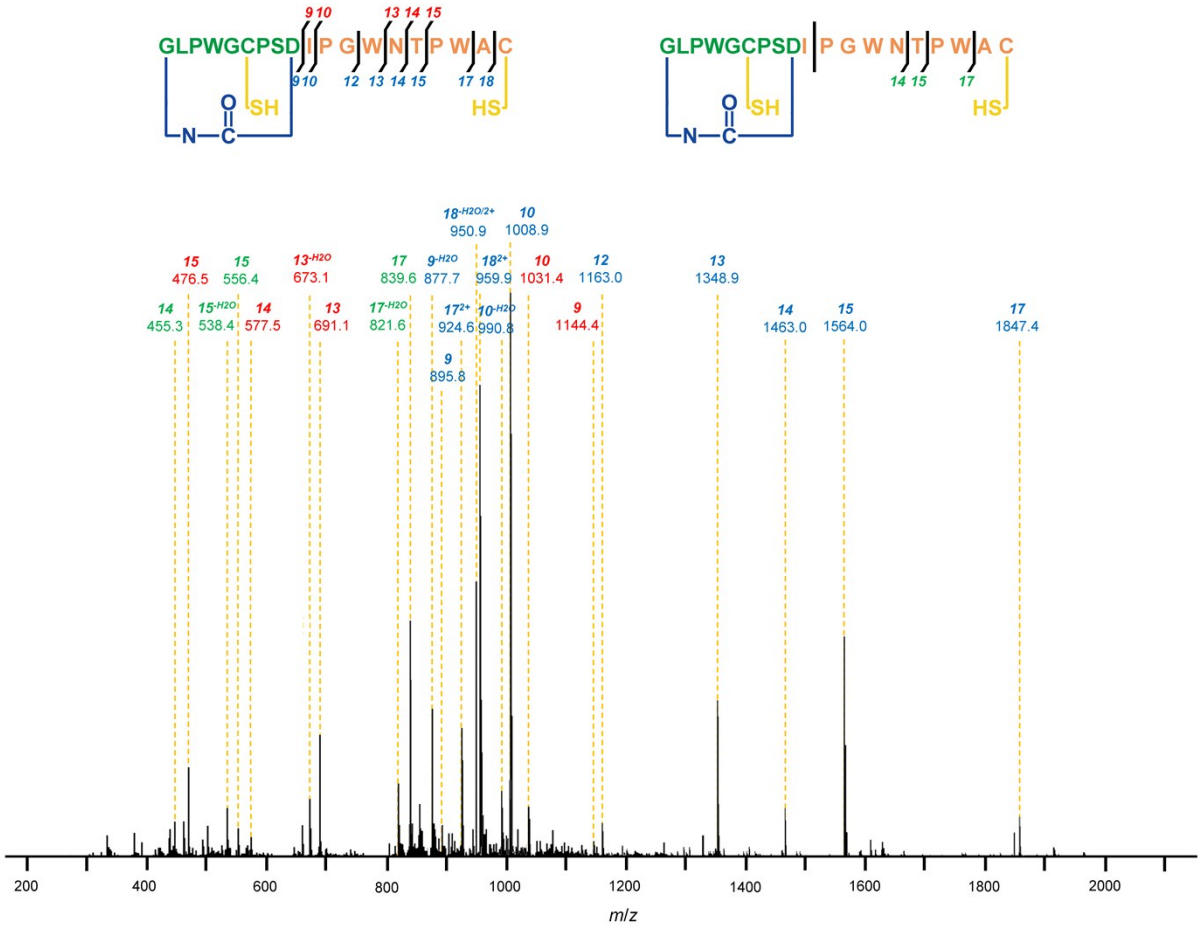

Figure **S66**. MS^2 spectrum of reduced BI-32169. Three series of fragment ions (singly and doubly protonated fragments) and their corresponding peaks (marked with italic serial numbers) were showed in green, red and blue, respectively.

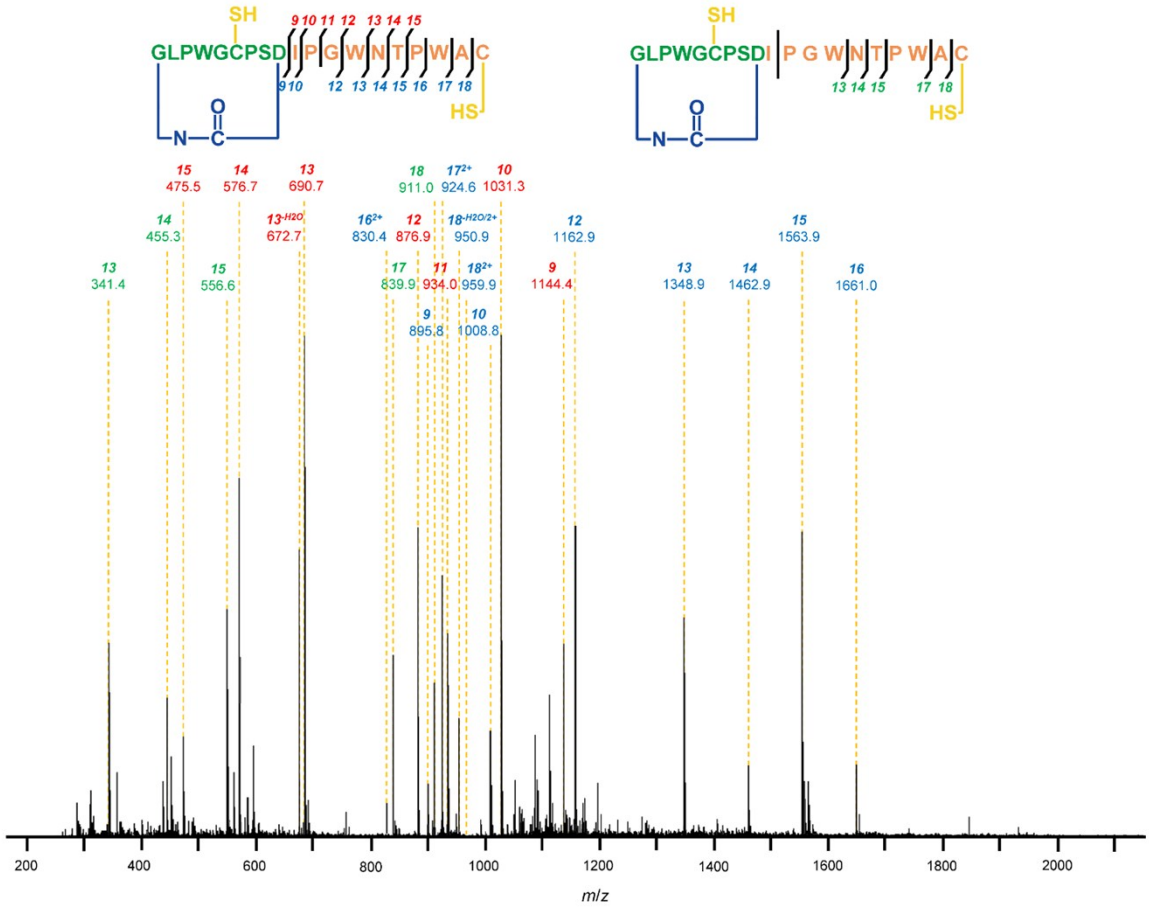

Figure **S67**. MS^2 spectrum of reduced unthreaded topoisomer of BI-32169. Three series of fragment ions (singly and doubly protonated fragments) and their corresponding peaks (marked with italic serial numbers) were showed in green, red and blue, respectively.

HPLC and MS spectrum of synthetic D*-BI-32169*

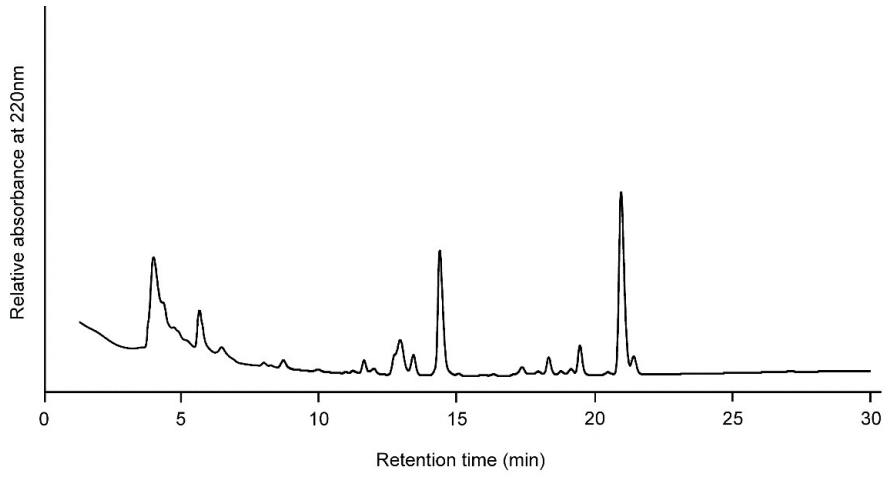

Figure **S68**. HPLC Chromatogram of crude synthesized D-BI-32169. (gradient: 0-40% acetonitrile in water + 0.1% TFA, at 1.0 mL/min, in 40 minutes).

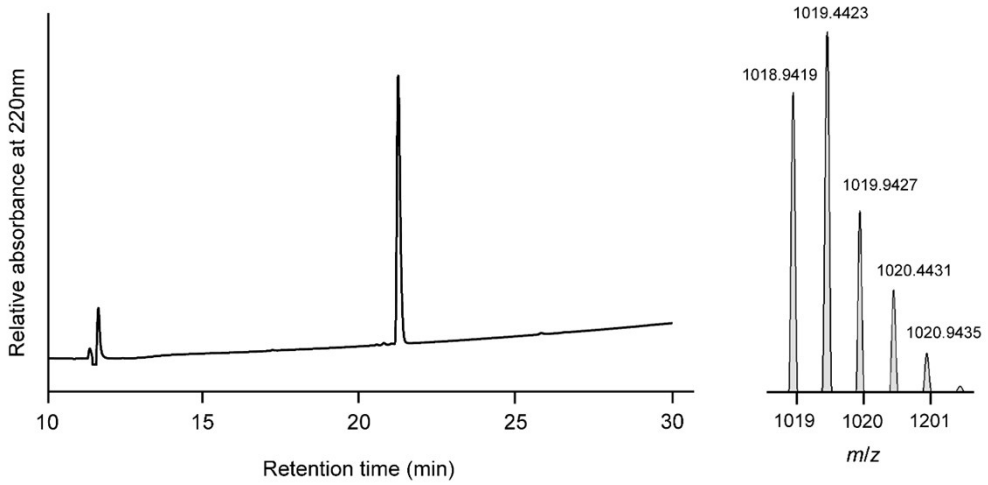

Figure **S69**. HPLC Chromatogram and ESI-FT mass spectrum of purified synthesized D-BI-32169 (T_R= 21.7 minutes, gradient: 0-40% acetonitrile in water + 0.1% TFA, at 1.0 mL/min, in 40 minutes; ESI-MS calculated for $C_{95}H_{125}N_{23}O_{24}S_2$ $[M+2H]^{2+}$: 1018.9433; Found 1018.9419).

NMR spectrum of synthetic D-BI-32169

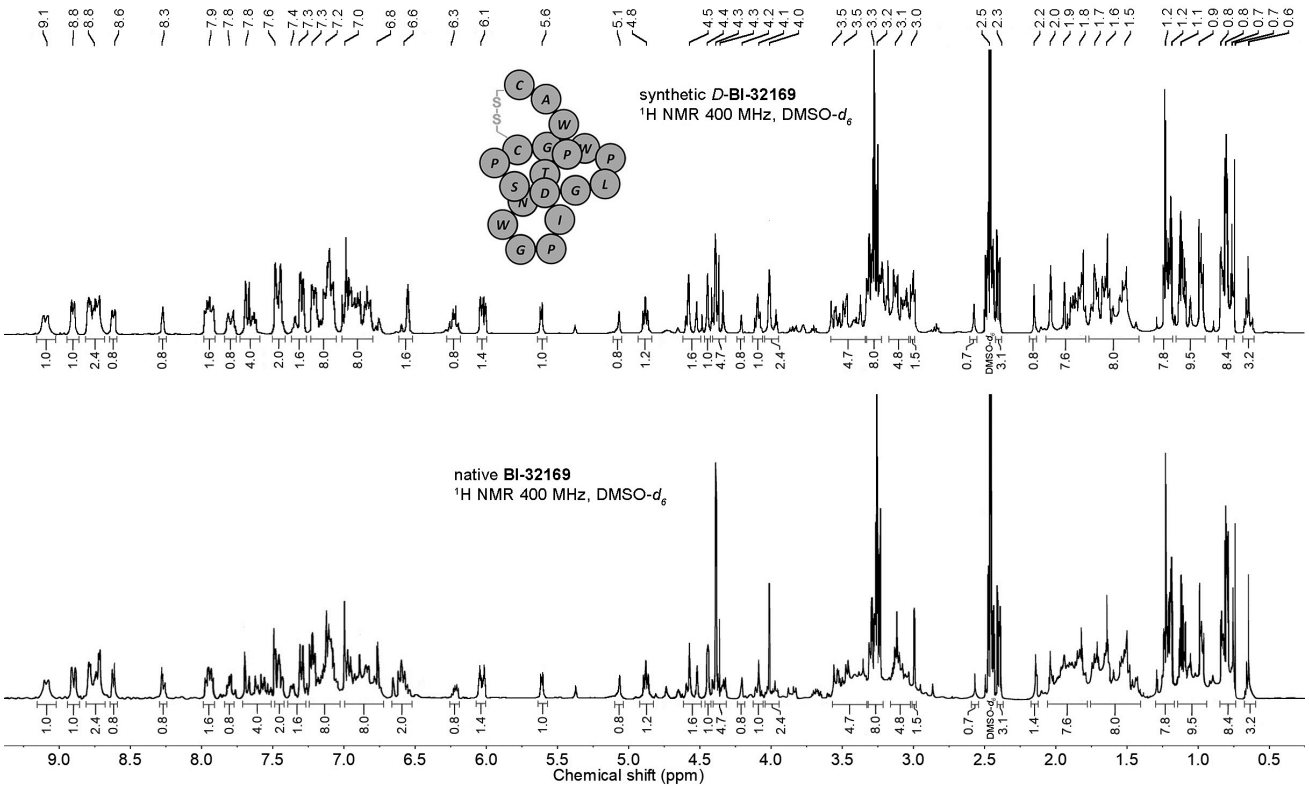

Figure **S70**. ^{1}H NMR spectra of synthetic D-BI-32169 and native BI-32169 (400 MHz, DMSO-d_6, 0.2 mM, 40 °C).

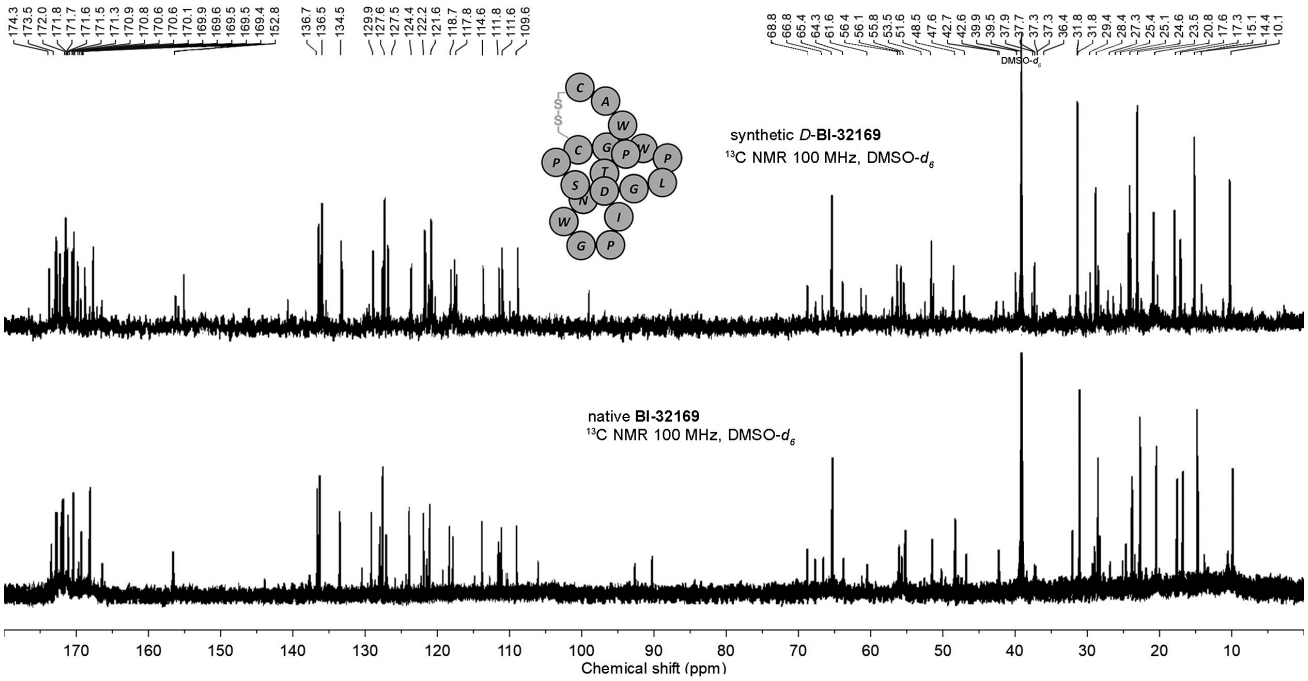

Figure **S71**. ^{13}C NMR spectra of synthetic D-BI-32169 and native BI-32169 (100 MHz, DMSO-d_6, 0.2 mM, 40 °C).

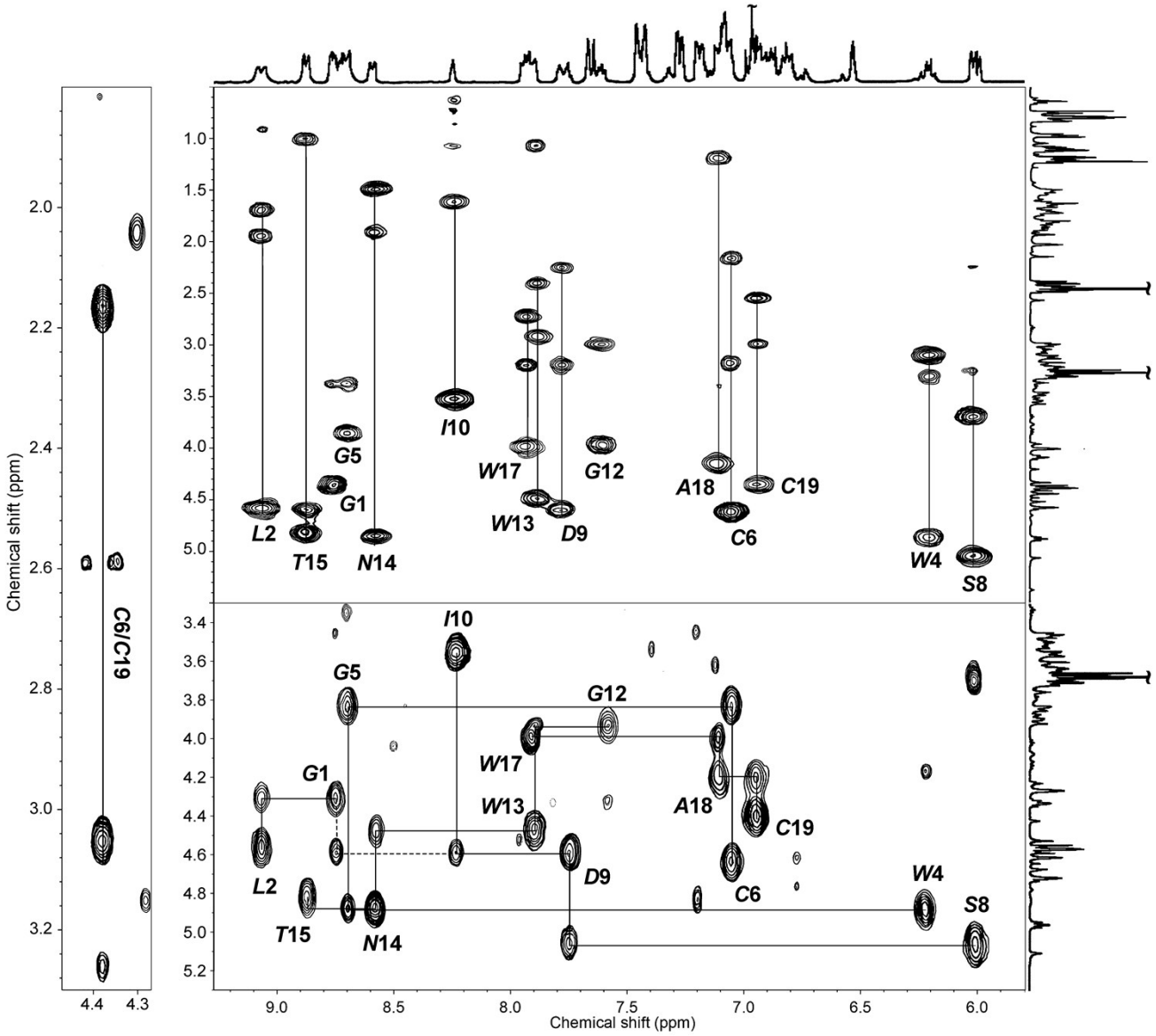

Figure **S72**. NMR spectra of synthetic D-BI-32169 (400 MHz, DMSO-d_6, 0.2 mM, 40 °C). *Top-right*: TOCSY spectrum (100 ms). Amino acid spin systems are labeled. *Bottom-right*: Fingerprint region of the NOESY spectrum (150 ms) showing sequential connectivity between the residues (solid line) and the isopeptide bond between D-**G**^{1} and D-**D**^{9} (dashed line). *Left*: Hα-Hβ region of NOESY spectrum (150 ms) showing the disulfide bond between D-**C**^{6} and D-**C**^{19}.

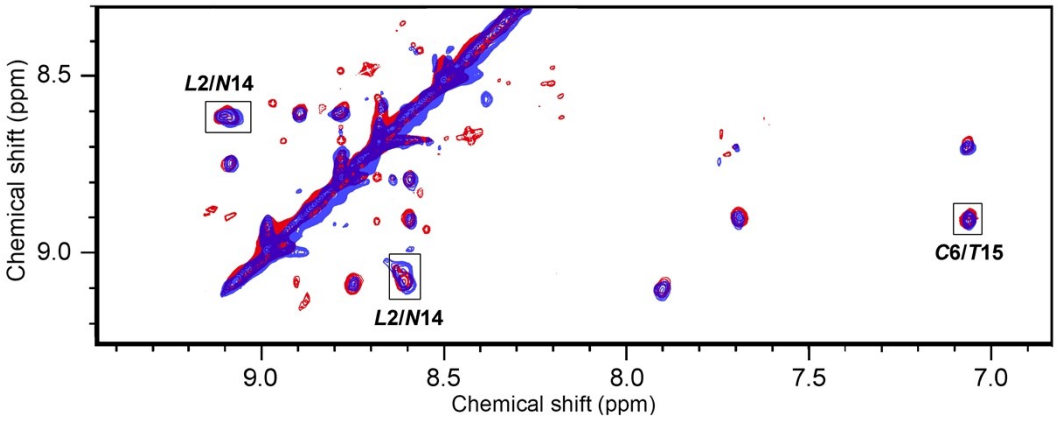

Figure **S73**. The NH/NH regions of NOESY spectra overlay of synthetic D-BI-32169 (blue) and native BI-32169 (red). The apparent long-range NOEs between the amide protons of D-**L**^{2} with D-**N**^{14} and d-**C**^{6} with D-**T**^{15} of synthetic D-BI-32169 are indicated, showing the lasso configuration of D-BI-32169.

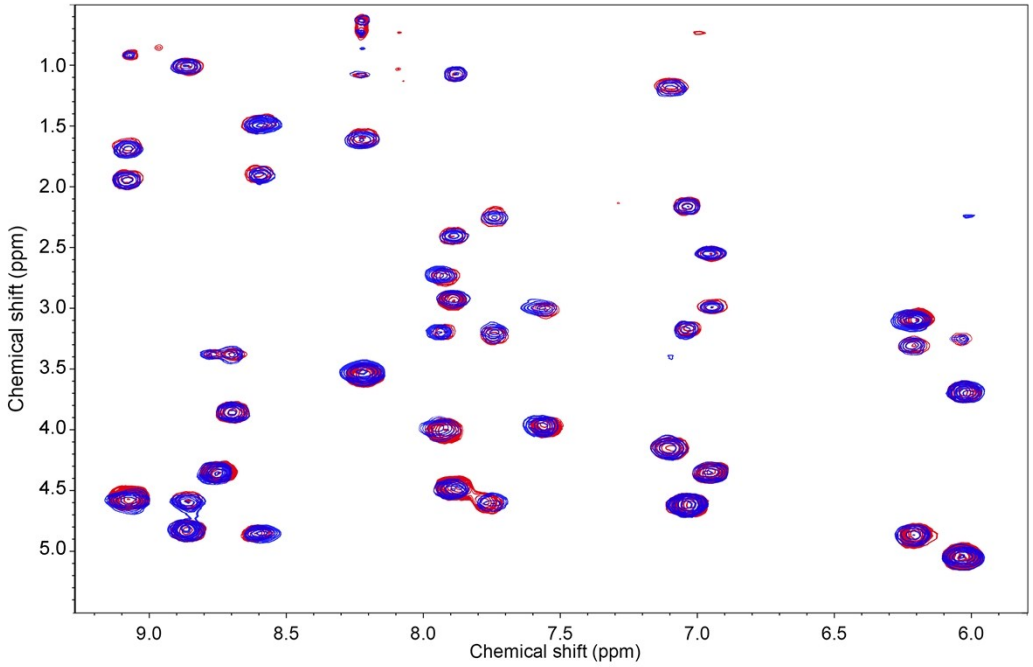

Figure **S74**. Superimposed TOCSY spectra (100 ms) of synthetic D-BI-32169 (blue) and native BI-32169 (red).

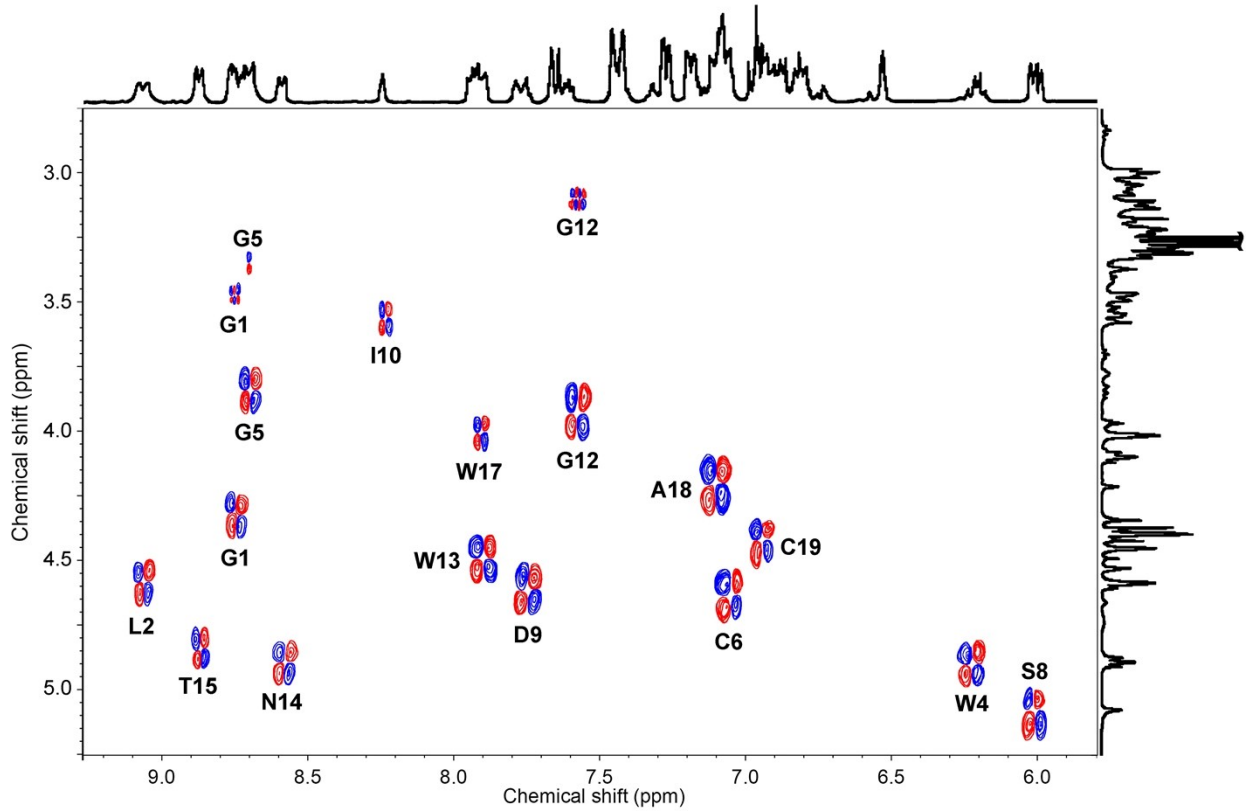

Figure **S75**. Fingerprint region of the 2D DQF-COSY spectrum of synthetic D-BI-32169 (400 MHz, DMSO-d_6, 0.2 mM, 40 °C).

Table **S3**. Comparison of assigned ^{1}H NMR chemical shifts of synthetic D-BI-32169 and native BI-32169

D-AA	Proton chemical shifts (synthetic/native, deviation), in DMSO-d_6 at 40°C (ppm)				
	NH	αH	βH	γH	others
G[1]	8.76/8.75, +0.01	3.39/3.39, ±0.00 4.32/4.32, ±0.00	-	-	-
L[2]	9.08/9.08, ±0.00	4.60/4.59, +0.01	1.68/1.67, +0.01 1.92/1.92, ±0.00	1.84/1.82, +0.02	δH: 0.91/0.90, +0.01 δH: 1.00/0.99, +0.01
P[3]	-	4.17/4.17, ±0.00	1.61/1.61; ±0.00 2.00/2.00; ±0.00	1.76/1.71, ±0.00 1.86/1.86, ±0.00	δH: 3.40/3.38, +0.02 δH: 3.58/3.58, ±0.00
W[4]	6.21/6.20, +0.01	4.83/4.83, ±0.00	3.10/3.09, +0.01 3.30/3.30, ±0.00	-	$2H_{indole}$: 7.25/7.25, ±0.00 NH_{indole}: 10.86/10.86, ±0.00 $4H_{indole}$: 7.55/7.55, ±0.00 $5H_{indole}$: 7.06/7.05, 0.01 $6H_{indole}$: 7.21/7.21, ±0.00 $7H_{indole}$: 7.42/7.41, +0.01
G[5]	8.72/8.73, -0.01	3.36/3.35, +0.01 3.82/3.82, ±0.00	-	-	-
C[6]	7.07/7.07, ±0.00	4.65/4.66, -0.01	2.19/2.19, ±0.00 3.13/3.13, ±0.00	-	-
P[7]	-	4.89/4.88, +0.01	1.92/1.91, +0.01 2.32/2.32, ±0.00	1.89/1.89, ±0.00 2.03/2.03, ±0.00	δH: 3.58/3.58, ±0.00
S[8]	6.03/6.03, ±0.00	5.16/5.18, -0.02	3.22/3.24, -0.02 3.70/3.70, ±0.00	-	-
D[9]	7.76/7.76, ±0.00	4.62/4.62, ±0.00	2.24/2.24, ±0.00 3.20/3.21, -0.01	-	-
I[10]	8.26/8.26, ±0.00	3.56/3.57, -0.01	1.62/1.61, +0.01	CH_2: 1.23/1.22, +0.01 1.74/1.74, ±0.00 CH_3: 0.93/0.92, +0.01	δH: 0.90/0.90, ±0.00
P[11]	-	4.32/4.32, ±0.00	1.66/1.66, ±0.00 2.10/2.09, +0.01	1.79/1.79, ±0.00 2.15/2.15, ±0.00	δH: 3.26/3.26, ±0.00 δH: 3.89/3.88, +0.01
G[12]	7.59/7.57, +0.02	3.04/3.05, -0.01; 3.95/3.95, ±0.00	-	-	-
W[13]	7.91/7.91, ±0.00	4.50/4.49, +0.01	2.40/2.40, ±0.00 2.91/2.92, -0.01	-	$2H_{indole}$: 6.95/6.95, ±0.00 NH_{indole}: 10.79/10.80, -0.01 $4H_{indole}$: 7.12/7.12, ±0.00 $5H_{indole}$: 6.86/6.86, ±0.00 $6H_{indole}$: 7.15/7.15, ±0.00 $7H_{indole}$: 7.38/7.38, ±0.00
N[14]	8.61/8.62, -0.01	4.88/4.88, ±0.00	1.49/1.49, ±0.00 1.91/1.89, +0.02	-	-
T$_{15}$	8.89/8.89, ±0.00	4.86/4.86, ±0.00	4.60/4.60, ±0.00	1.19/1.19, ±0.00	-
P[16]	-	4.48/4.48, ±0.00	1.48/1.48, ±0.00 2.25/2.25, ±0.00	1.58/1.57, +0.01 1.71/1.71, ±0.00	δH: 3.70/3.70, ±0.00 δH: 3.96/3.95, +0.01
W[17]	7.96/7.95, +0.01	4.00/4.01, -0.01	2.16/2.17, -0.01 3.20/3.20, ±0.00	-	$2H_{indole}$: 7.41/7.41, ±0.00 NH_{indole}: 11.13/11.12, +0.01 $4H_{indole}$: 7.66/7.66, ±0.00 $5H_{indole}$: 7.13/7.12, +0.01 $6H_{indole}$: 7.19/7.18, +0.01 $7H_{indole}$: 7.41/7.41, ±0.00
A[18]	7.18/7.18; ±0.00	4.20/4.19, +0.01	1.15/1.15, ±0.00	-	-
C[19]	6.95/6.95; ±0.00	4.36/4.36, ±0.00	2.58/2.58, ±0.00 3.01/3.00; +0.01	-	-

Table **S4**. *J* values and torsion angles of synthetic D-BI-32169 measured from DQF-COSY spectrum

D-AA	peak position (ppm-ppm)	assignment	*J* value (Hz)	backbone angle φ	sidechain angles χ1
G[1]	8.76-4.32	$^3J_{HHA3}$	11.1	-	
L[2]	9.08-4.60	$^3J_{HHA}$	9.8	-120°±30°	60°±30°
	4.60-1.92	$^3J_{HAHB3}$	9.8		
W[4]	6.21-4.83	$^3J_{HHA}$	9.8	-120°±30°	60°±30°
	4.83-3.30	$^3J_{HAHB3}$	6.5		
G[5]	8.72-3.82	$^3J_{HHA3}$	10.5	-	
C[6]	7.07-4.65	$^3J_{HHA}$	10.5	-120°±30°	-30°±30°
	4.65-3.13	$^3J_{HAHB3}$	6.1		
S[8]	6.03-5.16	$^3J_{HHA}$	9.9	-120°±30°	60°±30°
	5.16-3.70	$^3J_{HHB3}$	5.6		
D[9]	7.76-4.62	$^3J_{HHA}$	10.8	-120°±30°	60°±30°
	4.62-3.20	$^3J_{HAHB3}$	7.2		
I[10]	8.26-3.56	$^3J_{HHA}$	5.5	-60°±30°	-
	3.56-1.62	$^3J_{HAHB}$	10.8		
G[12]	7.59-3.95	$^3J_{HHA3}$	13.0	-	
W[13]	7.91-4.50	$^3J_{HHA}$	10.5	-120°±30°	-30°±30°
	4.50-2.91	$^3J_{HAHB3}$	5.5		
N[14]	8.61-4.88	$^3J_{HHA}$	10.0	-120°±30°	150°±30°
	4.88-1.91	$^3J_{HAHB3}$	10.5		
T$_{15}$	8.89-4.86	$^3J_{HHA}$	8.0	-120°±30°	-
	4.86-4.60	$^3J_{HAHB}$	13.5		
W[17]	7.96-4.00	$^3J_{HHA}$	7.5	-60°±30°	-30°±30°
	4.00-3.20	$^3J_{HAHB3}$	5.7		
A[18]	7.18-4.20	$^3J_{HHA}$	9.5	-120°±30°	-
	4.20-1.15	$^3J_{AB}$	7.6		
C[19]	6.95-4.36	$^3J_{HHA}$	8.0	-120°±30°	-30°±30°
	4.36-3.01	$^3J_{HAHB3}$	5.5		

* Conversion of *J* values into the torsion angle constraints was solved by a Karplus equation[9]. The information of χ1 rotameric state was obtained from ^{3}J-coupling constants and the NOE strengths between NH and βHs[10].

CD Spectrum

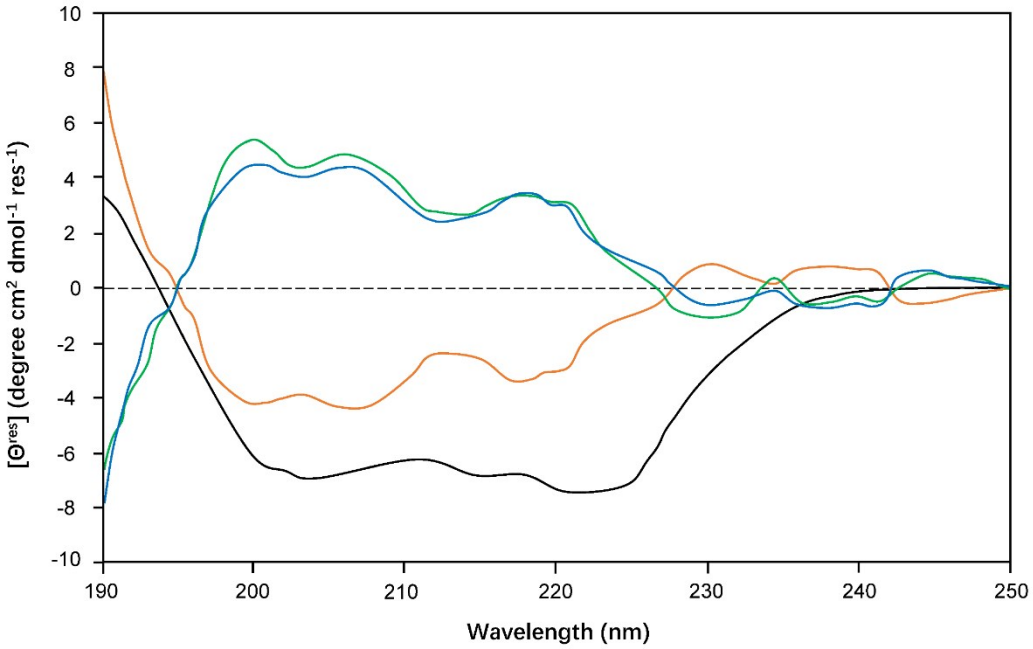

Figure **S76**. Circular dichroism spectra for synthetic BI-32169 (blue), synthetic D-BI-32169 (orange), native BI-32169 (green) and unthreaded topoisomer of BI-32169 (black).

5. Supplementary References

1 Potterat, O.; Wagner, K.; Gemmecker, G.; Mack, J.; Puder, C.; Vettermann, R.; Streicher, R. BI-32169, a Bicyclic 19-Peptide with Strong Glucagon Receptor Antagonist Activity from Streptomyces Sp. *J. Nat. Prod.* **2004**, *67*, 1528–1531.

2 Cudic, M.; Condie, B. A.; Weiner, D. J.; Lysenko, E. S.; Xiang, Z. Q.; Insug, O.; Bulet, P.; Otvos, L. Development of Novel Antibacterial Peptides That Kill Resistant Isolates. *Peptides* **2002**, *23*, 2071–2083.

3 Krakowiak, K. E.; Bradshaw, J. S.; An, H.; Izatt, R. M. Simple Methods for the Preparation of Cryptands. *Pure Appl. Chem.* **1993**, *65*, 511–514.

4 Naguib, Y. M. A. Synthesis of a [2.2.2] Cryptand Containing Reactive Functional Groups. *Molecules* **2009**, 14, 3600–3609.

5 Papageorgiou, G.; Ogden, D. C.; Barth, A.; Corrie, J. E. T. Photorelease of Carboxylic Acids from 1-Acyl-7-Nitroindolines in Aqueous Solution: Rapid and Efficient Photorelease of l-Glutamate. *J. Am. Chem. Soc.* **1999**, *121*, 6503–6504.

6 Kohl-Landgraf, J.; Buhr, F.; Lefrancois, D.; Mewes, J.-M.; Schwalbe, H.; Dreuw, A.; Wachtveitl, J. Mechanism of the Photoinduced Uncaging Reaction of Puromycin Protected by a 6-Nitroveratryloxycarbonyl Group. *J. Am. Chem. Soc.* **2014**, *136*, 3430–3438.

7 Wilson, K.-A.; Kalkum, M.; Ottesen, J.; Yuzenkova, J.; Chait, B. T.; Landick, R.; Muir, T.; Severinov, K.; Darst, S. A. Structure of Microcin J25, a Peptide Inhibitor of Bacterial RNA

Polymerase, is a Lassoed Tail. *J. Am. Chem. Soc.* **2003**, *125*, 12475–12483.

8 Knappe, T. A.; Linne, U.; Xie, X.; Marahiel, M. A. The Glucagon Receptor Antagonist BI-32169 Constitutes a New Class of Lasso Peptides. *FEBS Lett.* **2010**, *584*, 785–789.

9 Guentert, P.; Braun, W.; Billeter, M.; Wuethrich, K. Automated Stereospecific Proton NMR Assignments and Their Impact on the Precision of Protein Structure Determinations in Solution. *J. Am. Chem. Soc.* **1989**, *111*, 3997–4004.

10 Wagner, G. NMR Investigations of Protein-Structure; Elsevier BV: Amsterdam, 1990.